University of North Dakota
UND Scholarly Commons

Theses and Dissertations | Theses, Dissertations, and Senior Projects

12-1-2011

Amyloid-β Dependent Microgliosis Occurs Through Src Kinase Activation in Alzheimer's Disease

Gunjan Dhawan

How does access to this work benefit you? Let us know!

Follow this and additional works at: https://commons.und.edu/theses

Recommended Citation

Dhawan, Gunjan, "Amyloid-β Dependent Microgliosis Occurs Through Src Kinase Activation in Alzheimer's Disease" (2011). *Theses and Dissertations*. 3791.
https://commons.und.edu/theses/3791

This Dissertation is brought to you for free and open access by the Theses, Dissertations, and Senior Projects at UND Scholarly Commons. It has been accepted for inclusion in Theses and Dissertations by an authorized administrator of UND Scholarly Commons. For more information, please contact und.commons@library.und.edu.

AMYLOI D-β DEPENDENT MICROGLIOSIS OCCURS THROUGH SRC KINASE ACTIVATION IN ALZHEIMER'S DISEASE

by

Gunjan Dhawan
Bachelor of Science, University of Delhi, 2004
Master of Science, IIT Delhi, 2006

A Dissertation
Submitted to the Graduate Faculty

of the

University of North Dakota

in partial fulfillment of the requirements

for the degree of

Doctor of Philosophy

Grand Forks, North Dakota
December
2011

PERMISSION

Title	Amyloid-β dependent microgliosis occurs through Src kinase activation in Alzheimer's disease
Department	Pharmacology, Physiology and Therapeutics
Degree	Doctor of Philosophy

In presenting this dissertation in partial fulfillment of the requirements for a graduate degree from the University of North Dakota, I agree that the library of this University shall make it freely available for inspection. I further agree that permission for extensive copying for scholarly purposes may be granted by the professor who supervised my dissertation work or, in his absence, by the chairperson of the department or the dean of the Graduate School. It is understood that any copying or publication or other use of this dissertation or part thereof for financial gain shall not be allowed without my written permission. It is also understood that due recognition shall be given to me and to the University of North Dakota in any scholarly use which may be made of any material in my dissertation.

Signature Gwijun

Date 12/1/11

TABLE OF CONTENTS

LIST OF FIGURES

ACKNOWLEDGMENTS

First and foremost, I would like to thank my advisor Dr. Colin Combs for playing an instrumental role in my journey as a PhD student. I appreciate all his contributions of time, ideas and funding to make my graduate school experience productive and stimulating. He taught me everything I know of experimental neuroscience, starting from Western Blot experiments to animal surgeries. Not just Dr. Combs, but the whole Combs' lab has been a beautiful experience for me to work with. The joyous and motivational environment helped me through tough times during my Ph.D. This includes Angie Floden, who has been my driving force in the lab and outside, and has the solution to all my questions about lab experiments and/or everything North Dakota. Kendra Puig, for being the friend and a fun companion for all the regular and not so regular hours of work. Joy, for being a helpful lab mate and a shopping buddy. A big thank you to Jessi, Andrew and Keiko for being the coolest undergrads in the lab. The whole group has been a source of friendships, advice and collaboration.

I thank the members of my Faculty Advisory Committee, Dr. Holly BrownBorg, Dr. Saobo Lei and Dr. Brij Singh for all their support and encouragement all these years. I would like to acknowledge Dr. Jonathan Geiger, Department Chair and a member of my FAC for being an integral part of this whole journey, right from the very first step of applying for admission to this program.I am grateful to Dr. Eric Murphy for letting us use

his lab for all the amyloid peptide preparations, the fundamental component of my thesis work. I am extremely grateful to Julie Horn and Deb Kroese, Administrative Officers in the department for taking care of not just me but all the students in the department and their paper work. Deb was the first friendly face to greet me when I first came to the program and has been a tremendous help since then. A big thanks to Julie for all the sugary goodness every morning.

I greatly acknowledge the funding sources that made my PhD work possible. I was funded through Dr. Combs and the Doctoral Dissertation Award by NDEPSCoR. My work was also supported in part by travel grants from the Department of Pharmacology, Physiology and Therapeutics, UND, Office of Research Development and Compliance, UND, Office of Provost, UND, Graduate School, UND, Society for Neuroscience and American Society for Neurochemistry.

My time at UND was particularly made enjoyable due to my friends and groups I have been part of, here. Student Association of India has been a home away from home. I thank my friends Sumit, Malhar, Kirtipal, Malvika, Amar, Tanya, Tanveer, and Prasanna for being there for me always, and especially for the weekend parties. I would like to thank Dr. and Mrs. Seelan for treating me like their own daughter and for opening up their home for me with love and warmth. Lastly, I would like to thank my family for all their love and encouragement. For my parents who supported me in all my pursuits. For the presence of my brother, Mohit here at UND for two of my years here. And I am extremely thankful to my fiancé, Sachin for being the patient man he is and for dealing with the crazy me during my final stages of this Ph.D. I so appreciate that.

Grand Forks, ND has been good to me. Thank you.

Dedicated to

Mom and dad

ABSTRACT

The major histopathologic hallmark of Alzheimer's disease (AD) is the presence of β-amyloid plaques that are often associated with reactive microglia in the brain. It has been suggested modulating the microglial phenotype to attenuate an inflammatory response may prove to be useful in determining therapies for prevention or delay of the disease. My dissertation supports he hypothesis that Aβ stimulates microglial activation through a specific tyrosine kinase-dependent response involving the Src kinase family. Using primary mouse microglia we observed that both fibrillar and oligomeric Aβ stimulated increased microglial protein phosphotyrosine levels including active levels of the kinase Src and a subsequent increase in secretion of the cytokine, tumor necrosis factor alpha (TNFα). This response was attenuated by using a Abl/Src family kinase inhibitor, dasatinib. Intracerebroventricular infusions of Aβ oligomer into C57BL/6 adult mice elevated hippocampal phosphotyrosine levels and microgliosis that were attenuate by dasatinib treatment. To evaluate the efficiency of dasatinib in a relevant transgenic model of AD, drug was subcutaneously infused into 13-month old APP/PS1 transgenic mice. Behavioral testing using T-maze showed better performance from dasatinib infused mice as compared to vehicle treated and control animals. Biochemical analyses demonstrated that dasatinib infused animals had lower total protein phosphotyrosine and pSrc levels in the hippocampus. Dasatinib is an FDA approved drug for treating chronic myeloid leukemia and can cross the blood brain barrier. Our demonstration of the microglial inhibitory action of this drug defines a novel use. Based upon the observation

that AD brains showed increase in active, phosphorylated Lyn levels in reactive microglia, this kinase may also represent a possible microglial inhibitory target as well. Following a high throughput screening kinase assay, four drugs were identified. One compound LDDN-0003499 inhibited total protein phosphotyrosine as well as active pLyn levels in BV2 microglial cell line. LPS stimulated microglia treated with LDDN-0003499 demonstrated attenuation of TNF-α levels secretion. Collectively, our data supports the idea that non-receptor tyrosine kinase inhibition could be an important therapeutic goal for prevention and/or delay of AD.

CHAPTER 1

INTRODUCTION

Alzheimer's disease

Alzheimer's disease is the most common form of dementia. It affects mainly the elderly with a prevalence of 5% after 65 years of age and increases to about 30% at 85 years of age. AD is mainly characterized by cognitive impairment that affects thinking and behavior, severe enough to interfere with daily life (McKhann et al., 1984). It is a progressive form of disease that gets worse over time. At present, 5.3 million Americans are suffering from AD, with over 26 million people affected worldwide. According to the World Alzheimer's Report, the total estimated costs of dementia in US was $604 billion in 2010 with about 70% of that occurring in Western Europe and North America. Apart from the huge economic burden, this disease presents a tremendous amount of emotional and physical stress to not only the patients but also the care-givers of people suffering with Alzheimer's disease.

The disease was first described in 1906 by German psychiatrist and neuropathologist, Alois Alzheimer, when he observed in a patient, strange behavioral symptoms, including loss in short-term memory. Brain autopsy showed various abnormalities including a thinner cerebral cortex than normal and the presence of senile plaques and neurofibrilary tangles. Although the cause and progression of

Alzheimer's disease are not well understood, it has been very well established that the histopathology of AD consists of these two distinct characteristics, the presence of tangles and plaques (Dickson, 1997). These neurofibrilary tangles are mainly found in neurons in the brain regions affected by AD and are composed of protein tau, that is aggregated as paired helical filaments (PHF) (Hernandez and Avila, 2007). Tau is normally associated with microtubules that represent a component of structural support for intracellular transport (Weingarten et al., 1975; Drubin and Kirschner, 1986). Under normal conditions, tau has a role in stimulation and stabilization of microtubules. However in AD, tau is hyperphosphorylated which inhibits its ability to provide microtubule assembly and it aggregates as insoluble deposits within the cells (Grundke-Iqbal et al., 1986). The other major histopathological marker of AD is the presence of senile plaques, which are insoluble fibrous protein aggregates of amyloid-β peptide (Selkoe, 1994). This peptide is the cleavage product of a transmembrane integral protein, amyloid precursor protein. Plaques and tangles are predominantly found in frontal and temporal cortex regions of the brain, including the memory and visuospatial center, the hippocampus (Ray et al., 1998). Whether plaques and tangles play a causative or consequential role in the progression of Alzheimer's disease is still not well understood.

Clinically, Alzheimer's disease progression is marked by different stages of very mild/mild cognitive impairments (MCI), mild, moderate and severe dementia (Morris, 1993; Petersen et al., 1999). These stages correlate with increasing abundance of amyloid-plaques, neurofibrilary tangles and loss of neuronal and synaptic markers. Figure 1 adapted from (Perrin et al., 2009) illustrates the progression of changes of the various characteristic biomarkers of AD over time with relation to the appearance of

clinical stages in an AD brain. Amyloid-β plaques occur in the pre-clinical stages of AD for 10-15 years, eventually leading to damages in neuronal integrity (Morris, 1993). Neuronal loss is associated with onset of dementia as well as an increase in neurofibrilary tangles. The major biomarkers of AD include an increase in CSF tau and phosphorylated tau, a decrease in CSF Aβ42, microgliosis, inflammation, increase in markers oxidative stress, brain atrophy and genetic predisposition (Sunderland et al., 2003; Galimberti et al., 2008; Kauwe et al., 2009; Reddy et al., 2009). For diagnostic purposes, advanced medical imaging techniques like computer tomography (CT) or magnetic resonance imaging (MRI) and positron emission tomography (PET) can be used to determine the cerebral topography, but it is difficult to predict the earliest stages of AD. These diagnostic tools may predict the subtype of dementia or conversion from MCI to AD. However, apart from genetic predisposition, it is difficult to monitor the occurrence of AD progression in the early stages of the disease (Craig-Schapiro et al., 2009; Perrin et al., 2009)

AD can be classified into two forms, Familial Alzheimer's disease (FAD) and the Sporadic Alzheimer's disease (SAD). The familial form of the disease is uncommon and accounts for 5% of the cases and is usually defined at an earlier age. Also known as Early-onset AD, autosomal dominant mutations in APP, Presenilin 1 (PSEN1) and Presenilin 2 (PSEN 2) genes has been linked with the familial form of the disease. The sporadic form of AD accounts for 95% of the cases and has been linked to a number of environmental factors along with synergistic actions from genetic factors. These include cardiovascular diseases, Type 2 diabetes, mid-life obesity, increased age as well as

polymorphisms in apolipoprotein E (ApoE) as risk factors (Strittmatter and Roses, 1996; Lendon et al., 1997; Patterson et al., 2008).

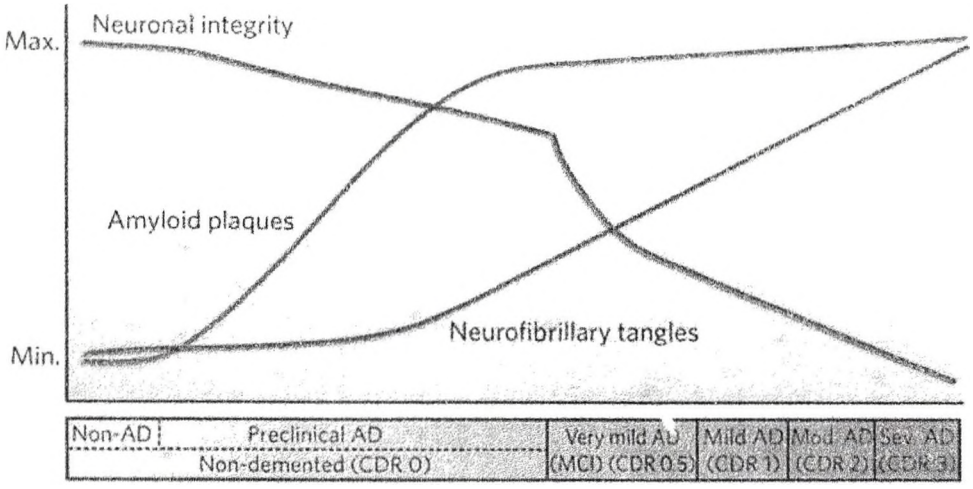

Figure 1. Proposed changes in biomarkers in relation to the time course of pathological and clinical stages (Adapted with permission from (Perrin et al., 2009))

APP and Amyloid-β peptide

A tremendous amount of research has been performed to try to identify the role of amyloid-β peptide in the pathogenesis of Alzheimer's disease. The peptide is derived from amyloid precursor protein (APP) which is ubiquitously expressed in neuronal and non-neuronal cells (Selkoe, 1994). Non-amyloidogenic cleavage of APP by α-secretase at a site within the Aβ domain, leads to the production of the soluble APP fragment, sAPPα, and prevents the formation of Aβ peptide (Lammich et al., 1999). But the amyloidogenic pathway of APP cleavage by β-secretase followed by gamma-secretase action generates the amyloid-β (Aβ) peptide (Fig. 2) (Gandy, 2005). Aβ is a 4KDa peptide with

microheterogeneiety in amino acid sequence with two physiologically relevant forms $A\beta_{1-40}$ and $A\beta_{1-42}$. $A\beta_{1-40}$ is the most abundant form of the Aβ present while $A\beta_{1-42}$ form is more prone to aggregation (Jarrett et al., 1993b; Yin et al., 2007). $A\beta_{42}$ readily multimerizes to form oligomers, then fibrils, and fully detergent resistant plaque aggregates (Gandy, 2005). $A\beta_{42}$, the more fibrillogenic form, is thus associated with disease states. Mutations in APP associated with early-onset Alzheimer's have been noted to increase the relative production of $A\beta_{42}$ perhaps leading to accommodation of plaque deposition and the early age of disease (Yin et al., 2007).

One of the leading theories behind understanding of the causes of AD pathology is the amyloid cascade hypothesis (Hardy, 2006). This theory was proposed in 1992 by Hardy and Higgins and has remained controversial over the years (Hardy and Higgins, 1992; Hardy, 1999, 2002). According to the hypothesis, Aβ plaque deposition is the main cause of AD pathogenesis. APP proteolysis leading to accumulation and deposition of Aβ plaques is the initiating event that then leads to Aβ dependent synaptic loss, neuritic injury, altered signaling events and subsequent formation of neurofibrilary tangles and cell death. Vascular damage and dementia follow as a direct effect of the deposition (Hardy and Selkoe, 2002; Hardy, 2006). Because Aβ peptide forms the fibrillar core of the senile plaques in both sporadic and autosomal dominant disease it has been hypothesized that fibrillar Aβ deposition is mechanistically critical for disease (Jarrett et al., 1993a; Pike et al., 1993). However, in recent years, evidence suggests a direct correlation between cognitive impairment and synaptic loss with the levels of soluble rather than fibrillar assemblies of Aβ extracted from AD brain (Lue et al., 1999; McLean

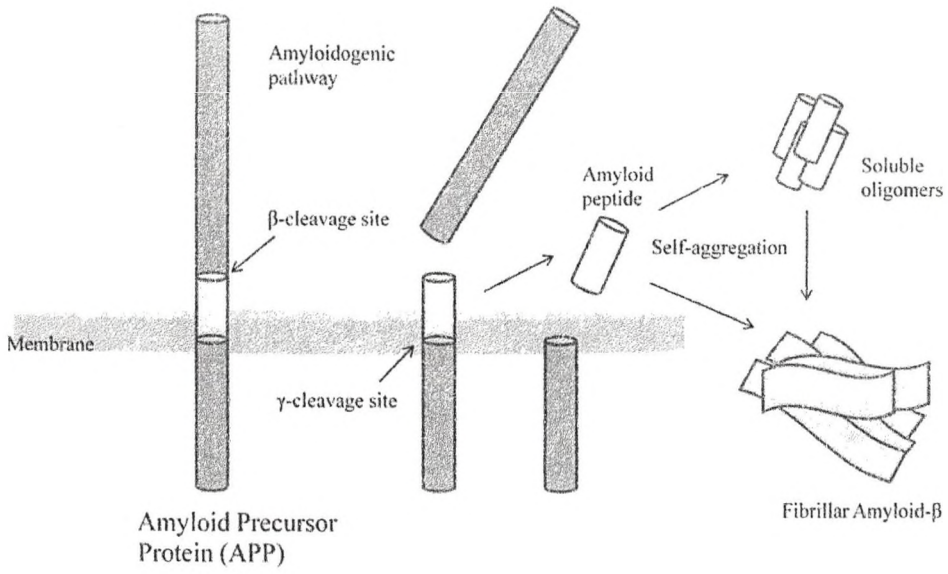

Figure 2: Schematic of Amyloidogenic APP processing

et al., 1999). Oligomeric Aβ has been shown to be neurotoxic and synaptotoxic *in vitro* studies as well (McLean et al., 1999; Sondag et al., 2009). Aβ oligomers have also been linked to gliotic pro-inflammatory changes *in vitro* (Roher et al., 1996; Cleary et al., 2005; Klyubin et al., 2005; Lesne et al., 2006; Klyubin et al., 2008). The exact contribution of the particular form of Aβ to disease, whether oligomeric or fibrillar, is yet to be fully defined. However, the issue remains that in order to identify a prevention or treatment therapy for AD, the role of Aβ and the mechanism behind its gliotic and neuronal actions need to be fully understood.

Microglia and AD

Microglia are the resident macrophages of the brain and the spinal cord. They form the first line of immune defense in the central nervous system. These cells constitute

about 5-20% of all glial cells (Lawson et al., 1992). In early stages of brain development, microglia generally represent an "amoeboid" phenotype. They show a macrophage-like morphology with a larger cell body and shorter processes (Ling, 1979). As the brain develops, these microglia obtain a "ramified" morphology. These are the resting microglia in a normal brain, with relatively longer processes and smaller cell bodies. In cases of brain injury, or other neurodegenerative diseases, ramified microglia may transform into activated states, also called "reactive microglia" (Nakajima and Kohsaka, 2001). These are morphologically distinct with longer, finger-like projections. The reactive microglia become proliferative at the affected site. Activated microglia have been implicated to play cytotoxic and inflammatory roles in the CNS (Poli, 1998; Weldon et al., 1998; Nakajima and Kohsaka, 2001; Rogers et al., 2002; Schlachetzki and Hull, 2009).

Microglia belong to the mononuclear phagocytic system, expressing characteristic markers of phagocytes and immune cells, such as complement components and their receptors, MHC glycoproteins and scavenger receptors (McGeer and McGeer, 1999; Streit et al., 2004). Activated microglia are known to secrete cytokines as well as toxic free radicals (Poli, 1998; Weldon et al., 1998; Akiyama et al., 2000; Jara et al., 2007). In neurodegenerative diseases, microglia are known to show increased secretion of pro-inflammatory cytokines, chemokines and free radicals and reduced clearance of pathological protein aggregates (like Aβ) and cell debris, thus contributing to disease pathogenesis (Dickson et al., 1993; Yates et al., 2000; Tuppo and Arias, 2005; Block et al., 2007).

The presence of increased number of reactive microglia has been very well characterized in Alzheimer's disease (Fig. 3). Besides the accumulation of plaques and tangles it has been shown in both human disease and transgenic mouse models, that reactive microglia numbers are increased compared to non-demented controls and wild-type mice, respectively (McGeer et al., 1987; Akiyama and McGeer, 1990; Cras et al., 1990; Styren et al., 1990; Frautschy et al., 1998; Stalder et al., 1999; Wegiel et al., 2001; Sasaki et al., 2002; Wegiel et al., 2003). The morphologically distinct, activated microglia are commonly associated with Aβ fibril containing plaques (Itagaki et al., 1989; Mattiace et al., 1990; Perlmutter et al., 1990; Mackenzie et al., 1995; Sasaki et al., 1997; Akiyama et al., 1999; Benzing et al., 1999; Morgan et al., 2005; Meyer-Luehmann et al., 2008). Numerous *in vitro* studies have demonstrated that Aβ fibrils can directly stimulate microglia to acquire a pro-inflammatory phenotype (Banati et al., 1993; Del Bo et al., 1995; Giulian et al., 1995; Klegeris et al., 1997; Combs et al., 2000; Combs et al., 2001a; Combs et al., 2001b). However oligomeric Aβ conformations have also been reported to stimulate gliosis (Martin et al., 1994; Sasaki et al., 1997; Sondag et al., 2009). Indeed, up to 70% of diffuse plaques in non-demented aged individuals contain microglia (Sasaki et al., 1997) suggesting that microglial interaction with nonfibrillar peptide is common. Work from primates even indicates that gliosis precedes fibrillar plaque deposition (Martin et al., 1994). Therefore, the fibrillar, insoluble form of the peptide may not be the only substrates mediating neuronal death/dysfunction. More importantly, the oligomeric peptide may represent a target for early disease therapy.

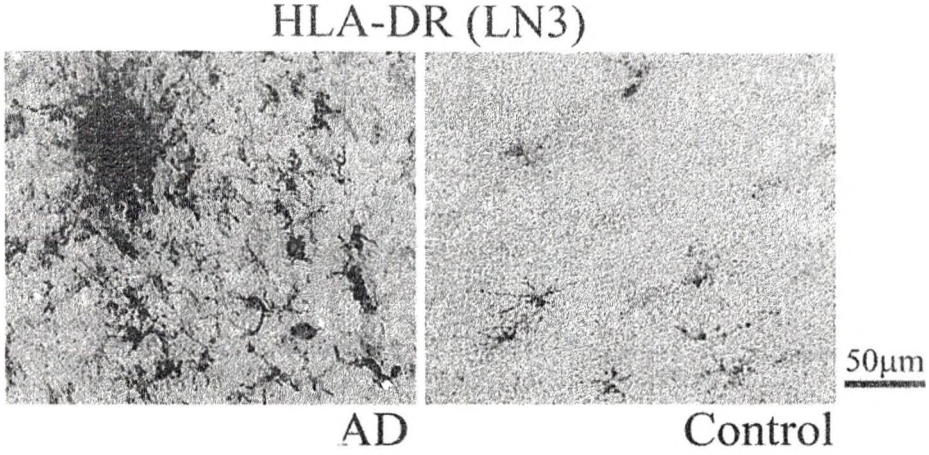

Figure 3. Presence of reactive microglia in AD brain

Anti-inflammatory approach to AD

A plethora of data over the past 2 decades have led to the conclusion that neuroinflammation forms an integral component of the pathogenesis of AD (Akiyama et al., 2000; Streit et al., 2004; Tuppo and Arias, 2005; Rojo et al., 2008; Agostinho et al., 2010; McNaull et al., 2010; Schwab et al., 2010). Up regulation of various pro-inflammatory cytokines has been widely reported in AD patients (McGeer and McGeer, 1999; Streit et al., 2001; Szczepanik et al., 2001; Moore and O'Banion, 2002; Wilson et al., 2002; Streit et al., 2004; Tuppo and Arias, 2005; Galimberti et al., 2008; Combs, 2009; McNaull et al., 2010). Microglia cultured from AD brains demonstrate marked chemotaxis to Aβ deposits (Rogers and Lue, 2001). Microglia adhesion to Aβ fibril coated surfaces substantially increases reactive oxygen species production (El Khoury et al., 1996). An increase in secretion of pro-inflammatory cytokines IL-1β, IL-6 and TNF-α, chemokines IL-8, macrophage and MLP-1α have been observed in microglia interacting with Aβ deposits (Rogers and Lue, 2001). Pro-inflammatory changes have

been widely reported in transgenic mouse models of AD as well. Brains of Tg 2576, TgAPPsw, PS1/APPsw and triple transgenic mice (3XTg-AD), have all been reported to have elevated levels of pro-inflammatory cytokines including IFN-γ, IL-12, TNF-α, IL-6,IL-1β, TGF-β, IL-10, MCP-1 and GM-CSF (Benzing et al., 1999; Apelt and Schliebs, 2001; Abbas et al., 2002; Janelsins et al., 2005; Patel et al., 2005).

Modulation of inflammatory activity in these mouse models produces changes in their AD-like pathology. For example, use of dominant negative-TNF inhibitors in triple transgenics prevents intraneuronal Aβ accumulation (McAlpine et al., 2009). IFN-γ knockdown reduces Aβ plaque load and gliosis in Tg2576 mice (Yamamoto et al., 2007). Up-regulating pro-inflammatory pathways has also been reported to give rise to AD pathology. For example, overexpression of CCL2 (MCP-1) increases microglial activation and Aβ deposition in APP/PS1 mice (Yamamoto et al., 2005).

Based upon the idea that manipulating microglial activity in various mouse models can affect disease histopathology, it is reasonable to expect that similar alteration of microglial phenotype will affect human disease. A number of epidemiological studies have demonstrated that long-term use of non-steroidal anti-inflammatory drugs (NSAIDs) could be helpful in reducing the risk of AD. The Rotterdam study in 2001 showed that long-term use of ibuprofen reduced relative risk of developing AD to 0.2 (95% CI 0.05-0.83)(in't Veld et al., 2001). Use of ibuprofen, naproxen and indomethacin, all NSAIDs demonstrated lower incidences of AD in the Baltimore study of Aging (Stewart et al., 1997). Use of NSAID was also associated with a decrease in microgliosis without affecting the Aβ fibrillar plaque load (Mackenzie and Munoz, 1998). The most

probable mechanism of action of NSAIDs is inhibition of COX-2 activity and prostaglandin production, both linked to pro-inflammatory effects (McNaull et al., 2010). In late onset AD, COX-2 activity has been found to be elevated in humans and it has also been linked to APP processing and cognitive decline in animal models (Pasinetti and Aisen, 1998; Tuppo and Arias, 2005; Rojo et al., 2008; McNaull et al., 2010). Besides cox inhibition, NSAIDs have been proposed to work through inhibition of cytokine expression as well as modulation of γ-secretase activity (Weggen et al., 2003). Some NSAIDs are known to be PPAR-γ agonists, modulating oxidative stress and inhibiting of expression of inflammatory genes (Lehmann et al., 1997; Landreth and Heneka, 2001; McNaull et al., 2010). However, a number of studies using rofecoxib (Reines et al., 2004), naproxen (Aisen et al., 2003), diclofenac (Scharf et al., 1999), celecoxib (Soininen et al., 2007), dapsone (Eriksen et al., 2003), hydroxychloroquine (Aisen et al., 2001) and nimesulide (Aisen et al., 2002) failed to slow progression of cognitive decline in patients with mild to moderate AD. A number of factors may be responsible for the failure or disappointing results in the clinical studies involving the use of NSAIDs. These include inadequate drug penetration into the brain, inadequate doses and the variability in diagnosis and progression of AD in individuals (Rojo et al., 2008). Indeed a very recent study indicates that prolonged use of NSAIDs decreases the incidence of AD when taken by only asymptomatic individuals (Breitner et al., 2011). This suggests that timing of anti-inflammatory use is critically important when considering any therapeutic strategies for AD.

Structure, function and inhibition of Src family of tyrosine kinases

Tyrosine kinases are enzymes that catalyze the transfer of phosphate groups from ATP to the tyrosine residues within proteins. Tyrosine kinases are part of the larger family of protein kinases. Proteins that become phosphorylated by tyrosine kinases, or by other kinases, allow for the signal transduction pathways that regulate many of the functions of cells. The Src family of tyrosine kinases (STKs) is a non-receptor kinase family with nine members: Lyn, Fyn, Lck, Hck, Fgr, Blk, Yrk, Yes and c-Src. c-Src (henceforth referred to a Src) is the best studied non-receptor tyrosine kinase and is commonly implicated in oncogenesis (Yeatman, 2004), cellular proliferation, survival, migration, and angiogenesis (Hanahan and Weinberg, 2000; Yeatman, 2004).

Proteins in the Src family have a conserved organization consisting of four Src homology (SH) domains and a C-terminal segment containing a negative regulatory tyrosine residue (Tyr530) (Fig. 4). Src exists in both active and inactive conformations. Negative regulation occurs through phosphorylation of Tyr530, resulting in an intramolecular association between phosphorylated Tyr530 and the SH2 domain of Src, thereby locking the protein in a closed conformation. Further stabilization of the inactive state occurs through interactions between the SH3 domain and a proline-rich stretch of residues within the kinase domain (Sicheri and Kuriyan, 1997). Conversely, dephosphorylation of Tyr530 allows Src to assume an open conformation (Aleshin and Finn, 2010). Full activity requires additional autophosphorylation of the Tyr419 residue within the catalytic domain (Lowell, 2004) . The intramolecular activity of Src is regulated by a balance between kinases and phosphatases including other receptor

tyrosine kinases such as epidermal growth factor receptor (EGFR), fibroblast growth factor receptor (FGFR) and platelet-derived growth factor receptor (PDGFR) as well as direct binding of Focal Adhesion Kinases (FAK), that mainly act at the C-terminal Tyr530 residue (Sakai et al., 1994; Parsons and Parsons, 1997).

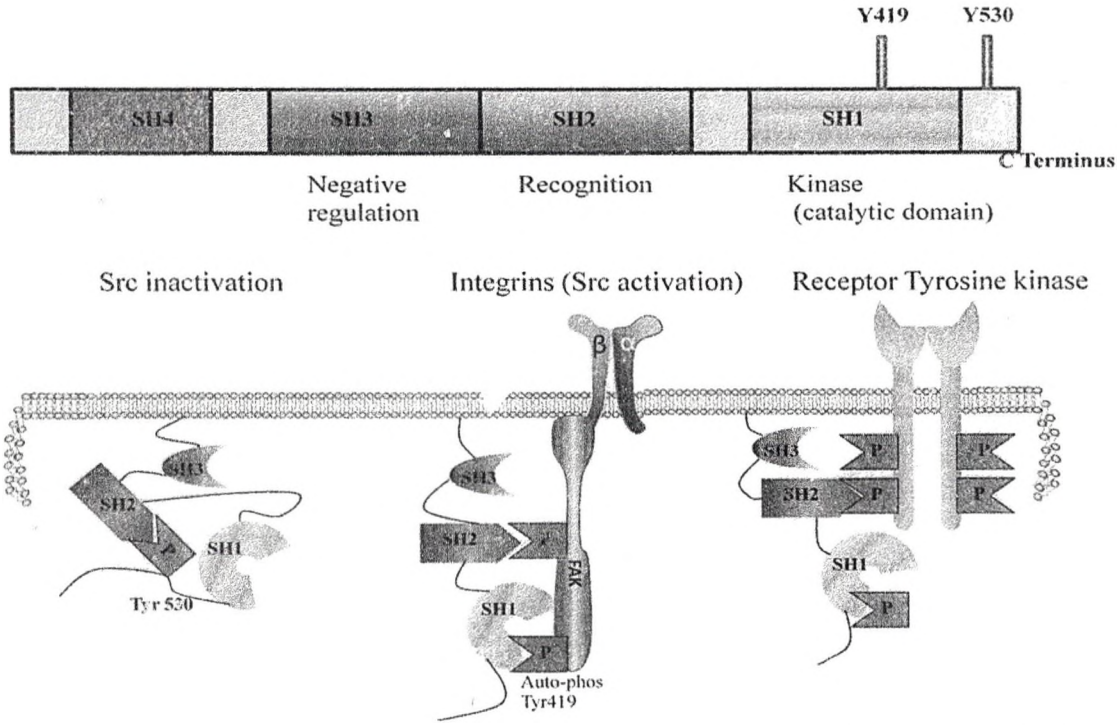

Figure 4. Src activation and inactivation (adapted and modified from (Aleshin and Finn, 2010) and (Tatosyan and Mizenina, 2000)

As mentioned, Src activation is an important event in various cell processes in normal and malignant cells. Src plays a key role in regulation of cell adhesion and migration. Dynamic turnover of cell-cell (adherence junctions) and cell-matrix (focal adhesions) junctions is crucial for normal cellular adhesion, migration, and division (Biscardi et al., 1999; Playford and Schaller, 2004; Yeatman, 2004; McLean et al., 2005;

Guarino, 2010). The subcellular localization of Src is critical to its function of regulating the assembly and disassembly of these junctions. An increase in Src signaling deregulates cell-cell adhesion. In association with FAK, Src mediates signals from extracellular matrix–integrin complexes to the cell interior, thereby influencing cell motility, survival, and proliferation (Roche et al., 1995; Prathapam et al., 2006). Src is also suggested to be involved in regulating cell cycle progression and mitogenesis (Weng et al., 1994; Roche et al., 1995; Prathapam et al., 2006). Src activation is associated with increased expression of proangiogenic cytokines such as VEGF and interleukin 8 (IL-8) (Kanda et al., 2007). Treatment with 4-amino-5-(4-chlorophenyl)-7-(t-butyl)pyrazolo[3,4-d] pyrimidine (PP2), a potent and selective inhibitor of SFKs, inhibits angiogenesis *in vivo* and blocks endothelial cell differentiation *in vitro* (Kilarski et al., 2003). Inhibiting Src blocks IL-8–mediated VEGFR2 activation and decreases vascular permeability (Yeh et al., 2004; Petreaca et al., 2007). Furthermore, SFKs are implicated in endothelial cell function, with inhibition of Src, Fyn, and Yes decreasing VEGF-induced endothelial cell migration (Werdich and Penn, 2005).

The Src family of tyrosine kinases has been identified as important for recruitment and activation of immune cells like monocytes, macrophages and neutrophils into pro-inflammatory sites. Several Src family members, Blk,Fgr, Hck, Lck, Lyn and Yes have been implicated in signaling responses in hematopoetic lineage cells (De Franceschi et al., 1997; Lowell and Berton, 1999; Gardai et al., 2002; Nijhuis et al., 2002; Rane and Reddy, 2002). Src family members, Lck and Fyn are expressed in T-cells and are known to become activated directly downstream of the T-cell receptors (Barber et al.,

1989). Macrophage and monocytes have been reported to express Fyn, Yes, Src, Hck and Lyn kinase (Okutani et al., 2006). LPS stimulation increases the expression of Hck in monocytes, human peripheral blood monocyte-derived macrophages and murine-bone marrow derived macrophages (Ziegler et al., 1988; Boulet et al., 1992; Beaty et al., 1994; Cohen, 2002). Lyn expression and activity is also increased in LPS stimulated macrophage and monocytes (Ziegler et al., 1988; Boulet et al., 1992; Beaty et al., 1994). Blocking tyrosine kinase activity also reduces low-dose LPS induced TNF-α production as well as LPS-induced NF-kB translocation in macrophage (Khadaroo et al., 2003; Khadaroo et al., 2004). LPS stimulation recruits Src protein tyrosine kinases into the LPS receptor complex via CD14 (Stefanova et al., 1993). Other pro-inflammatory mediators have also been reported to be associated with Src family members, besides LPS. Src protein tyrosine kinases bind to IL-6 receptor b-chain, gp130 in macrophage (Schaeffer et al., 2001). In addition to the involvement in pro-inflammatory pathways, Src kinases play critical roles in other cellular functions of macrophage. Src kinases are known to associate with integrin heterodimers that play important role in migration and adhesion of macrophage (Suen et al., 1999; Caveggion et al., 2003). Macrophage with Src family kinases knockdown display alterations in cytoskeleton dynamics and polarization.

Abundant evidence of pharmacological intervention against Src protein tyrosine kinase in acute inflammation responses has been reported *in vivo*. Use of the selective Src kinase inhibitor PP1 in brain injury models in rats has been shown to reduce brain edema and mortality as well as suppressed vascular permeability in a mouse model of stroke (Paul et al., 2001; Kusaka et al., 2004; Lennmyr et al., 2004). Another Src kinase

inhibitor PP2, reduces alveolar macrophage priming in an acute lung injury model (ALI) *in vivo* (Khadaroo et al., 2004). Decreased LPS-induced acute lung injury and LPS-induced mortality were reported with PP2 injections as well (Severgnini et al., 2005).

With a key role in cell proliferation, invasion and metastasis, Src has been identified as a major target for therapeutic intervention with various Src inhibitors being identified for clinical purposes. One of the most studied Src inhibitors finds relevance in our study as well. Dasatinib, commercially available as Sprycel (Bristol-Myers Squibb) is an FDA approved drug for Chronic Myelogenous Leukemia. Dasatinib is an orally available, small-molecule Src/Abl inhibitor that has robust antitumor and antiproliferative activity against numerous hematologic and solid tumor cell lines (Lombardo et al., 2004; Das et al., 2006; Chang et al., 2008). In addition to inhibiting Src and Bcr-Abl in the subnanomolar range, dasatinib also variably inhibits other SFKs, c-KIT, PDGFR, and ephrin A2 (Chang et al., 2008). The mechanism of Src inhibition results from a hydrogen bond–mediated association with the ATP binding site, resulting in competitive restriction of ATP binding by Src (Lombardo et al., 2004). This compound emerged from a series of Lck inhibitors originally synthesized as anti-inflammatory compounds. Dasatinib (BMS-354825) is potent against cAbl and BCR-Abl, inhibiting the pure enzyme with an IC50 of <1 nM(Jakubowska and Czyz, 2006). According to the Cancer Drug Information, National Cancer Institute, due to the activity of dasatinib against BCR-Abl, especially its activity against mutant forms of BCR-Abl that are resistant to Gleevec treatment, Bristol-Myers developed this compound as a therapy against CML and ALL in pre-clinical and clinical trials. As shown *in vitro*, Dasatinib was effective on patients harboring mutations

resistant to Gleevec but not in those patients whose CML cells contained mutation T315I. This mutant proved to be resistant to Dasatinib *in vitro* (Quintas-Cardama et al., 2007). These results led to FDA approval of dasatinib for Gleevec-resistant CML in June 2006 at a recommended dose for CML(Gnoni et al., 2011). Dasatinib is also known to cross the blood brain barrier, although the efficiency of the transport is not yet known (Porkka et al., 2008).

During microglia stimulation, tyrosine phosphorylation systems have been found to be particularly activated *in vitro* and *in vivo* (Tillotson and Wood, 1989b). Elevated protein phosphotyrosine levels have been reported, selectively in ramified microglia (Wood and Zinsmeister, 1991). Tyrosine phosphorylation of a variety of substrates is quantitatively enriched in microglia compared to other neural cell types. Therefore, protein tyrosine kinases have been seen as reliable markers for microglial activation in Alzheimer's disease (Karp et al., 1994). *In vitro* studies using monocytic lineage cells (Combs et al., 1999) as well as microglia (Sondag et al., 2009) have supported these data by demonstrating that Aβ fibrils and oligomers stimulate a specific increase in overall protein tyrosine phosphorylation. This supports the idea that tyrosine kinase inhibition may be useful for attenuating microgliosis in AD.

Hypothesis

Microglial-dependent proinflammatory changes are a component of Alzheimer's disease process suggesting that strategies to limit acquisition of a reactive phenotype may be therapeutically useful. However, in order to modulate microglial behavior during disease it is necessary to understand their source of stimulation and the resultant

mechanism of activation. One possibility is that Aβ peptide in both its fibrillar and oligomeric form may activate microglia during disease. As already mentioned, prior work from our lab as well as others has demonstrated the ability of fibrillar peptide to stimulate microglia. Prior work has shown that the oligomeric peptide is a potent proinflammatory stimulus also utilizing tyrosine kinase mechanism (Sondag et al., 2009). This increase in tyrosine kinase activity is required for subsequent secretion of the neurotoxic cytokine, TNFα. Aβ oligomers were also shown to be toxic to cultured neurons only in the presence of microglia (Sondag et al., 2009).

Therefore, targeting Aβ oligomer and fibril dependent signaling mechanism in microglia, especially those including the Src family of kinases, presents a therapeutically attractive target to attenuate microgliosis in AD. This work aims to indentify Src kinase inhibitory properties of a commercially available cancer drug, dasatinib as well as characterizing novel Src kinase inhibitors, for attenuating Aβ oligomer and fibril dependent microgliosis in various disease models including primary microglia cultures, Aβ infused *in vivo* models and a transgenic mouse model of AD.

CHAPTER 2

METHODS

Materials

Anti-oligomer antibody (I11) and anti-fibril antibody (O.C.) have been previously described (Kayed et al., 2007). The anti-oligomer antibody (A11) was purchased from Invitrogen (Camarillo, CA). Anti-Aβ, clones 6E10 and 4G8 were from Covance (Emeryville, CA). The anti-Lyn antibody, anti-Src, anti-α-tubulin antibodies and horseradish peroxidase conjugated secondary antibodies were purchased from Santa Cruz Biotechnology (Santa Cruz, CA). Mouse TNF-α ELISA kit was obtained from R&D Systems (Minneapolis, MN). Anti-phospho-tyrosine (4G10) antibody was from Upstate (Temecula, CA), HLA-DR Ab-1 (LN3) antibody was from Neomarkers (Fremont, CA) and anti-pLyn (396) antibody was purchased from Abcam (Cambridge, MA). Anti-CD68 was obtained from Serotec (Raleigh, NC). Anti-APP antibody was purchased from Invitrogen (Camarillo, CA). The non-receptor tyrosine kinase inhibitor, dasatinib, was obtained from LC Laboratories (Woburn, MA). Elite Vectastain ABC avidin and biotin, biotinylated anti-rabbit, anti-mouse, anti-rat antibodies and the Vector VIP chromogen kits were from Vector Laboratories Inc. (Burlingame, CA). Anti-PSD95 and anti-pSrc (Tyr 416) antibody was purchased from Cell Signaling Technology (Danvers, MA). Anti-synaptophysin and anti-βIII tubulin antibodies were purchased from Chemicon

International, Inc (Temecula, CA, USA). The transgenic mouse line, strain 005864 B6.Cg-Tg(APPswe,PSEN1dE9)85Dbo/J and wild-type mouse line, C57BL/6J were obtained from the Jackson Laboratory (Bar Habor, Maine).

Animal Use

All animal use was approved by compliance with the University of North Dakota Institutional Animal Care and Use Committee (UND IACUC). Mice were provided food and water *ad libitum* and housed in a 12 h light/dark cycle. The investigation conforms to the National Research Council of the National Academies Guide for the Care and Use of Laboratory Animals (8th edition).

Human Tissue

Human AD and age-matched control tissue was obtained from the University of Washington Alzheimer's Disease Research Center, Grant # P50AG05136 and University of Iowa Brain Bank. The investigation conforms to the principles outlined in the Declaration of Helsinki. All human tissue use was approved by the University of North Dakota Institutional Biosafety Committee/Institutional Review Board.

Preparation of Peptides

Aβ1-42 was purchased from Bachem (Torrance, CA) or American Peptide (Sunnyvale, CA) for fibril and oligomer preparations, respectively. Aβ1-42 peptide was dissolved in 1:1 acetonitrile-water, aliquoted and dried. The aliquoted peptides were stored at –20 degree C until use. For oligomer preparation, each tube was dissolved in 50 μL HFIP and then diluted with 175 μL of sterile water and stirred at room temperature for 48h. The peptide was then spun at 14,000 rpm, for 10 min and the supernatant quantified using the method of Bradford (Bradford, 1976). For Aβ fibril preparations,

Aβ1-42 peptide was dissolved in deionized water and incubated for a week at 37 degrees C. Before use, the fibril was mixed well and quantified using the Bradford assay.

Structural Peptide Analyses

For Western blot analysis of SDS-stable multimeric forms of oligomers, the peptide was diluted to different concentrations, separated by 15% SDS-PAGE and analyzed by Western blot using 6E10 (anti-Aβ) as the primary antibody. For dot-blot analyses of oligomers and fibrils, 1μg each of Aβ oligomer or fibril were dot blotted onto polyvinylidene flouride (PVDF) membrane and incubated with A11 (anti-oligomer) and 6E10 (anti-Aβ) antibodies and analyzed via enhanced chemiluminescence (GE Healthcare, Piscataway, NJ).

BV2 Cell Line

Immortalized murine microglial BV2 cells were obtained from Dr. Gary E. Landreth, Cleveland, Ohio. The cells were maintained at 3×10^6 cells/dish in 100-mm dishes in DMEM/F12 (Gibco RBL, Rockville, MD) supplemented with 10% heat-inactivated FBS (U.S. Biotechnologies Inc., Parkerford, PA), 5% horse serum (Equitech-Bio, Inc., Kerrville, TX), penicillin G (100 units/ml), streptomycin (100 mg/ml), and l-glutamine (2 mM) and incubated at 37 °C in a humidified atmosphere containing 5% CO_2 and 95% air.

Tissue Culture

Microglia cultures were derived from the brains of postnatal day 1-3 C57BL/6J mice (Floden and Combs, 2006). Briefly, cortices were removed and trypsinized. The trypsin was inactivated in microglial growth media (DMEM/F-12 with L-glutamine (Invitrogen) containing 10% heat-inactivated FBS, 5% heat-inactivated horse serum, and

antibiotics, penicillin, streptomycin and neomycin (Gibco, Invitrogen). The tissue was triturated and plated into tissue culture flasks. After 24 hours all media and cellular debris was replaced with fresh media. After 7 more days one half of the media was replaced and cells were maintained as a mixed glia culture until day 14. At 14 days *in vitro*, microglia were shaken from the mixed glial culture at 200 rpm for 45 min and collected for use.

Cell Stimulation

BV2 cells and/or microglia were placed into serum-free DMEM/F12 media for stimulations with Aβ oligomers or fibrils. To inhibit tyrosine kinases, cells were pretreated with drug or vehicle (DMSO) for 30 min before adding the appropriate concentrations of peptides. For ELISA analysis, cells were stimulated in 96-well plates (20,000 cells/ well, 75 µL serum-free DMEM/F12) for 24 hours with 8 replicates per condition repeated 4-5 independent times. Experiments for Western blot analyses were performed for 5 minutes to assess signaling changes. After stimulation, cells were lysed in RIPA buffer (20mM Tris, pH 7.4, 150mM NaCl, 1mM Na_3VO_4 10mM NaF, 1mM EDTA, 1mM EGTA, 0.2mM phenylmethylsulfonyl fluoride, 1% Triton X-100, 0.1% SDS, and 0.5% deoxycholate) with protease inhibitors (AEBSF 104mM, Aprotinin 0.08mM, Leupeptin 2.1mM, Bestatin 3.6mM, Pepstatin A 1.5mM, E-64mM). Protein concentrations were determined using the Bradford method (Bradford, 1976). For toxicity analyses, cells stimulated for 24 hours were used for MTT reduction toxicity assay.

Enzyme Linked-immuno-sorbent Assay (ELISA)

Media was collected from microglia following 24 hour stimulation for ELISA analysis. Levels of mouse TNF-α in the media were determined using commercially available ELISA kits according to the manufacturer's protocol (R&D Systems).

Cell Viability Assay

The MTT reduction assay was performed to assess changes in cell survival. In brief, the media was removed from cells stimulated with or without Aβ and dasatinib and replaced with media containing 3[4,5-dimethylthiazol-2-y1]-2,5-diphenyltetrazolium bromide (MTT, 100μg/mL) for 4 hours. The media was aspirated and the reduced formazan precipitate was dissolved in isopropanol and absorbances read at 560/650nm via plate reader and averaged. For the Lactate Dehydrogenase Release (LDH) Assay, media was collected following 24 hour cell stimulation and centrifuged (14,000xg, 2 min, 25°C). Aliquots were then added to a 96-well plate and LDH concentrations assayed according to manufacturer's instructions (Promega Corporation, Madison, WI). Background absorbance was subtracted from each condition. Values were averaged (± SD).

Western Blot Analysis of BV2 Cells and Microglia Cultures

Cell lysates from 5 minute stimulations were resolved by SDS-PAGE and transferred to PVDF membranes. Western blots were blocked and incubated in anti-phospho-tyrosine (4G10), anti-pSrc (Tyr 416) and anti-pLyn (Tyr 396) as primary antibodies with α-tubulin, Src and Lyn antibodies as the respective loading controls. Blots were washed followed by incubation with HRP-conjugated secondary antibodies and antibody binding was detected via enhanced chemiluminescence (GE Healthcare, Piscataway, NJ).

Intracerebroventricular Infusion of Aβ 1-42 Oligomers and Dasatinib

Aβ oligomers with or without dasatinib were infused into the right ventricle of C57BL/6 female mouse brains at 12 months of age. Mice were anesthetized with sodium

pentobarbital (Nembutal, 70mg/kg) and a scalp incision made for stereotaxic placement of the cannula. Blunt end dissection caudally from the base of the scalp incision were performed to generate a small subcutaneous pocket for placement of an Alzet (model 1004, 0.25μL/hour delivery rate, Cupertino, CA) osmotic pump in the sub-scapular region. A cannula (Brain infusion kit, Alzet) was stereotaxically placed into the right lateral cerebral ventricle at coordinates –1.0 mm mediolateral and –0.5 mm anterioposterior from Bregma; –1.5 mm dorsal-ventral from skull. The cannulae were connected to subscapularly placed miniosmotic pumps (Alzet, model 1004) delivering either Aβ oligomers (1.6μg/day) or vehicle (4mM Hepes, 250μg/mL human high density lipoprotein) with or without dasatinib (500ng/kg/day) for 14 days. At the end of the infusion period, mice were euthanized, brains perfused with PBS-$CaCl_2$ and rapidly collected. The right hemispheres were collected for cryosectioning and the left hemispheres were flash frozen in liquid nitrogen and lysed in RIPA buffer for biochemical analysis.

Collection of Brains from Different Age APP/PS1 Mice

Brains from different aged APP/PS1 mice were collected for longitudinal analyses. 2, 4, 6 and 12 month old transgenic mice (n=5-6) along with their age-matched C57BL/6 wild type controls were euthanized and perfused with PBS-$CaCl_2$. Brains were rapidly dissected and divided into left and right hemispheres, with right hemispheres fixed in 4% paraformaldehyde for sectioning. The left hemispheres were further dissected into different brain regions to obtain hippocampus, temporal cortex, frontal cortex and cerebellum and flash frozen using liquid N_2. The frozen tissue was lysed using RIPA with protease inhibitor and quantified by the method of Bradford.

Subcutaneous Infusions of Dasatinib into APP/PS1 mice

Dasatinib was infused subcutaneously into female APP/PS1 mice at 13 months of age. Dasatinib was delivered via mini-osmotic pumps (model 1004, 0.25μL/hour delivery rate, Alzet, Cupertino, CA). Pumps delivered either vehicle (DMSO/Hepes) (n=6) or dasatinib (500ng/kg/day) (n=7) for 28 days. At the end of the infusion period, mice were euthanized, brains perfused with PBS-$CaCl_2$, and rapidly collected. The right hemispheres were collected for fixing in 4% paraformaldehyde and the left hemispheres were flash frozen in liquid nitrogen for biochemical analysis.

Immunostaining Mouse Brains

The paraformaldehyde fixed right hemispheres for different age mice or from dasatinib treated mice were sectioned using a freezing microtome. Briefly, paraformaldehyde fixed tissue was embedded in a 15% gelatin (in 0.1M phosphate buffer) matrix and immersed in a 4% paraformaldehyde solution for 2 days to harden the gelatin matrix. The blocks were then cryoprotected through 3 cycles of 30% sucrose for 3-4 days each. The blocks were then flash frozen using dry-ice/isomethylpentane, and serial sections (40μm) were obtained using a freezing microtome. Serial sections were used for immunostaining with anti- pTyr (4G10) antibody at a dilution of 1:1000, anti-Aβ (4G8) and anti-CD68 at a dilution of 1:500, anti-pSrc as 1:250, anti-GFAP antibody at a dilution of 1:1000, anti-A11 antibody at 1:250, O.C. antibody at 1:4000, and anti-I11 antibody at a dilution of 1:500 followed by incubation with biotinylated secondary antibodies (1:2000 dilution) (Vector laboratories Inc. Burlingame, CA) and avidin/biotin solution (Vector ABC kit). Immunoreactivity was visualized using visible light chromogens VIP, Vector Blue, and DAB (Vector Laboratories). The slides were

dehydrated and cover slipped using VectaMount (Vector Laboratories) following a standard dehydrating procedure through a series of ethanol solutions and Histo-Clear (National Diagnostics, Atlanta, GA). Images were taken using an upright Leica DM1000 microscope and Leica DF320 digital camera system. Figures were made using Adobe Photoshop 7.0 software. For quantitation purposes, 1.25X images were taken from 3 consecutive serial sections, (960μm apart) throughout the hippocampal region. Optical densities from the temporal cortex and CA1 regions from the same serial sections were measured using Adobe Photoshop software (Adobe Systems, San Jose, CA). All sections were immunostained at the same time to minimize background variability and background values in an unstained area of tissue for each section was set to zero using the curve tool before measuring optical density values. The optical density of the entire temporal cortex region/CA1 region from a representative section was selected via marquee. The same size marquee was applied to all sections across all conditions to allow comparison of optical densities independent of area changes. The values for each section were averaged (3sections/brain, 5-7 brains per condition) and plotted for Aβ, immunoreactivity for dasatinib infusion animals and Aβ and CD68 immunoreactivities for longitudinal study animals. For quantitating phosphotyrosine immunostaining for different aged APP/PS1 and wild type mice, the serial sections were viewed under a microscope and the number of 4G10 positive plaques were counted from the entire CA1 and temporal cortex regions for all the animals in each condition. The numbers of plaques were averaged (3 sections/brain, 5-7 brains per condition) and plotted.

Double Label Immunofluorescence

For double label immunofluorescence staining, tissue was incubated in the desired primary antibodies and then corresponding Texas red and FITC-conjugated secondary antibodies (Santa Cruz Biotechnology, Santa Cruz, CA). Tissue was counterstained with DAPI and visualized using a Zeiss LSM-510 META Confocal Microscope (Thornwood, NY).

Western Blot Analyses of Mouse Brains

Hippocampus and temporal cortex were removed from flash frozen brains of treated mice, lysed, sonicated in RIPA buffer, and quantitated using the Bradford method (Bradford, 1976). The lysates were resolved using a custom-built 28-well comb and 10% SDS-PAGE and transferred to polyvinylidene difluoride membranes for Western blotting using anti-pTyr (4G10), anti-APP, anti-Aβ (6E10), anti-GFAP, anti-TNF-α and anti-CD68 antibodies with α-tubulin as their loading control, anti-pSrc (Tyr 416), anti-pLyn (Tyr 396) antibodies with anti-Src and anti-Lyn as their respective loading controls and anti-PSD95 and anti-synaptophysin with βIII-tubulin as the loading control. Antibody binding was detected using enhanced chemiluminescence. Western blots were quantified using Adobe Photoshop software. Optical density (O.D.) of bands were normalized against their respective loading controls and averaged (+/-SEM).

Thioflavin Staining

Mouse brain sections from Aβ oligomer and vehicle infused animals were stained with thioflavin (0.1g/10mL) and counterstained with 4,6-diamidino-2-phenylindole (DAPI) (Invitrogen) to visualize the nucleus. To quench lipofuscin autofluorescence, the

sections were then incubated in 0.1% Sudan Black for 30 min, rinsed with PBS and cover slipped using PBS-glycerol (1:1).

Human Tissue Double Staining

Human tissue was obtained from University of Washington Alzheimer Disease Research Center (ADRC, NIH P50AG05136) and was sectioned via freezing microtome (40μm) for immunostaining using DAB or Vector Red (Vector Laboratories, Burlingame, CA, US) as the first chromogen. The sections were then stripped using 0.2N HCl, 5 min. and incubated with the second primary antibody for immunostaining using Vector Blue or Vector SG (Vector Laboratories) as the second chromogen.

T-maze

T-maze analysis was performed as described preciously (Wenk, 1998). Briefly, upon completion of the *in vivo* infusion period mice were placed into the starting arm, and the door was raised to allow animals to walk down the stem and choose an arm. Once the mice entered an arm with all four feet, they were returned to the starting arm and the door was closed. After 30 sec, the door was opened and the mice were allowed to choose an arm again. The process was repeated for 9 trials with a 30 sec interval between each trial. The choice of arms was noted each time and the number of alternations between trials for each mouse was averaged and plotted.

Dot Blot

To obtain a dose response curve for the LDDN drugs on BV2 cells, the cells were untreated (control), vehicle-treated, or treated with 0.0005 μM, 0.005 μM, 0.05 μM, 0.5 μM, 5 μM and 50 μM of the drug for 30 minutes. The cells were then lysed in RIPA containing protease inhibitor and Bradford quantified. Lysates were diluted with 3X

sample buffer, boiled, and stored in -20° for use. For dot blot analyses, PVDF membranes were prepared by first incubating in methanol solution for 5 minutes, and then soaking in Tris-Glycine solution for 10 minutes. The membranes were then placed into a dot blot apparatus and the apparatus was closed to create an air-tight seal for the vacuum to work. Using a narrow-mouth pipet, 2 microgram of lysate was blotted onto each well. After the loading was complete, the vacuum pump was turned on for 30sec-1min, to make sure all the solution was pulled through the membrane allowing protein to adhere. The membranes were then blocked in 3%BSA solution and incubated in anti-pTyr (4G10), anti-pLyn, anti-pSrc and anti-pERK antibodies with α-tubulin, Lyn, Src and ERK2 antibodies as loading controls overnight at 4°C. Blots were rinsed the next day and incubate in secondary antibodies and detected with enhanced chemiluminescence (GE Healthcare). Dot blots were quantified using Adobe Photoshop software. Optical densities of bands were normalized using appropriate loading controls and averaged (+/-) SD.

Statistical Analysis

Data are presented as mean +/− standard deviation. Values statistically different from controls were determined using one-way ANOVA. The Turkey-Kramer multiple comparisons post test was used to determine p values.

CHAPTER 3

OLIGOMERIC Aβ STIMULATES MICROGLIA THROUGH A TYROSINE KINASE MECHANISM

$A\beta_o$ oligomer stimulated increased total protein phospho-tyrosine levels in primary microglia cultures that were attenuated by a non-receptor tyrosine kinase inhibitor, dasatinib.

In order to characterize the form of Aβ oligomer used in our studies, we first performed a structural analyses of the prepared peptide. Preparations were separated via 15% SDS-PAGE to demonstrate that the major detergent resistant multimer of Aβ migrated with an apparent molecular weight loosely correlating with a trimeric/tetrameric form of the peptide that was stable even after incubation at 37 degree C (Fig. 5A). Larger amounts of loaded peptide demonstrated larger molecular weight multimers that were lesser species (Fig. 5A). This low molecular weight migration pattern correlates approximately with the multimeric confirmations of Aβ oligomers isolated from human cerebral cortex as well as cerebrospinal fluid in which dimer/trimer forms of Aβ have been the primary forms observed (Klyubin et al., 2008; Shankar et al., 2008; Villemagne et al., 2010; Shankar et al., 2011). This demonstrates that several detergent resistant species of oligomers are present in our preparation validating their use for subsequent cellular stimulations. In order to further confirm that the peptides were in a stable oligomeric conformation, dot blot analyses were performed after a period of 48h at 37 degree C. Oligomeric peptides were compared to fibrillar peptide. As expected, both

fibrils and oligomers were immunodetected with an anti-Aβ antibody 6E10 (Fig. 5B). However, only the oligomeric preparation was detected by the anti-oligomer antibody A11 (Kayed et al., 2003) (Fig. 5B).

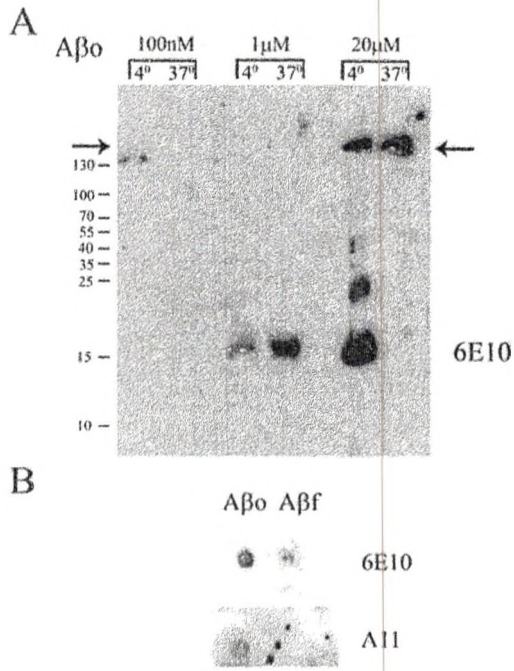

Figure 5. Structural characterization of Aβ1-42 oligomers ($Aβ_o$) and Aβ1-42 fibrils ($Aβ_f$). The peptide (**A**) $Aβ_o$ was prepared and stored overnight at 4 or 37 degree C to assess multimer stability. Increasing concentrations of peptide were separated by 15% SDS-PAGE and Western blotted with anti-Aβ antibody, 6E10. (**B**) Alternatively, prepared $Aβ_o$ and $Aβ_f$ were dot blotted (1μg each) onto PVDF and incubated with anti-Aβ antibody, 6E10, or anti-oligomer antibody, A11. Arrows indicate border between stacking and resolving gels for 6E10 Western blots.

We next determined the appropriate concentration of Aβo for stimulating microglia. Our prior studies demonstrated that oligomeric peptide was sufficient to

increase primary murine microglia total protein phospho-tyrosine levels although the concentrations employed were above the physiologic range and included a larger range of multimeric species in the preparation (Sondag et al., 2009). Primary murine microglia cultures were treated with varying concentrations of $A\beta_o$ for 5 minutes in order to assess the signaling response stimulated by peptide interaction. Oligomeric peptide stimulated an increase in total protein phospho-tyrosine levels (Fig. 6A) that was significantly different from controls even as low as 100nM (Fig. 6B). Importantly this concentration is similar to that reported from human CSF and human cell culture conditioned medium (Seubert et al., 1992; Podlisny et al., 1995).

Because different proteins are recognized with anti-phospho-tyrosine antibodies, it is very common to see different overall Western blot banding patterns with different concentrations of ligands and different time courses of stimulation since protein phosphorylation/dephosphorylation is dynamically regulated during all of the signaling events initiated during any acute stimulation. Indeed, as can be seen from Figure 6, some phospho-tyrosine immunoreactive bands steadily increase with dosage while others demonstrate a biphasic response. To further validate this point, we examined the changes of two specific tyrosine kinases in these experiments. The non-receptor tyrosine kinase, Src, was elevated in its active, phosphorylated form at 100nM $A\beta_o$ stimulation, while there was no change in the levels of active, Lyn kinase levels with either of the $A\beta_o$ doses (Fig.6B). Because of this complex dynamic change we focused on the concentration that provides a maximal change for overall tyrosine phosphorylation rather than any particular molecular weight species.

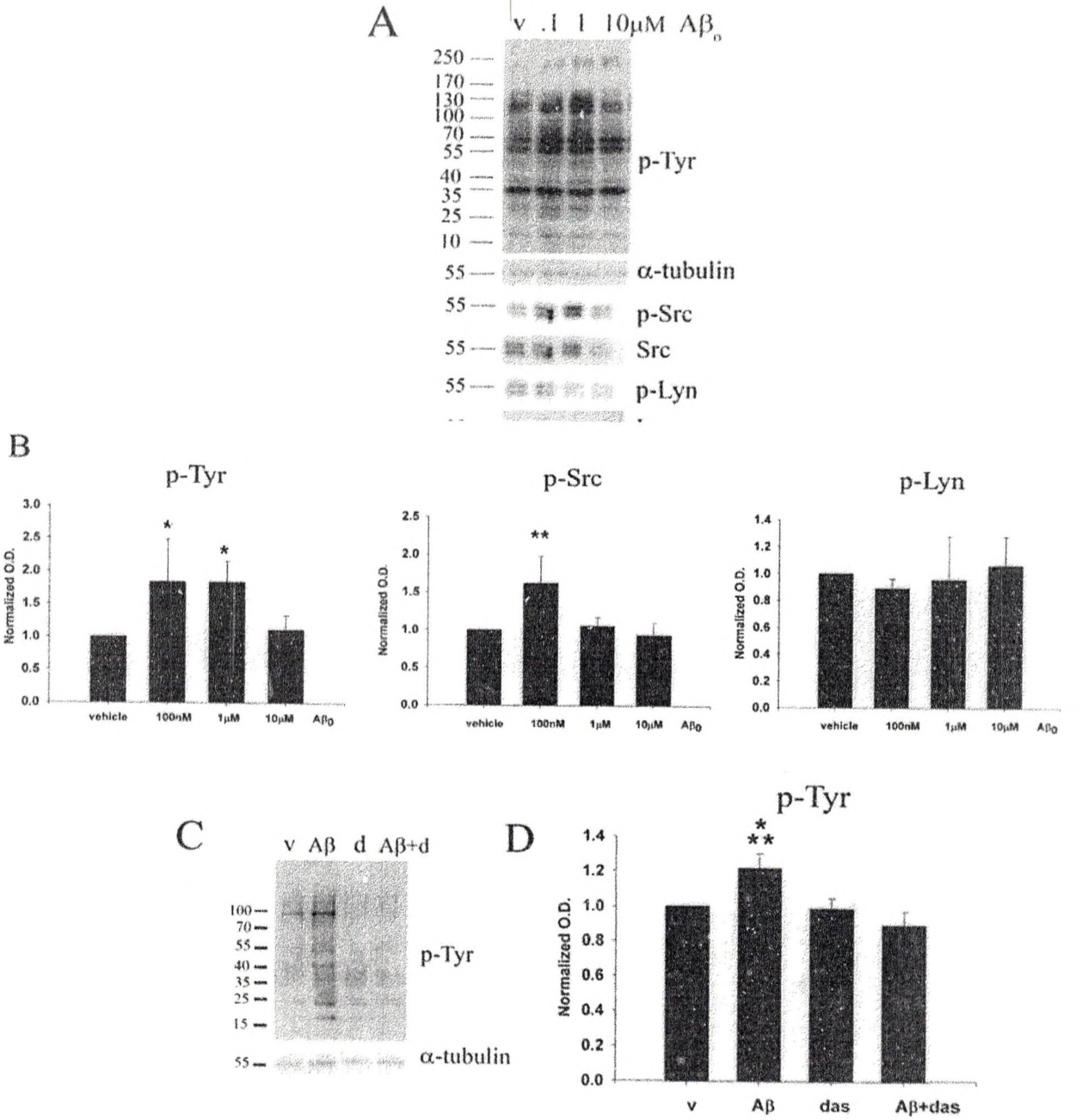
A
v .1 1 10μM Aβ0
250
170
130
100
70
55
40
35
25
10
p-Tyr
55
α-tubulin
55
p-Src
55
Src
55
p-Lyn
B
p-Tyr
Normalized O.D.
3.0
2.5
2.0
1.5
1.0
0.5
0.0
*
*
vehicle
100nM
1μM
10μM
Aβ0
p-Src
Normalized O.D.
2.5
2.0
1.5
1.0
0.5
0.0
**
vehicle
100nM
1μM
10μM
Aβ0
p-Lyn
Normalized O.D.
1.4
1.2
1.0
0.8
0.6
0.4
0.2
0.0
vehicle
100nM
1μM
10μM
Aβ0
C
v Aβ d Aβ+d
100
70
55
40
35
25
15
p-Tyr
55
α-tubulin
D
p-Tyr
*
**
Normalized O.D.
1.4
1.2
1.0
0.8
0.6
0.4
0.2
0.0
v
Aβ
das
Aβ+das

Figure 6. Oligomeric Aβ1-42 stimulated increased microglial protein phospho-tyrosine levels that were attenuated by the tyrosine kinase inhibitor, dasatinib. (**A**) Primary microglia were vehicle treated (v), or stimulated for 5 min with 0.1μM, 1μM and 5μM $A\beta_o$. Cell lysates were resolved by 10% SDS-PAGE and Western blotted using anti-phospho-Tyr (4G10), anti-pSrc, anti-pLyn antibodies or anti-α-tubulin, anti-Src and anti-Lyn (loading controls) antibodies. A Representative blot from 5 independent experiments is shown. (**B**) Densitometric analyses of the Western blots was performed normalizing protein phospho-tyrosine, pSrc and pLyn levels against their respective α-tubulin, Src and Lyn controls and averaging +/-SD. Percent fold changes in phospho-tyrosine levels were plotted (*$p< 0.05$ from vehicle). (**C**) Primary microglia were stimulated for 5 min with 1μM $A\beta_o$ with or without 30 min pretreatment with 100pM dasatinib (d). A representative Western blot from 3 independent experiments is shown. **(D)** Densitometric analyses of Western blots were performed for protein phosphotyrosine levels normalized to their respective α-tubulin control (*$p<0.05$ from vehicle and dasatinib, **$p<0.01$ from Aβ+dasatinib).

In order to determine whether this Aβ stimulated increase in protein phospho-tyrosine levels could be inhibited pharmacologically, a clinically relevant non-receptor tyrosine kinase Src/Abl inhibitor, dasatinib, was used to assess its ability to attenuate the oligomer stimulated change in total protein phospho-tyrosine levels (Shah et al., 2004; Das et al., 2006) (Fig.6C). As expected, dasatinib pretreatment attenuated the Aβo stimulated increase in total protein phospho-tyrosine levels (Fig. 6D). This data indicates that $A\beta_o$ is able to stimulate increased tyrosine kinase activity in primary murine microglia at physiologically relevant concentrations and this can be attenuated through the use of a non-receptor tyrosine kinase inhibitor, dasatinib.

$A\beta_o$ oligomer stimulated increased TNF-α secretion from primary microglia cultures

To assess cell viability in the presence of oligomeric Aβ for microglia, primary microglia cultures were treated with different doses of Aβo. The cells were then used for MTT assay to determine the toxicity levels. 10μM Aβo proved to be toxic to the cells as compared to control and vehicle treated microglia (Fig 7A). In order to determine whether the increase in tyrosine kinase activity was responsible for a change in secretory phenotype, microglia were stimulated with Aβ oligomers and fibrils with or without increasing concentrations of dasatinib for 24 hours. A concentration of 1μM $A\beta_o$ was used for the stimulations based upon the fact that a robust stimulatory change in protein phospho-tyrosine levels was observed with this concentration (Fig. 6A) as well as the toxicity data from MTT analyses of microglia cells (Fig. 7A). Both fibrillar and oligomeric Aβ stimulated a significant increase in TNF-α secretion that was attenuated in

a dose dependent fashion (Fig. 7B). Since dasatinib attenuated TNF-α secretion maximally at the lowest concentration employed, 100pM, this suggests that the drug concentration curve employed was already above the IC_{50} (Johnson et al., 2005). This data demonstrated that oligomer Aβ stimulated a proinflammatory cytokine secretory phenotype that was dependent upon propagation of the tyrosine-kinase based signaling response. The cell viability MTT reduction assay demonstrated that neither the peptide nor drug treatments were toxic to the microglia (Fig. 7C).

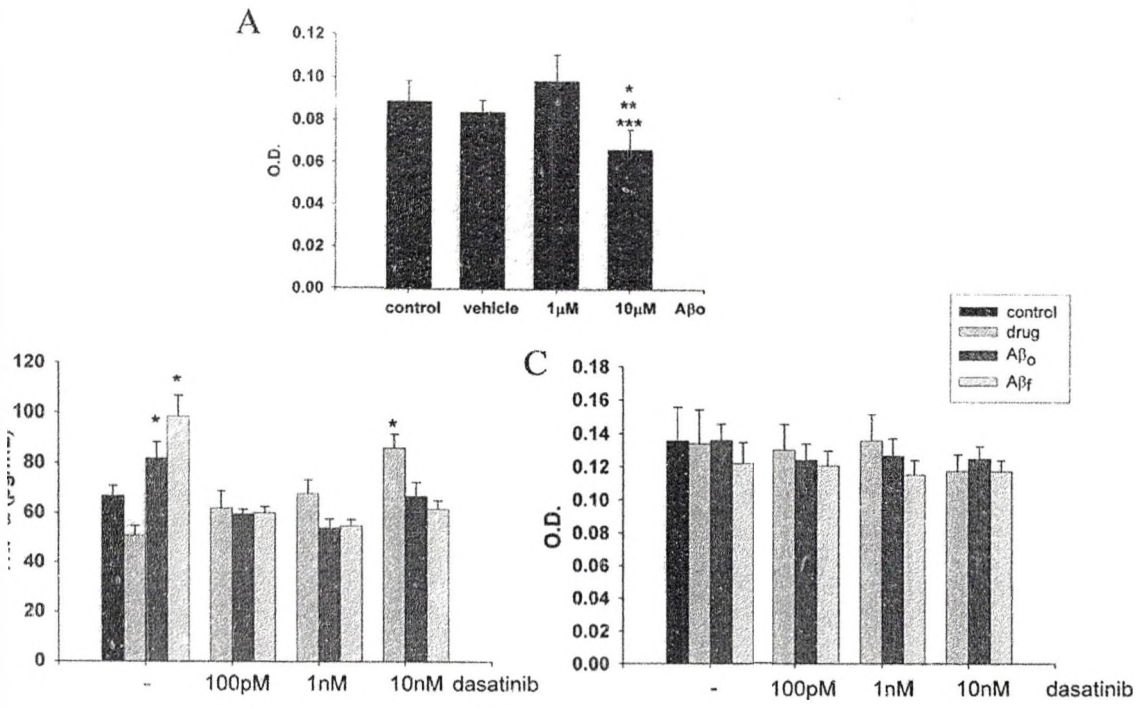

gure 7. Oligomeric Aβ1-42 stimulated increased microglial secretion of the oinflammatory cytokine, TNF-α, that was attenuated by dasatinib. (A) Primary croglia were untreated (control), vehicle treated, or stimulated with 1μM and 10μM o for 24 hr to assess cell viability using the MTT assay. Absorbance values 60/650nm) were averaged+/-SD. (*p<0.05 from vehicle). **(B)** Primary microglia were stimulated (control), DMSO vehicle treated (v), or stimulated for 24 hours with 1μM $_o$ or 10μM $A\beta_f$ in the presence/absence of 100pM, 1nM and 10nM dasatinib. Media s collected from treated cells and used to quantify changes in TNF-α secretion via ISA. Secreted values were averaged +/-SD (*p< 0.05 from control and vehicle). (**C**) er media removal, the treated cells were used to assess cell viability via the MTT uction assay. Absorbance values (560/650nm) were averaged+/-SD.

$A\beta_o$ oligomers stimulated tyrosine kinase dependent microgliosis in vivo

In order to validate the relevance of the *in vitro* findings, we next determined whether $A\beta_o$ could stimulate a tyrosine kinase associated microgliosis *in vivo*. $A\beta_o$ was intracerebroventricularly infused into the right lateral ventricle of 12 month old C57BL/6 mice for 14 days to stimulate gliosis in the absence or presence of co-administered dasatinib. $A\beta_o$ infused animals demonstrated a robust increase in microglial-like phospho-tyrosine immunoreactivity that spatially correlated with increased reactive microglial CD68 immunoreactivity (Fig.8A). Densitometric analysis of the immunostaining demonstrated that dasatinib significantly attenuated the $A\beta_o$-dependent increase in both phospho-tyrosine (Fig.8B) and CD68 (Fig. 8C) immunoreactivity. To validate the correlation between increased phosphotyrosine immunoreactivity and microgliosis, $A\beta_o$-infused tissue was double labeled using anti-phosphotyrosine (4G10) antibody and CD68 antibody, along with control brain sections. CD68-positive microglia co-localized with phosphotyrosine immunoreactivity in the Aβ-infused mouse brains (Fig. 8D).

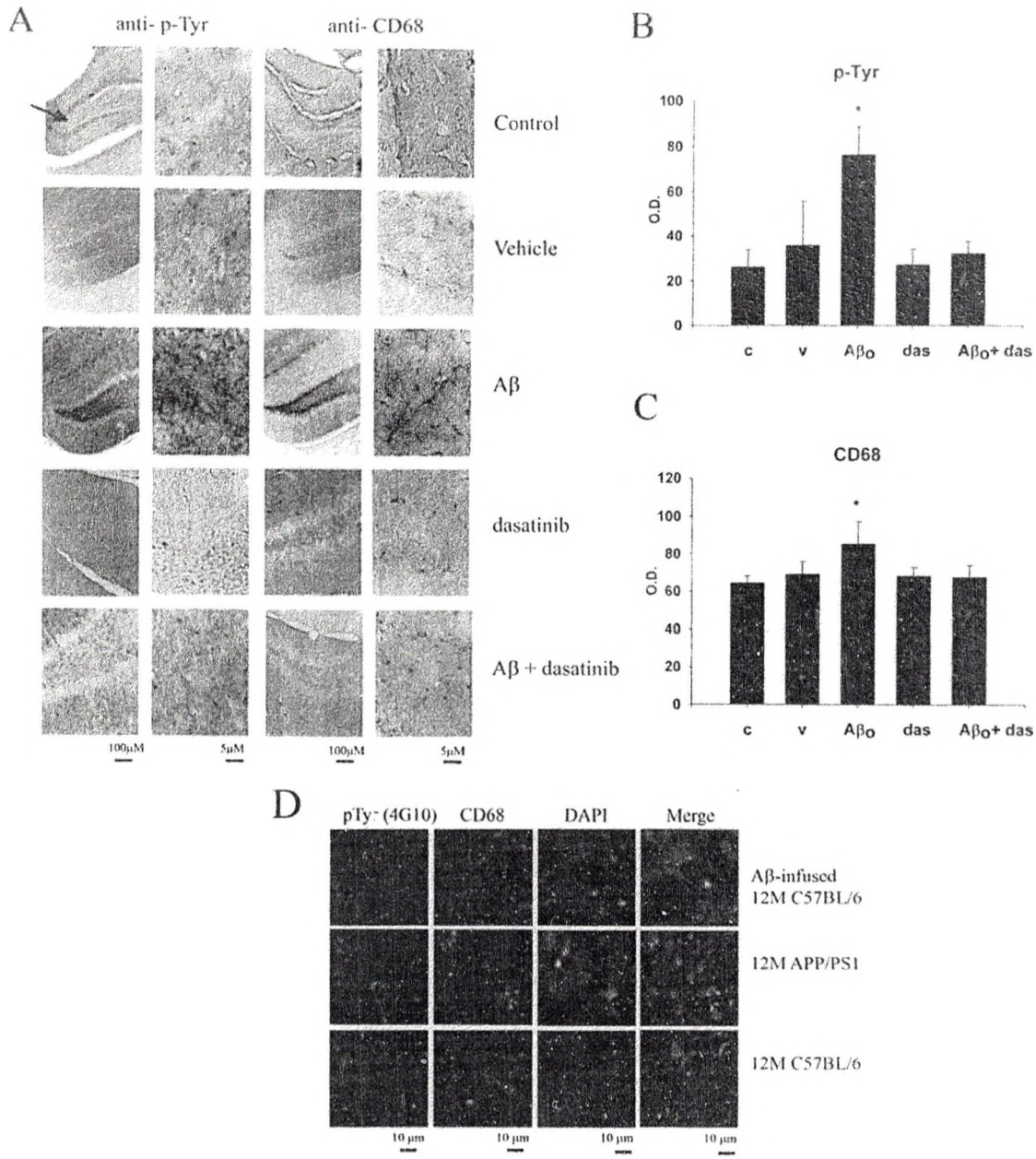

Figure 8. Intracerebroventricular infusion of oligomeric Aβ1-42 stimulated increased protein phospho-tyrosine and CD68 immunoreactivity that was attenuated by dasatinib. Aβ oligomer (1.2mg/day) or vehicle control (human HDL in artificial CSF) in the presence or absence of drug (500ng/kg/day) were infused into the right lateral ventricle of 12 month old male C57BL6/J mice for 14 days (n=6). Brains

were fixed, sectioned, and immunostained using anti-phospho-tyrosine (4G10) and CD68 antibodies. (**A**) Representative images from the dentate gyrus of the right hippocampus are shown. The arrow indicates the region imaged for the high magnification insets. Optical density (O.D.) of immunoreactivities for (**B**) phospho-tyrosine and (**C**) CD68 were quantified from serial sections of the CA1 region. (*$p < 0.001$ from c, v, dasatinib (das) and Aβ+dasatinib). (**D**) Aβ oligomer infused brains along with 12-month APP/PS1 and control mouse brains were double-immunostained using anti-phospho-tyrosine, 4G10 (red) and anti-CD68 (green) antibodies and counterstained with DAPI. Images shown are 40x magnification.

In order to compare this acute model of Aβ oligomer stimulated increase in protein phospho-tyrosine immunoreactivity to more chronic gliosis paradigms, microgliosis in infused brains was compared to that observed in a common transgenic mouse model of AD. This particular APP/PS1 model is a double transgenic line that expresses chimeric mouse/human amyloid precursor protein (Ms/Hu APPswe) and a mutant human presenilin 1 (PS1dE9), allowing the mice to secrete human Aβ peptide. This mouse model of AD shows a progressive increase in Aβ deposition with age (Garcia-Alloza et al., 2006). As expected, CD68 positive microglia in this model but not C57BL/6J controls correlated with increased phospho-tyrosine immunoreactivity (Fig. 8D). This demonstrated that elevated phosphotyrosine immunoreactivity was a common presentation of reactive microglia across disease model paradigms including both acute and transgenic models.

However, it was not clear whether the phospho-tyrosine immunoreactive, activated microglia in the Aβ oligomer infused brains correlated with oligomeric Aβ

deposition. In order to determine whether microgliosis in the infusion model correlated with oligomeric Aβ deposits, immunohistochemical analyses of Aβ in infused brains was performed. Staining with the anti-Aβ antibody, 4G8, demonstrated immunoreactivity (Fig. 9A) broadly correlating with the same localization pattern of CD68 and phospho-tyrosine immunoreactivity observed in the peptide infused animals (Fig 8A). To determine whether the infused, immunodetected Aβo had remained oligomeric rather than converting to fibrils, sections of treated brains were stained using anti-oligomer antibodies, A11 and I11 to detect oligomeric species. Both A11 and I11 antibodies demonstrated positive immunoreactivity in the $A\beta_o$ infused brains compared to vehicle-infused and control animals (Fig. 9B). This was supported by the fact that $A\beta_o$ infused animals were negative for thioflavin staining and comparable to the vehicle treated group, suggesting that the immunodetected Aβ in infused brains had not fibrillized (Fig. 9C). To further validate the use of anti-oligomer antibodies at recognizing non-fibril confirmations in situ, again, the transgenic APP/PS1 model was used. Immunostaining of brains from 12 month old animals demonstrated robust immunoreactivity with anti-fibril antibody, OC, compared to control animals (Fig. 9D). However, abundant immunoreactivity of non-fibril, oligomeric Aβ was also observed using A11, anti-oligomer antibody in these brains. Indeed, although OC and A11 immunoreactivity co-localized to the same plaque structures, each antibody often displayed unique immunoreactivities within plaques (Fig. 9D). This not only indicates that plaques contain heterogeneous Aβ conformations but also suggests that anti-oligomer antibodies are useful for immunodetecting peptide conformations in situ, particularly in the infusion model employed.

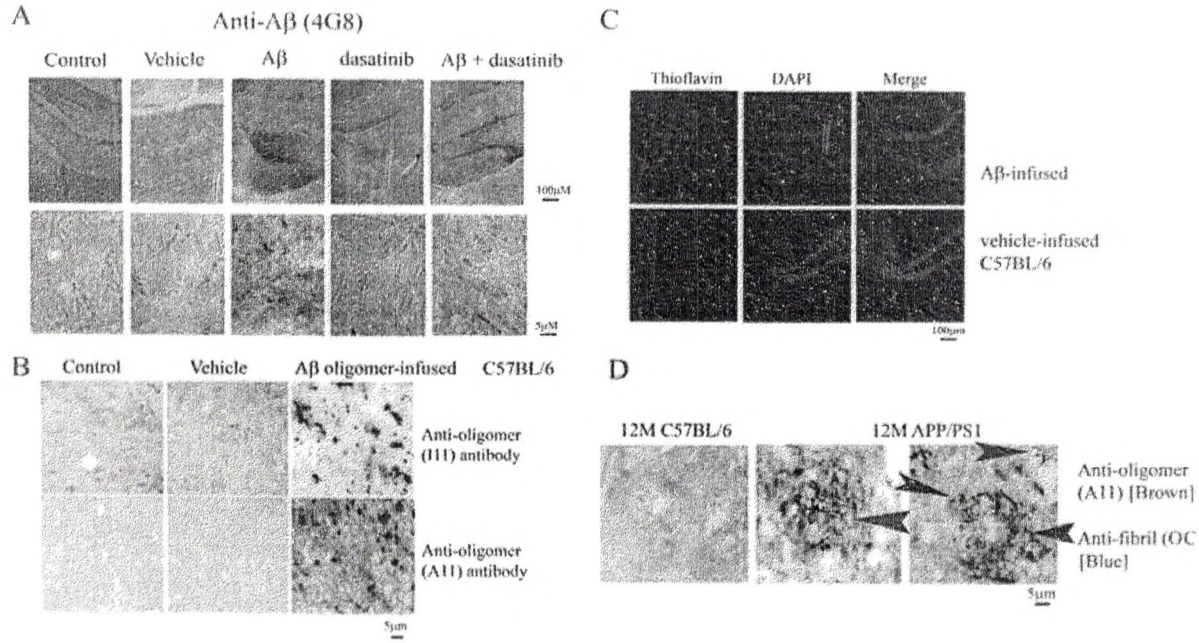

Figure 9. Brains of Aβ oligomer-infused animals were thioflavin negative but displayed immunoreactivity with anti-Aβ, 4G8, and anti-oligomer, A11 and I11 antibodies. **(A)** Brains from wild-type control, vehicle-infused, and Aβ oligomer-infused animals (+/-) dasatinib were immunostained with anti-Aβ (4G8) antibody. Representative images from the dentate gyrus of the right hippocampus are shown. **(B)** Brains were also immunostained with anti-oligomer antibodies, A11 and I11, to detect infused peptide. Representative images of control, vehicle-infused, and Aβ oligomer-infused animals are shown. **(C)** Brains from vehicle-infused and Aβ oligomer- infused C57BL/6J mice were stained with thioflavin to identify the presence of any fibrils and counterstained with DAPI as a nuclear stain and Sudan black to quench autofluorescence. Representative images from the dentate gyrus are shown from 6 animals per group. **(D)** Brains from 12 month old C57BL/6J control and APP/PS1 mice were immunostained with A11 and OC antibodies to visualize fibrillar and oligomeric Aβ peptide deposition. Representative

double label with A11 (brown) and OC (blue) is shown. Arrows indicate only A11 immunoreactivity (brown), only OC immunoreacitvity (blue) and co-localization (black).

AD brains demonstrated increased protein phospho-tyrosine, Aβ, and active Src kinase levels compared to age matched controls

To further establish the correlation between Aβ oligomer levels and tyrosine kinase dependent microgliosis during disease, we compared human AD tissue with age matched non-demented controls. As seen in the *in vitro* and *in vivo* rodent data, examination of temporal cortex from human AD brains demonstrated a significant increase in overall protein phospho-tyrosine levels (Fig. 10A,B). This correlated with a significant increase is phosphorylated active forms of the tyrosine kinase, Src, as well as Lyn kinase, in diseased brains versus their corresponding age- matched controls suggesting that the protein phospho-tyrosine changes could be related to increased activity of the Src family of kinases (Fig. 10C,D). AD and control tissue lysates were also analyzed via Western Blot analyses to examine levels of multimeric forms of Aβ oligomers. Densitometric analysis of the multimeric SDS-stable species (Fig. 5A) demonstrated that AD brains had a significantly higher level than age-matched controls (Fig. 10A,B) correlating well with the changes in protein phospho-tyrosine, active Src and active Lyn levels.

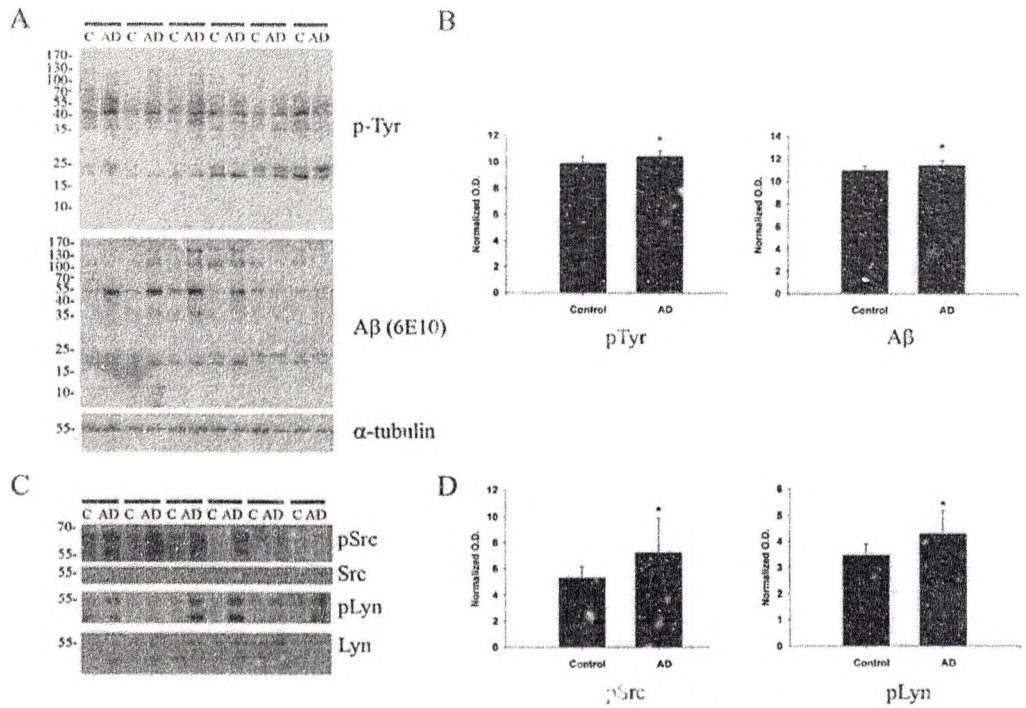

Figure 10. AD brains had elevated protein phospho-tyrosine, active phospho-Src and phospho-Lyn levels compared to age-matched controls. AD and age-matched control (c) temporal lobe lysates (n=6) were resolved by 10% SDS-PAGE and Western blotted using (**A**) anti phospho-Tyr (4G10), anti-Aβ (6E10), anti-α-tubulin (loading control) antibodies, (**C**) anti-Lyn, anti-phospho-Lyn (Tyr396), anti-Src, and anti-phospho-Src antibodies. Optical density of (**B**) Total phospho-Tyr or Aβ multimers and (**D**) pLyn and pSrc from 6 AD and age-matched control brain blots were normalized to their respective α-tubulin blots or total protein levels (Lyn/Src) then averaged and graphed (+/-SD). (*$p < 0.001$)

In order to verify whether the changes in protein phospho-tyrosine and Aβ oligomers correlated with microglial activation in the AD brains, immunostaining of fixed AD tissue was compared to age-matched controls. As expected, AD brains demonstrated defined, plaque-like deposits that were immunoreactive with the anti-oligomer (A11) antibody (Fig. 11A). Although A11 positive deposits were not uniformly associated with activated microglia there were clear instances of HLA-DR (LN3) positive activated microglia directly associated with oligomeric deposits (Fig. 11A). This supported the *in vitro* (Fig. 7) and *in vivo* (Fig. 8) rodent observations of the ability of oligomeric Aβ to stimulate microglia and suggested that a similar activation occurs during disease. To further support the rodent observations, the AD and control brain sections were immunostained to determine whether HLA-DR positive, reactive microglia demonstrated increased protein phospho-tyrosine levels indicative of increased tyrosine kinase activity. AD brains demonstrated increased immunostaining for reactive microglia compared to age-matched controls (Fig. 11B). More importantly, reactive HLA-DR positive microglia co-localized with anti-phospho-tyrosine immunoreactivity in both diffuse and clustered cell patterns supporting the idea that tyrosine kinase-dependent changes were a component of the microglial activation process during disease (Fig. 11B).

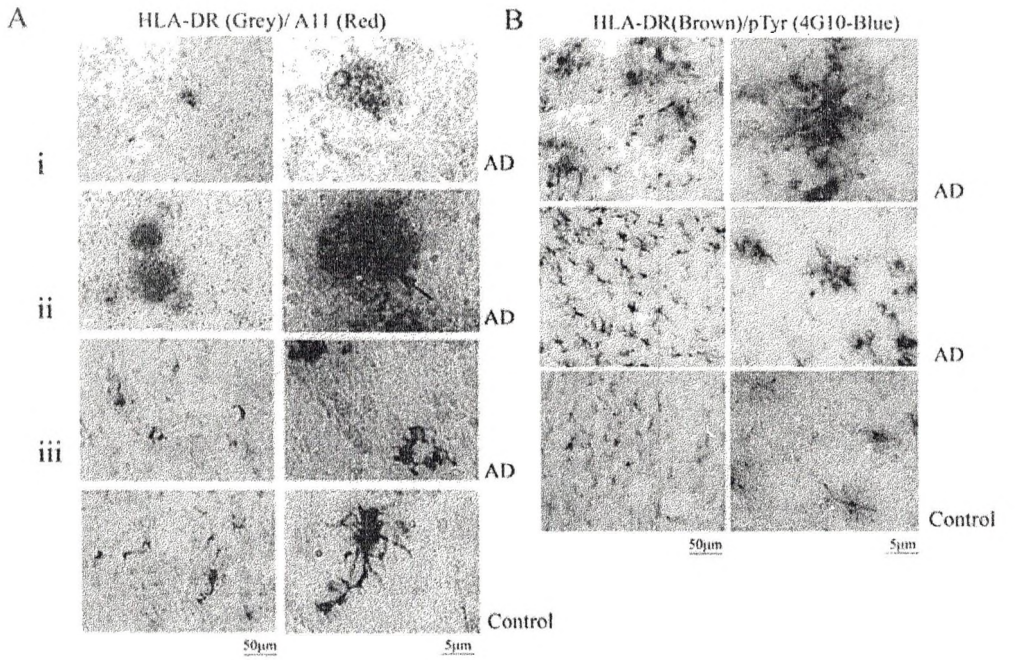

Figure 11. A population of AD brain microglia was phospho-tyrosine immunoreactive and localized to Aβ oligomers. AD and control (c) temporal lobe sections were immunostained using anti-HLA-DR antibody to identify microglia, anti-oligomer antibody, A11, to visualize prefibril peptide, and anti-phospho-Tyr (4G10) antibodies. (**A**) A11/HLA-DR double label is shown with (i) only A11 (red) immunoreactivity, (ii) double label (black arrow) and (iii) only HLA-DR (grey) immunoreactivity in the AD brain. (**B**) A double label for HLA-DR (brown)/phospho-Tyr (blue) is also shown. Images are representative of three cases each.

HLA-DR positive microglia from AD brains displayed increased immunoreactivity for active, phosphorylated Src and Lyn kinases.

To begin identifying the specific enzymes responsible for the increased protein phospho-tyrosine levels, additional immunostaining of activated microglia in AD versus age-matched control brains was performed. Based upon the Western blot analysis of increased levels of active phosphorylated Src in AD brains (Fig. 10) immunostaining of active Src was again compared to the related family member, Lyn. Double label immunostaining using anti-HLA-DR to identify reactive microglia verified that a heterogeneous portion of the activated microglia also demonstrated increased phosphorylated, active Src immunoreactivity compared to age-matched control brains (Fig. 12A). A small amount of reactive microglia in AD versus control brains also demonstrated immunoreactivity for phosphorylated active, Lyn (Fig. 12C). The immunostaining correlated well with the Western blot analysis changes (Fig. 10) and supported the idea that tyrosine kinase-dependent activation of microglia occurred in AD brains involving at least the non-receptor kinase, Src. Immunofluorescence and confocal imaging confirmed the colocalisation of reactive microglia (using HLA-DR antibody) and active Src immunoreactivity (Fig. 12B) as well as active Lyn immunoreactivity (Fig. 12D)

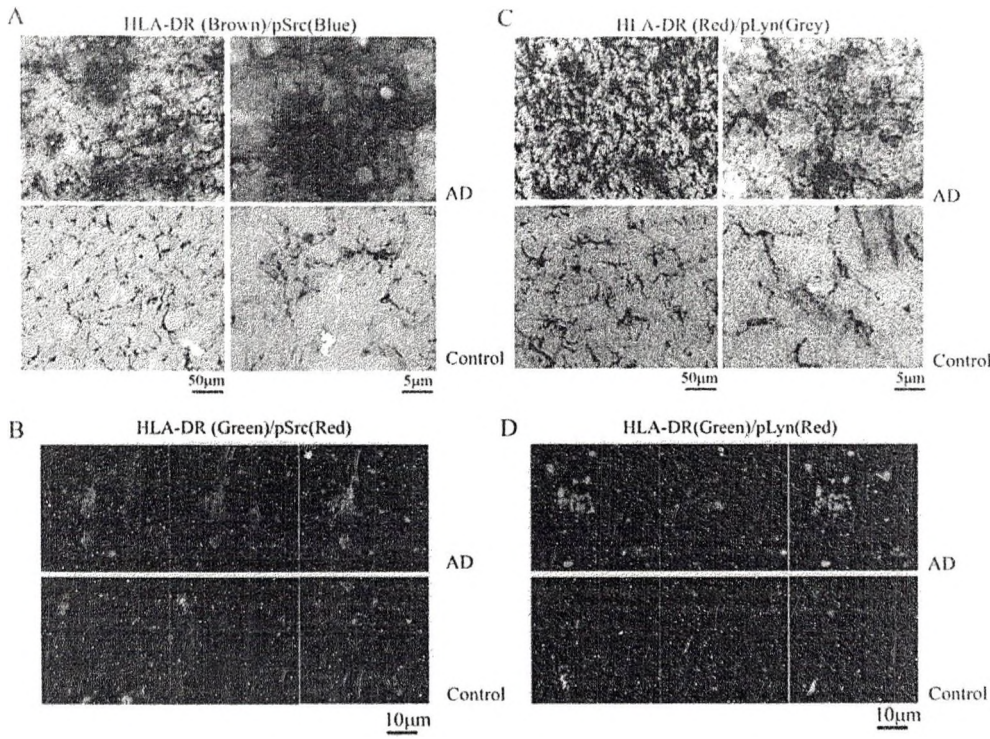

Figure 12. A population of AD brain microglia was immunoreactive for phospho-Lyn and phospho-Src. AD and control temporal lobe sections were immunostained using anti-HLA-DR antibody to identify microglia, anti-phospho-Lyn-396 antibody to identify activated Lyn kinase and anti-phospho-Src antibody to identify activated Src kinase. (**A**) p-Src (blue)/HLA-DR (brown) double label and (**C**) p-Lyn (grey)/HLA-DR (red) double label images are shown. Images are representative of three cases each. AD and control temporal lobe sections were also double-labeled using immunofluorescence using **(B)** anti-HLA-DR (green) and anti-pSrc (red) antibodies or **(D)** anti-HLA-DR (green) and anti-pLyn (red) antibodies.

CHAPTER 4

ROLE OF SRC KINASE IN AMYLOID DEPENDENT MICROGLIOSIS IN AD

Based upon our prior work demonstrating that both fibrillar and oligomeric Aβ stimulate increased non-receptor tyrosine kinase activity in microglia (Sondag et al., 2009), we determined whether a brain penetrant tyrosine kinase inhibitor, dasatinib, could attenuate activity of Src kinase *in vitro.*

The non-receptor tyrosine kinase inhibitor, dasatinib, decreased active-phospho Src levels in microglia BV2 cells

In order to validate the Src-kinase inhibitory ability of dasatinib, the mouse microglia cell line, BV2, was treated with varying concentrations of dasatinib. Dasatinib is a small molecule ATP-competitive inhibitor of BCR/Abl and Src kinase with IC50s for the isolated kinases of 0.55 and 3.0 nM, respectively (Lombardo et al., 2004; Nam et al., 2005). FDA approved for use in cases of Chronic Phase Philadelphia chromosome-positive Chronic Myelogenous Leukemia (CP-CML), dasatinib (Sprycel, Bristol-Myers Squibb), has been shown to the cross the blood brain barrier (Porkka et al., 2008). As expected, active, phosphorylated Src levels significantly decreased with increasing dasatinib concentrations from 1nM to 1μM compared to vehicle treated BV2 cells (Fig.13). For subsequent treatments of microglial cells *in vitro*, a dose of 100nM dasatinib was chosen to obtain an optimum effect of Aβ-dependent tyrosine kinase inhibition in primary cultures.

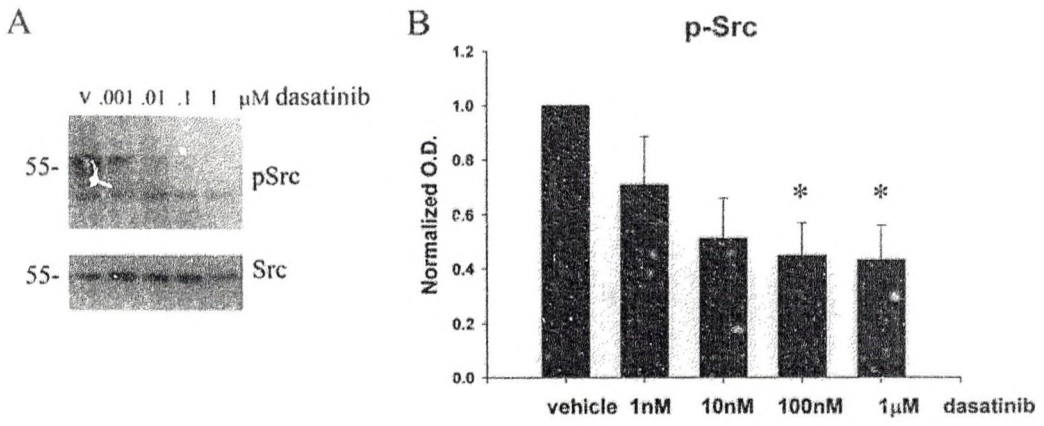

Figure 13. Dasatinib dose-dependently attenuated active, phospho-Src kinase levels in the BV2 cell line. (A) Microglial BV2 cells were vehicle treated (v), or treated with 1nM, 10nM, 100nM and 1μM dasatinib for 30 min. Cells lysates were resolved by SDS-PAGE and Western blotted using anti-phospho-Src, and Src antibodies. **(B)** Densitometric analyses of the Western blots were performed normalizing active-pSrc levels against their respective Src controls and averaging +/-SEM. Blots are representative of 6 independent experiments.

Dasatinib attenuated the Aβ-stimulated increase in active-phospho Src levels in primary murine microglia cultures

In order to determine whether dasatinib was able to reduce an Aβ stimulated increase in active tyrosine kinase levels, primary microglia cultures were treated with Aβ fibril with or without dasatinib. Microglial cells were pretreated with 100nM dasatinib followed by 5 minute stimulation by 10μM $A\beta_f$ to detect changes in the activated, phosphorylated forms of the specific non-receptor tyrosine kinases, Src and Lyn. As expected, Aβ fibrils stimulated an increase in active-phospho Src levels compared to vehicle treated cells (Fig. 14). The Aβ-dependent increase in phospho-Src levels was significantly attenuated when cells where stimulated in the presence of dasatinib (Fig. 14). Although Aβ fibrils did not significantly increase the levels of active, phosphorylated Lyn kinase at the concentrations used, dasatinib was still able to significantly reduce levels of active phospho-Lyn indicating that the drug was not specific to any particular Src family member (Fig 14). In addition, the data demonstrated that the Aβ stimulated increase in microglial active Src kinase levels could be inhibited using a clinically relevant non-receptor tyrosine kinase Src/Abl inhibitor, dasatinib.

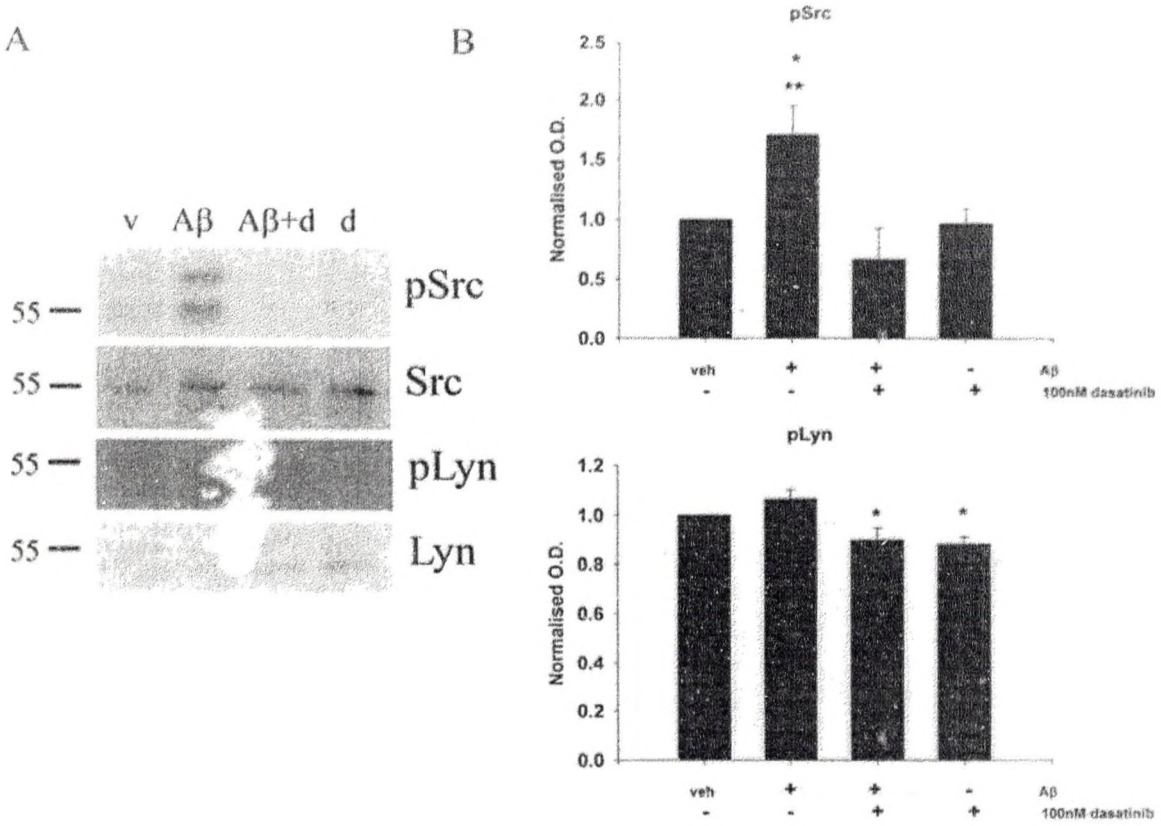

Figure 14. Dasatinib attenuated an Aβ-stimulated increase in active, phospho-Src kinase levels in primary microglia cultures. (**A**) Primary microglia were vehicle treated (v,veh), or stimulated for 5 min with 10μM $A\beta_f$ in presence or absence of 30 min pretreatment of 100nM dasatinib. Cells lysates were resolved by 10% SDS-PAGE and Western blotted using anti-pSrc or Src (loading control) antibodies and anti-pLyn or Lyn (loading control) antibodies. A Representative blot from 6 independent experiments is shown. (**B**) Densitometric analyses of the Western blots was performed normalizing active, phospho-Src levels against Src control and active, phospho-Lyn levels against Lyn control and averaging +/-SE. Percent fold changes in phospho-Src levels were plotted. (*$p<0.05$ vs. vehicle, dasatinib, **$p<0.01$ vs. Aβ+dasatinib for pSrc and *$p<0.01$ vs. Aβ for pLyn)

Dasatinib attenuated Aβ-stimulated TNF-α secretion in primary microglia cultures

In order to determine whether the Aβ-stimulated change in active Src levels was required for changes in phenotype, changes in secretion of the pro-inflammatory cytokine, TNF-α, was quantified from the primary microglia cultures in the presence or absence of dasatinib. Fibrillar Aβ stimulated a significant increase in TNF-α secretion compared to control or vehicle treated microglial cells (Fig. 15). This increase in TNF-α secretion was attenuated by 100nM pretreatment of dasatinib with no effect on cellular viability (Fig. 15). The data demonstrated that inhibition of Src family kinase activity was sufficient to prevent microglia from acquiring a reactive secretory phenotype upon Aβ fibril stimulation *in vitro*.

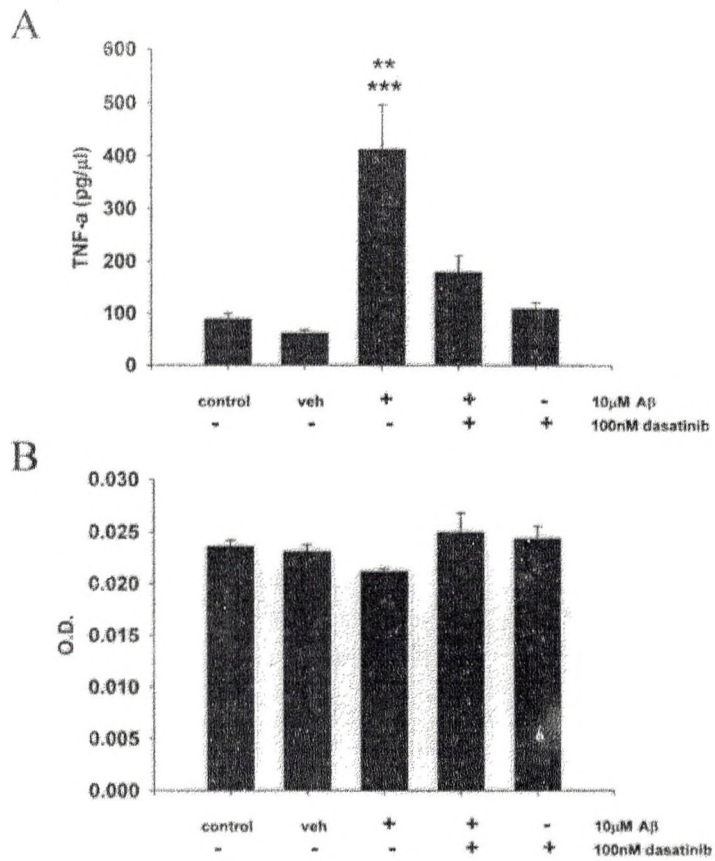

Figure 15. Dasatinib attenuated Aβ1-42 stimulated-microglial secretion of the proinflammatory cytokine, TNF-α. Primary microglia were unstimulated (control), DMSO vehicle treated (veh), or stimulated for 24 hours with 10μM $A\beta_f$ in the presence/absence of 100nM dasatinib. (**A**) Media was collected from treated cells and used to quantify changes in TNF-α secretion via ELISA. Secreted values were averaged +/-SE. (**B**) After media removal, the treated cells were used to assess cell viability via the MTT reduction assay. Absorbance values (560/650nm) were averaged+/-SE. (**p< 0.01 from control, ***p<0.001 vs veh,dasatinib and Aβ+dasatinib).

An age-dependent increase in Aβ plaque density correlated with microgliosis in a transgenic mouse model of AD

To determine an appropriate age *in vivo* for examining increased tyrosine kinase activity and Aβ-associated microgliosis, a transgenic APP/PS1 mouse model of AD was used. Brains of varying aged APP/PS1 mice were compared to age-matched controls to validate the use of this transgenic mouse model for our study. The APP/PS1 mice were collected at 2, 4, 6 and 12 months of age along with their age-matched wild type (C57BL/6) mice and brains were sectioned for histology. Immunostaining demonstrated a significant increase in APP/PS1 temporal cortex CD68 immunoreactivity in 6 and 12 month old mice compared to the earlier 2 and 4 month APP/PS1age groups and their age-matched C57BL/6 controls (Fig. 16). This increase correlated precisely with increased plaque-associated Aβ immunoreactivity in the 6 and 12 month old APP/PS1 mice (Fig. 16). Analyses of hippocampi from all groups showed similar results to the temporal cortex (data not shown). These data supported the notion that microglial activation in AD and its mouse models may be a consequence of Aβ fibril interaction. However, to validate an involvement of tyrosine kinase activity in microglial phenotype changes during disease, APP/PS1 brains were next immunostained with anti-phosphotyrosine antibody as an indirect method to assess overall tyrosine kinase activity changes. Immunostaining mouse brains with anti-phosphotyrosine antibody, 4G10, demonstrated positive microglial-like as well as neuronal-like immunoreactivity (Fig.17). Counting plaque-associated 4G10 positive staining as putative microglia demonstrated a trend of age-associated increase in APP/PS1 temporal cortex staining with a significant increase by 4 months of age with significantly higher immunoreactivity at 6 and 12

months (Fig. 17). Similar trends were observed in the hippocampus (data not shown). These data validated that by 12 months of age, this particular transgenic line had robust phosphotyrosine microglial reactivity in association with Aβ plaques providing us with the appropriate time point for use.

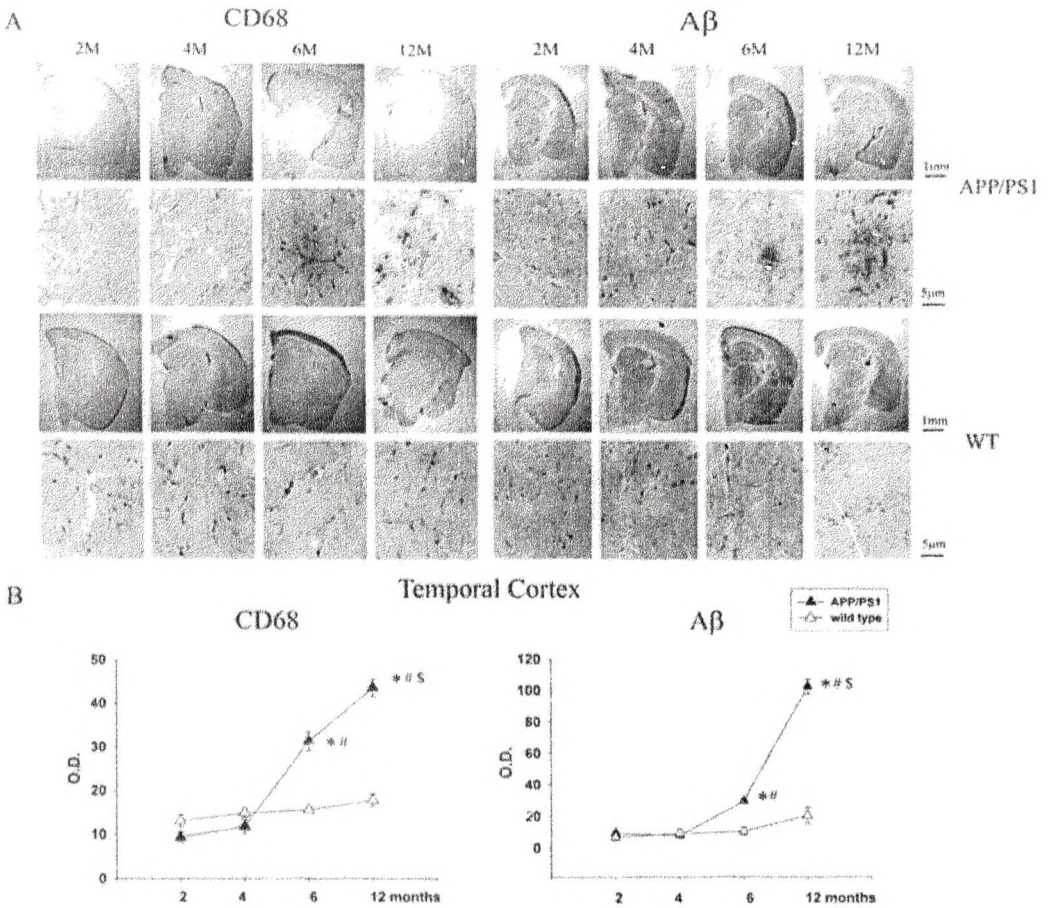

Figure 16. Microgliosis in the APP/PS1 model of AD positively correlated with increased Aβ plaque density. Serial coronal sections from 2 month, 4 month, 6 month and 12 months old control (C57BL/6) animals and age-matched transgenic animals (APP/PS1) (n=6) were immunostained for **(A)** activated microglia (anti-CD68) and Aβ (anti-4G8 antibody) plaques. Representative hemi sections are shown with select high magnification panels. **(B)** Immunoreactivity densities from the temporal cortex region for CD68 and 4G8 were quantified, averaged and graphed (+/-SE) *$p< 0.001$ from 2 and 4 month APP/PS1 animals, $^{\#}p<0.001$ from 2, 4, 6 and12 month wild type animals for CD68, $^{\#}p<0.001$ from 2, 4, 6 month wild type mice for 4G8, and $^{\$}p<0.001$ from 6 month APP/PS1 animals.

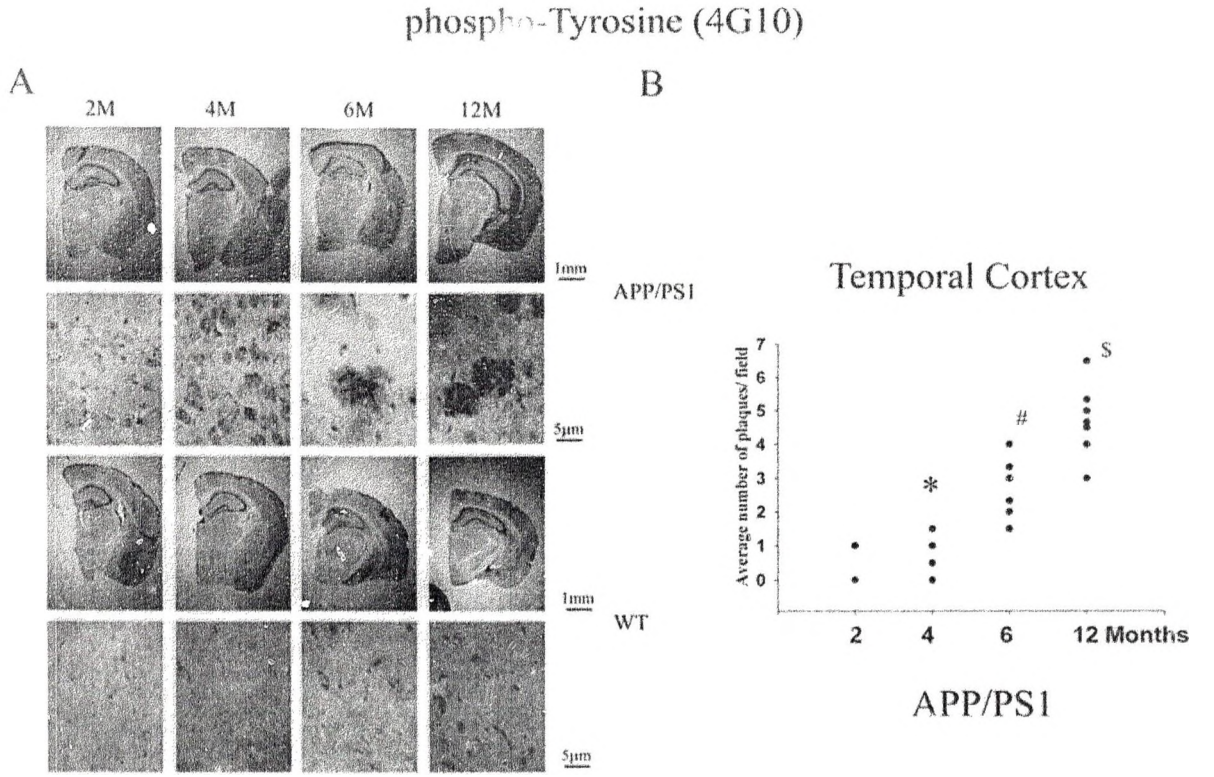

Figure 17. There was an age-dependant increase in total phospho-tyrosine immuno-positive plaques in a transgenic mouse model of AD (APP/PS1). (A) Serial coronal sections from 2 month, 4 month, 6 month and 12 months old control (C57BL/6) animals and age-matched transgenic animals (APP/PS1) (n=6) were immunostained using phospho-tyrosine antibody (4G10). **(B)** To omit the inclusion of neuronal phosphotyrosine staining, 4G10 positive plaques were counted from the temporal cortex and the hippocampus regions and averaged and graphed (+/-SE) *$p<0.001$ from 2 month APP/PS1 mice, $^{\#}p<0.001$ from 2 month and 4 months APP/PS1 animals, $^{\$}p<0.001$ from 2, 4 and 6 month APP/PS1 animals.

Dasatinib infusion decreased phospho-Src but not phospho-Lyn levels in APP/PS1 mice

Based upon the temporal profiling of microgliosis we next determined whether inhibition of tyrosine kinase activity could attenuate the microglial reactivity in this line. Based upon our *in vitro* data we hypothesized that dasatinib treatment would attenuate the Aβ-associated increase in tyrosine kinase activity, particularly Src, and subsequent inflammatory changes in the mice. In order to answer this question, 13 month old APP/PS1 female mice were sub-cutaneously infused with dasatinib for 28 days. Dasatinib infusion significantly decreased protein phosphotyrosine levels in the hippocampus but not the temporal cortex compared to vehicle infused control animals (Fig. 18). More importantly, dasatinib infusion significantly decreased levels of active, phospho-Src in both temporal cortex and hippocampus compared to vehicle treated mice (Fig. 18). However, dasatinib infusion had no effect on the active, phosphorylated levels of the related Src family member, Lyn kinase, demonstrating some specificity of the drug (Fig. 18). These data demonstrated that a subcutaneous route of dasatinib delivery was able to inhibit levels of active Src in the brains of the APP/PS1 mice.

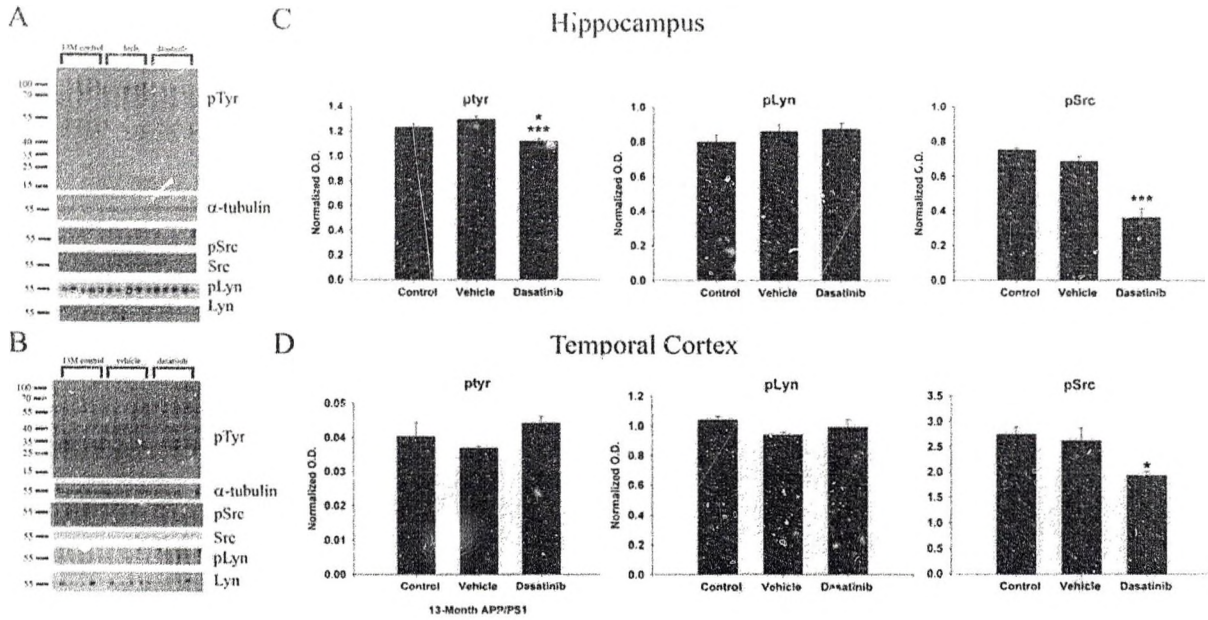

Figure 18. Dasatinib infusion reduced protein phosphotyrosine and active phospho-Src kinase levels in APP/PS1 brains *in vivo*. Vehicle or dasatinib (500ng/kg/day) was infused sub-cutaneously into 13-month old APP/PS1 for 28 days (n=7). Hippocampus and temporal cortex regions were dissected from the left hemispheres and flash frozen for protein analyses. The frozen tissue was lysed in RIPA with protease inhibitor. **(A)** Hippocampal and **(B)** temporal cortex brain lysates from control (13 month APP/PS1), vehicle infused, and dasatinib infused animals were used for Western blot analyses using pTyr (4G10), pSrc, pLyn, α-tubulin, Src, and Lyn antibodies. **(C)** Optical densities were averaged and graphed (+/-SEM) for hippocampus *$p < 0.05$, ***$p < 0.001$ from control and for **(D)** temporal cortex *$p<0.05$ from control.

Dasatinib infusion decreased TNF-α levels and microgliosis in APP/PS1 mice

Based upon the encouraging findings that dasatinib was able to exert brain effects and inhibit active Src levels we expected that dasatinib infusion should also attenuate microgliosis and TNFα secretion as observed in our *in vitro* findings. Dasatinib infusion significantly decreased TNFα levels in both the hippocampus and temporal cortex correlating with the decrease in active Src levels and demonstrating a clear brain anti-inflammatory effect of the drug (Fig. 19). Moreover, levels of CD68, the reactive microglial marker protein, were significantly decreased in the hippocampus of dasatinib infused brains but not the temporal cortex. This data demonstrated that dasatinib inhibition of brain active Src levels correlates with a significant anti-inflammatory, microglial-inhibitory effect in APP/PS1 mice. Interestingly, these effects appeared most robust in the hippocampus compared to the temporal cortex (Fig. 18,19).

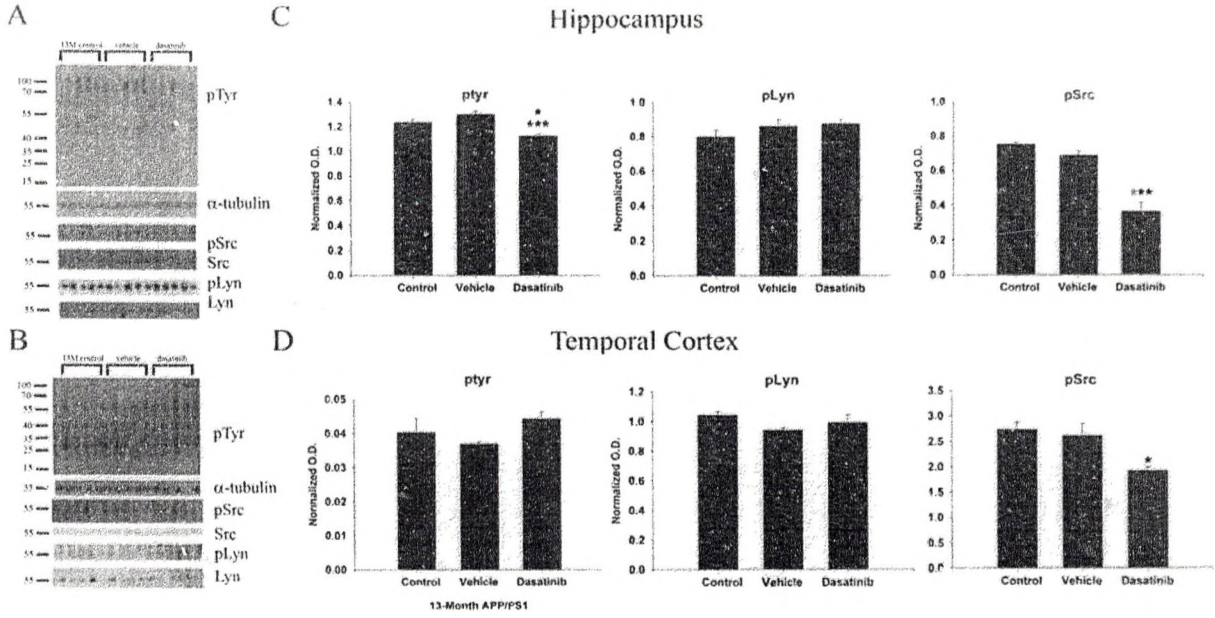

Figure 19. Dasatinib infusion reduced CD68 and TNF-α protein levels in hippocampus of 13 month old APP/PS1 brains *in vivo*. **(A)** Hippocampal and **(B)** temporal cortex brain lysates from control (n=7), vehicle (n=6), and dasatinib infused animals (n=7) were used for Western blot analyses for activated microglia (using CD68 antibody) and pro-inflammatory cytokine TNF-α (anti-TNF-α antibody) antibodies with α-tubulin as the loading control. **(C)** Optical densities were averaged and graphed (+/- SEM) for hippocampus **p< 0.01 from controls and **(D)** temporal cortex *p<0.05 from controls.

Dasatinib infusion did not alter APP, Aβ, or synaptic protein levels in APP/PS1 mice

To examine the breadth of changes that might result from dasatinib infusion we also determined whether adverse effects on neurons, astrocytes, or Aβ deposition resulted from drug treatment in addition to the anti-inflammatory, microglial-inhibitory changes. However, dasatinib administration had no effect on either total APP levels or Aβ levels in the hippocampus or temporal cortex of treated mice compared to vehicle controls (Fig. 20). In addition, dasatinib treatments did not increase levels of the reactive astrocyte marker protein, GFAP, in the infused animals compared to vehicle control mice (Fig. 8). Finally, dasatinib treatment did not have any significant effects on levels of either presynaptic (synaptophysin) or post-synaptic (PSD 95) proteins in either the temporal cortex or hippocampus compared to vehicle treated mice (Fig. 20). These data demonstrated that the Src inhibitory, anti-inflammatory, microglia-inhibitory effects of dasatinib treatment did not correlate with any adverse effects such as increased astrogliosis, neuron or synaptic loss, and increased Aβ deposition.

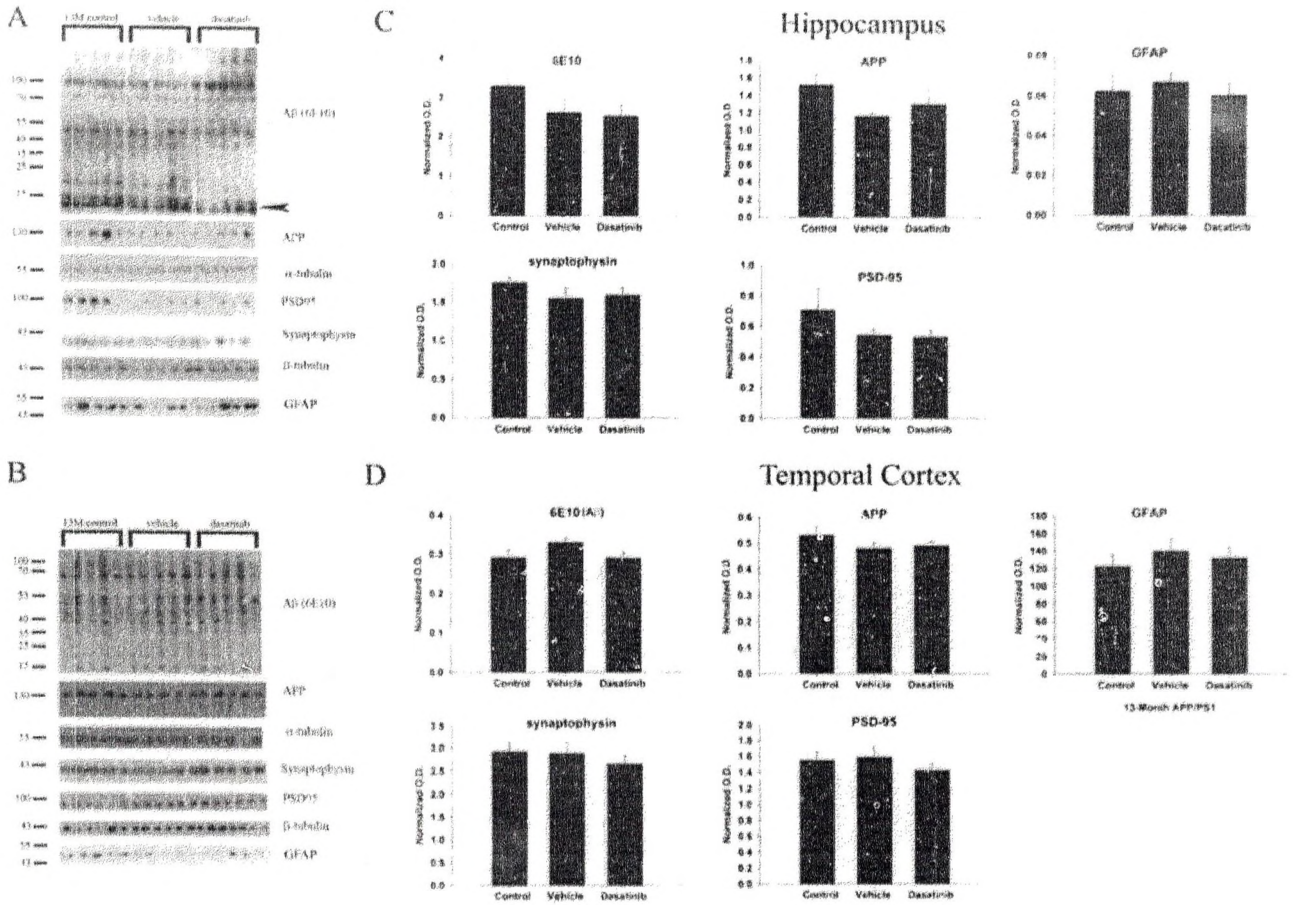

Figure 20.Dasatinib infusion did not alter levels of APP, Aβ, synaptic markers, synaptophysin, PSD95, or GFAP in hippocampus of 13 month old APP/PS1 brains *in vivo*. **(A)** Hippocampal and **(B)** temporal cortex brain lysates from control (n=7), vehicle (n=6), and dasatinib (n=7) infused animals were used for Western blot analyses using anti-Aβ clone 6E10 antibody, anti-APP, anti-synaptophysin, anti-PSD95 and anti-GFAP antibodies. **(C)** Optical densities were averaged, and graphed (+/-SEM) for hippocampus and **(D)** temporal cortex.

Dasatinib infusion decreased immunoreactivity for protein phosphotyrosine, phospho-Src and CD68 in APP/PS1 mice

To provide qualitative assessments along with the quantitative Western blot analyses, immunohistochemical studies were also performed from the treated animals. As expected, protein phosphotyrosine immunoreactivity in dasatinib infused mouse brains appeared dramatically less then vehicle treated mice in both the hippocampus and temporal cortex (Fig. 21). A similar trend of decreased immunoreactivity was observed for active phospho-Src in dasatinib treated animals versus vehicle controls (Fig. 21). Importantly, the decrease in immunoreactivity was observed in plaque-associated microglial-like cells demonstrating that the significant decreases in active Src and phosphotyrosine levels observed by Western blot analyses were a reflection of microglial changes due to the drug. Also as predicted, levels of CD68 reactive microglial immunoreactivity in dasatinib infused mice was noticeably decreased compared to vehicle treated mice in both the hippocampus and temporal cortex (Fig. 21). Consistent with the Western blot analysis, GFAP immunoreactivity for reactive astrocytes was not visually different between dasatinib and vehicle infused mice in either temporal cortex or hippocampus (Fig. 21). The qualitative immunostaining findings corroborated the quantitative Western blot analyses and validated that the significant decreases in pSrc levels were largely due to decreased microglial immunoreactivity, our intended target for the drug.

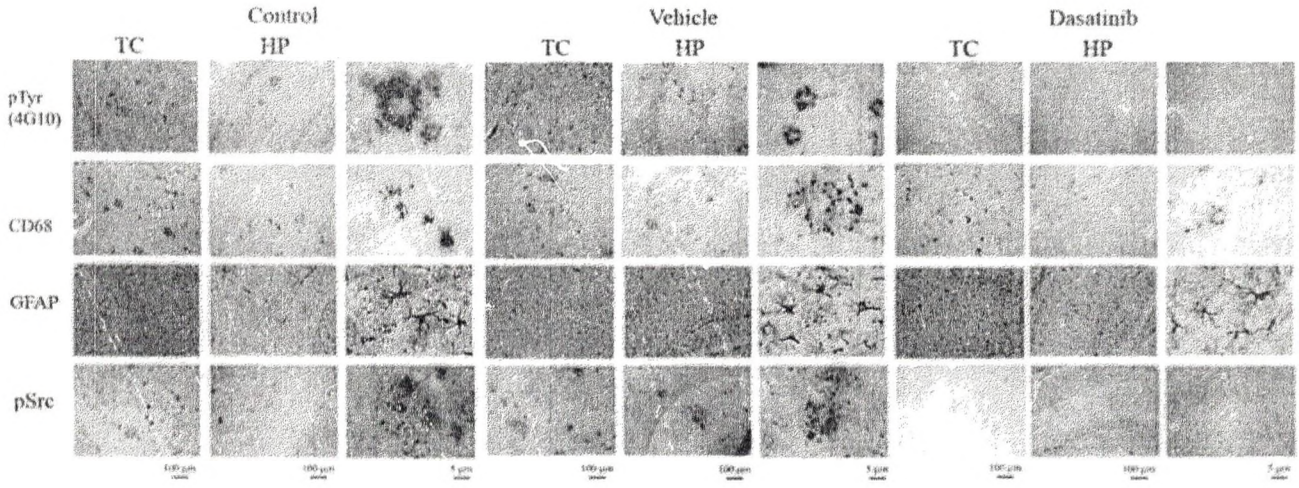

Figure 21. Dasatinib infusion attenuated microgliosis, protein phospho-tyrosine levels and active phospho-Src levels but not GFAP immunoreactivity in the APP/PS1 model of AD. Right hemispheres from brains of dasatinib infused, vehicle infused and 13 month old APP/PS1 controls animals were fixed, sectioned and immunostained using anti-phosphotyrosine (4G10) antibody, CD68 antibody, and active, phospho-Src (anti-pSrc) antibody. Representative 10X sections from the CA1 region of the hippocampus are shown with select high magnification fields.

Aβ plaque load was not affected by dasatinib infusions into the APP/PS1 mice

One possible consequence of attenuated tyrosine kinase activity in microglia could be inhibition of phagocytic ability. It is well known, for instance, that tyrosine kinase activity can affect macrophage phagocytic ability (Greenberg et al., 1996; Aderem and Underhill, 1999; Fitzer-Attas et al., 2000). Therefore, inhibition of Src or related kinase activity might attenuate any ability microglia have to clear Aβ deposits in the brain producing an unwanted side-effect of increased plaque load. Based upon the Western blot analysis dasatinib treatment had no effect on altering APP or Aβ levels in the brains of mice (Fig. 21). However, to better assess whether the drug had any effects on insoluble fibrillar deposits in the brain, quantitative immunostaining of Aβ plaques was performed. Dasatinib treatment had no effect on plaque load in treated mice compared to vehicle controls in either the hippocampus or temporal cortex (Fig. 22). These data demonstrate that the microglial-inhibitory effects of dasatinib do not result in unwanted effects of increasing Aβ deposition or accumulation

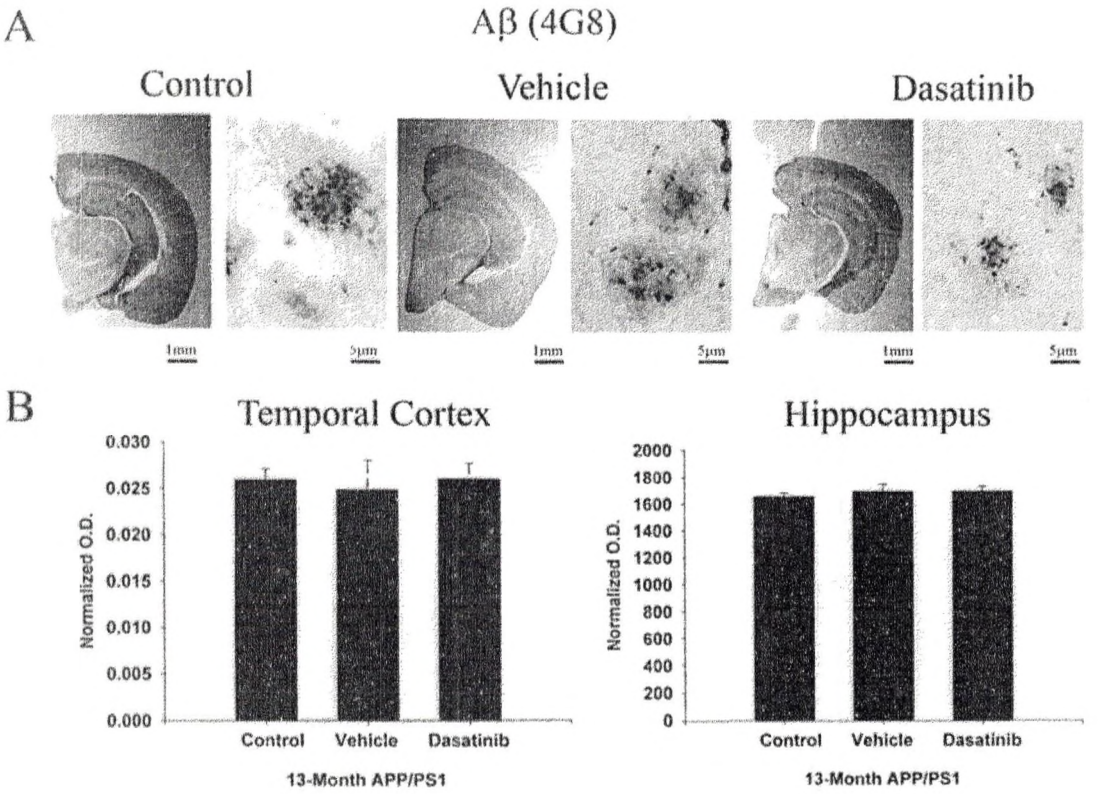

Figure 22. Dasatinib infusion did not change the Aβ plaque load in the brain of APP/PS1 mice. Serial sections from right hemishperes of brains of dasatinib infused, vehicle infused and 13 month old APP/PS1 mice were immunostained using anti-Aβ antibody, clone 4G8, and quantified for plaque load. **(A)** Representative 1.25X sections of the brain hemipsheres are shown with select high magnification fields. **(B)** Optical density measurements from the CA1 region of hippocampus and temporal cortex regions are shown +/- SE.

Dasatinib infusion improved T maze performance in APP/PS1 mice

Although there was no effect of dasatinib treatment on Aβ deposition, the clear and somewhat specific effect of Src inhibition correlating with anti-inflammatory and microglial-inhibitory effects provided an opportunity to assess whether dasatinib could also provide cognitive improvement to the mice. After treatments, spontaneous alternations from dasatinib treated, vehicle treated, and control animals were quantified during T maze analyses. This particular model of spatial memory was selected based upon its sensitivity of detection of cognitive deficit in AD mouse models (Stewart et al., 2011) and its preference for detecting changes in hippocampal-based performance differences (Duncan and Duncan, 1971; Loesche and Steward, 1977) since our most significant effects of drug were observed in hippocampus. Dasatinib infused animals demonstrated improved cognitive performance represented by a significant increase in spontaneous alternations compared to vehicle treated mice (Fig. 23). These data validated that subcutaneous administration of the Src/Abl tyrosine kinase inhibitor, dasatinib, is able to provide cognitive enhancing effects to APP/PS1 mice while attenuating microglial activation and proinflammatory cytokine, TNFα, levels in the brain.

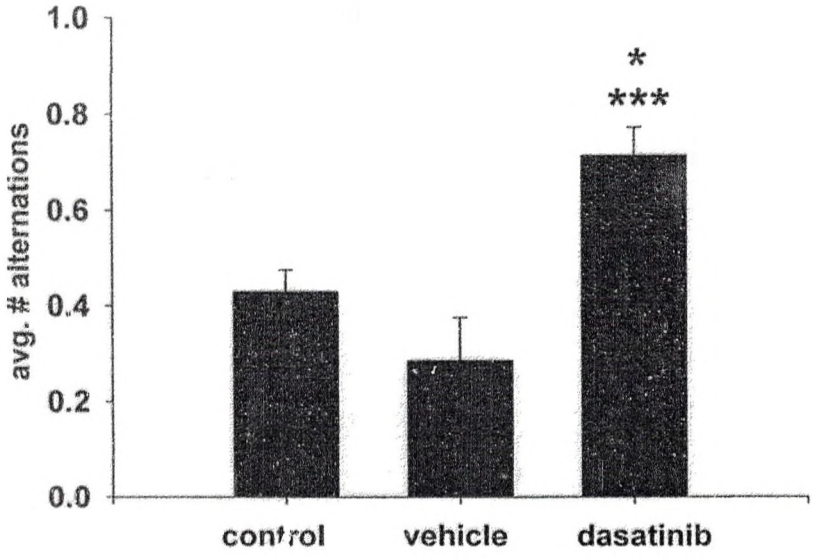

Figure 23. Dasatinib infused APP/PS1 mice demonstrated increased spontaneous alternations during T maze testing. Dasatinib or vehicle DMSO was infused sub-cutaneously via min-osmotic pump into 13-month old APP/PS1 mice (n=7) for 28-days. T-maze performance and numbers of spontaneous arm entry alternations was assessed on day 29. Mean number of alternations +/- SE were graphed. (*$p<0.05$ vs control, ***$p<0.001$ vs. vehicle).

CHAPTER 5

CHARACTERIZATION OF NOVEL SRC FAMILY KINASE INHIBITORS

Although dasatinib exerted anti-inflammatory effects *in vivo* correlating with decreased levels of active Src, it had no effect on active Lyn. Based upon the data that increased active pLyn levels were observed in AD brains, Lyn kinase still represents a valid microglial inhibitory target in AD. In order to identify a Lyn selective inhibitor, a high throughput screening *in vitro* and kinase assay was performed screening over 20,000 compounds. Four novel compounds were chosen to be characterized in cellular assays for their ability to inhibit two target kinases, Src and Lyn. The murine BV2 microglial cell line and primary microglial cultures were selected as the screening cells. These novel drugs, LDDN-0003499, LDDN-0075935, LDDN-0125694 and LDDN-0127164, were used to treat microglial BV2 cells to determine their ability to decrease basal total protein phosphotyrosine levels as well as active, phosphorylated forms of Src, Lyn and ERK kinases. Of the four drugs, LDDN-0003499 dose-dependently inhibited active, phosphorylated Lyn kinase levels. To determine whether the drug could attenuate stimulated kinase activity, Aβ and LPS stimulated primary microglia cultures were treated with LDDN-0003499 to assess effects on active levels of Src and Lyn. This study characterized the ability of LDDN-0003499 to attenuate microgliosis via particularly Lyn inhibition *in vitro*. Further work is required to modify this compound for *in vivo*

testing to determine whether it can attenuate microgliosis and Lyn activity in an AD mouse model.

Assessment of LDDN drugs effects on viability

Before screening drugs for any ability to alter cellular kinase activities, we first determined whether the drugs were toxic or not. Microglial BV2 cells were treated with LDDN-0003499, LDDN-0075935, LDDN-0125694 and LDDN-0127164 with increasing concentrations ranging from 0.5nM up to 50 μM for 24h. The media was removed and used for LDH release assays to determine cell viability. Quantitation of LDH released from the media following drug treatment demonstrated that none of the four drugs were toxic at any of the concentrations used for treatment (Fig. 24). For subsequent experiments to assess effects on tyrosine kinase inhibition, 0.5nM, 5nM, 50nM, 0.5μM, 5μM and 50μM concentrations were chosen for treatment of BV2 cells line as well as primary microglia cultures.

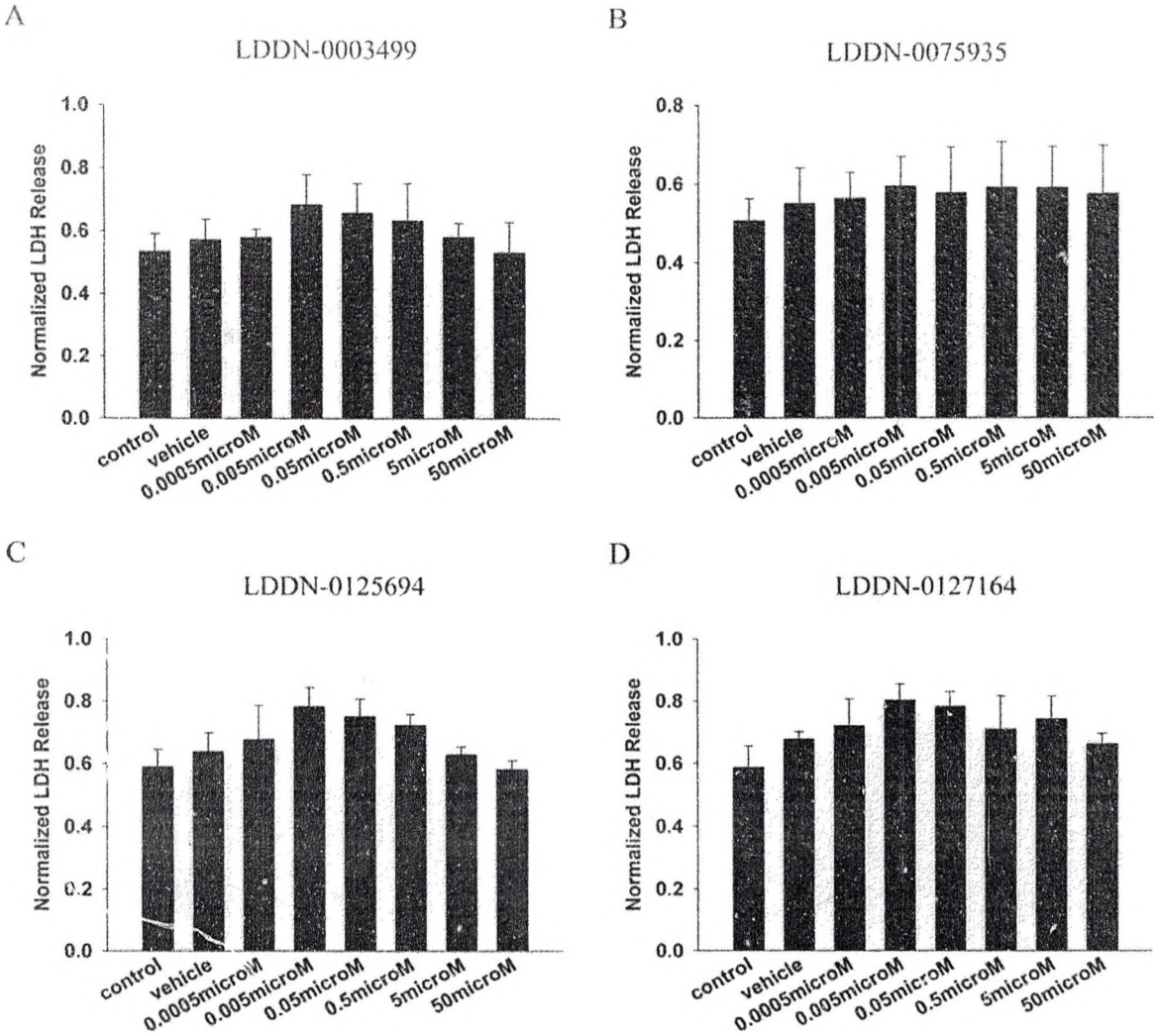

Figure 24. LDDN drugs were not toxic to microglial BV2 cells. Microglial BV2 cells were untreated (control), vehicle treated, or treated with 0.5nM, 5nM, 50nM, 0.5 μM, 5μM and 50 μM **(A)** LDDN-0003499, **(B)** LDDN-0075935, **(C)** LDDN-0125694 and **(D)** LDDN-0127164 for 24h. Media was removed and used for an LDH release assay to determine cell viability. 3 independent experiments with 8 replicates each were performed and absorbance values graphed and averaged +/- SD.

LDDN-0003499 decreased total protein phosphotyrosine level in microglia BV2 cells

In order to validate a tyrosine kinase inhibitory ability of the drugs in cells, the mouse microglia cell line, BV2, was treated with increasing concentrations of LDDN-0003499, LDDN-0075935, LDDN-0125694 and LDDN-0127164. Of the four drugs analyzed using dot blot analyses, 50μM LDDN-0003499 was able to significantly decrease the levels of total protein phosphotyrosine in these cells as compared to vehicle treated cells (Fig. 25). LDDN-0075935, LDDN-0125694 and LDDN-0127164 were not able to inhibit protein phosphotyrosine levels at the concentrations used. The cell lysates were also analyzed using Western blot analysis to completely resolve the protein phospho-tyrosine profile. A dose-dependent inhibition of overall protein phosphotyrosine levels was observed with LDDN-0003499 whereas the other 3 drugs failed to show any inhibitory effects in these cells.

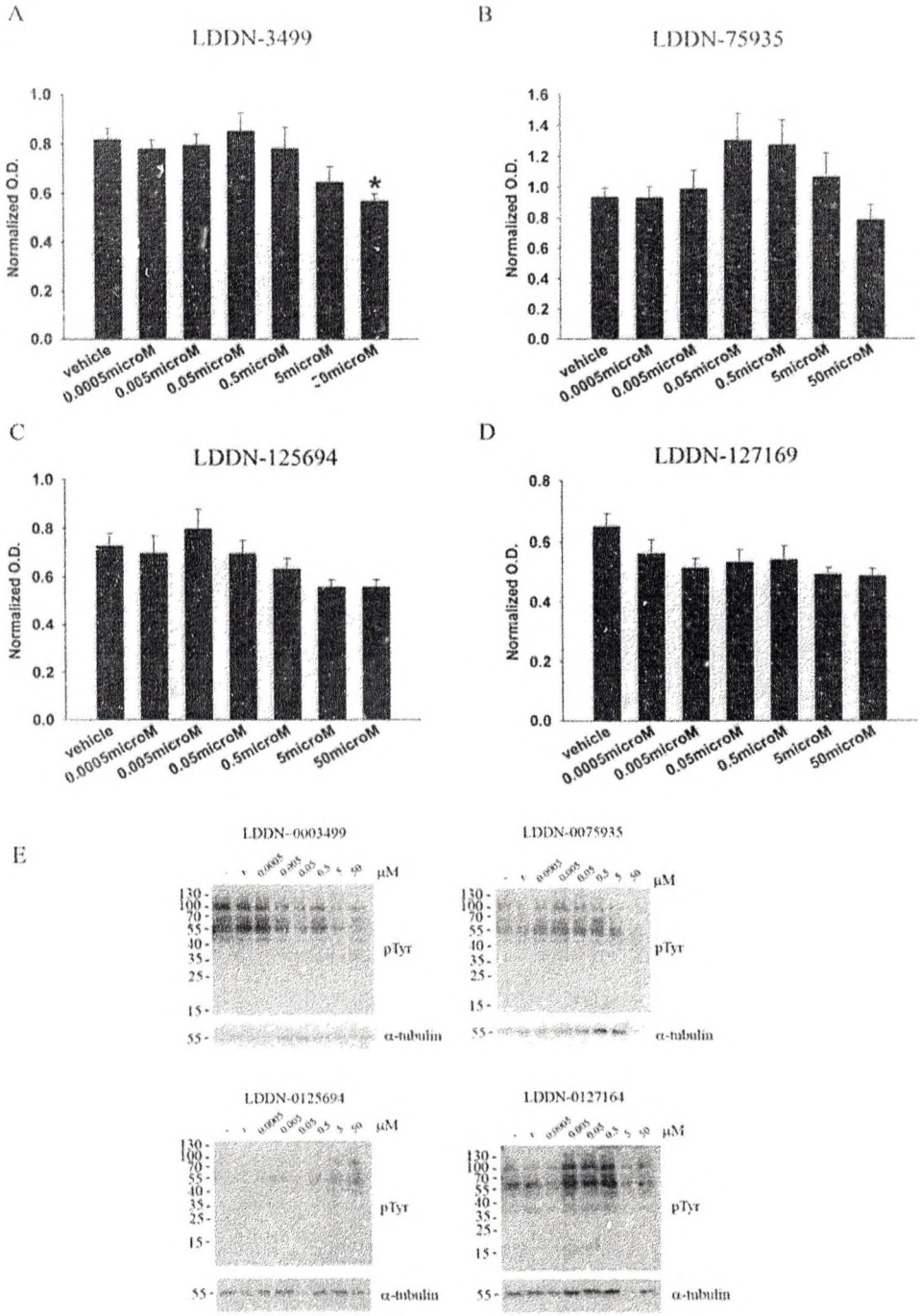

Figure 25. LDDN-0003499 attenuated total protein phosphotyrosine levels in the microglial BV2 cell line. Microglial BV2 cells were vehicle treated, or treated with 0.5nM, 5nM, 50nM, 0.5 μM, 5μM and 50 μM **(A)** LDDN-0003499, **(B)** LDDN-0075935,

(C) LDDN-0125694 and **(D)** LDDN-127164 for 24h. Cells lysates were used for dot-blot analyses using anti-phosphotyrosine (4G10) antibody with α-tubulin as the loading control. Optical densities were graphed and averaged +/- SD (*$p<0.05$ vs. control and vehicle). **(E)** Cell lysates were resolved via SDS-PAGE and Western blotted using anti-pTyr and α-tubulin (loading control) antibodies. A representative Western blot is shown.

LDDN-0003499 dose-dependently attenuated levels of active, phosphorylated Lyn in BV2 cells.

Although the drugs were tested for an ability to decrease total protein phosphotyrosine levels, the *in vitro* kinase assay target for these drugs was Lyn kinase. Therefore, in order to validate a cellular Lyn inhibitory ability of these drugs, BV2 cells were treated with increasing concentrations of LDDN-0003499, LDDN-0075935, LDDN-0125694 and LDDN-0127164 for 24h. Cell lysates were analyzed using dot blot analyses for pSrc, pLyn and pERK levels. Quantitation of the blots demonstrated a dose-dependent decrease in active, phosphorylated Lyn kinase levels in the cells treated with LDDN-0003499 (Fig. 26). LDDN-0075935 and LDDN-0127164 were not able to attenuate or affect pLyn levels in the cells at any of the doses (Fig. 27-29). LDDN-0125169 inhibited pLyn at a number of doses, as compared to vehicle treated cells, but this response was not dose dependent. LDDN-0003499 was also able to significantly reduce pSrc levels in these cells, although the response was not dose dependent. LDDN-0075935 and LDDN-0127164, again did not affect any change in pSrc levels. LDDN-0125169 was able to inhibit pSrc at a lower dose of 0.5nM only, as compared to vehicle treated cells. As an unrelated kinase control, each drug was tested for ability to alter active levels of the Ser/Thr kinase extracellular signal regulated kinase 2 (ERK2). There were no changes in active, phosphorylated ERK kinase levels in BV2 cells with treatment of any of the four drugs at the concentrations used. Western blot analysis of the microglial BV2 cells treated with LDDN-3499 revealed a dose-dependent attenuation in pLyn levels, but not pSrc levels. The other three drugs failed to affect any changes in active levels of Src, Lyn or ERK kinases.

This data suggests that LDDN-0003499 may be a promising drug for specifically inhibiting active pLyn levels in a dose dependant manner in microglia. To assess the specific kinase inhibition on microgliosis, 50μM of LDDN-0003499 was chosen to obtain a maximal inhibitory effect on tyrosine kinases in stimulated primary microglia cultures.

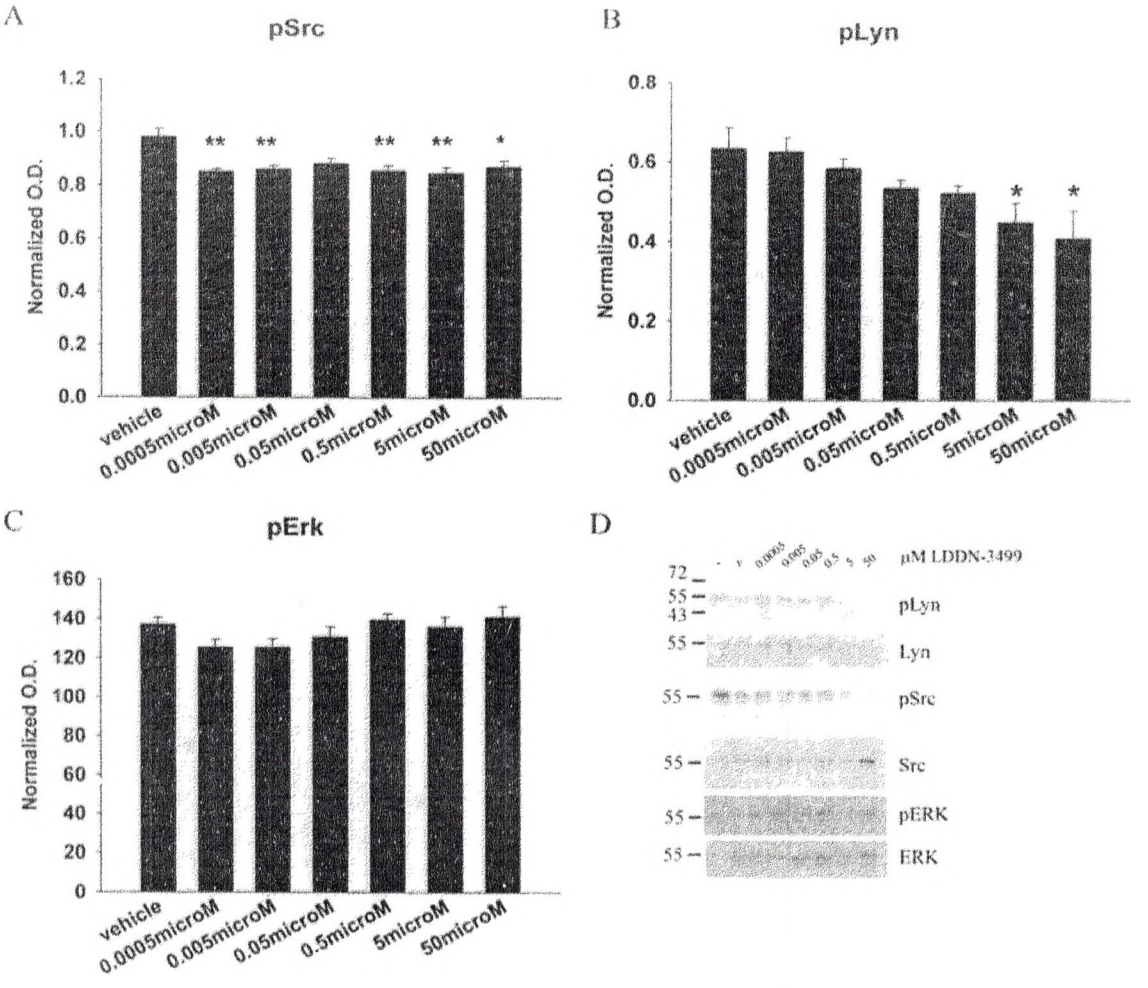

Figure 26. LDDN-0003499 dose-dependently attenuated active, phosphorylated Lyn levels in BV2 cells. Microglial BV2 cells were vehicle treated, or treated with 0.5nM, 5nM, 50nM, 0.5 μM, 5μM and 50 μM LDDN-0003499 for 24h. Cells lysates were collected for dot-blot analyses with anti-pSrc (Tyr 416) **(A)**, anti-pLyn (Tyr 396) **(B)** and anti-pERK **(C)** antibodies with Src, Lyn and ERK2 antibodies as their respective loading controls. Optical densities were graphed and averaged +/- SD (*$p<0.05$, **$p<0.01$ vs. control and vehicle). **(D)** Cell lysates were resolved via SDS-PAGE and western blotted using anti-pSrc, anti-pLyn, anti-pERK, anti-c-Src, anti-Lyn and anti-ERK2 antibodies. A representative Western blot is shown.

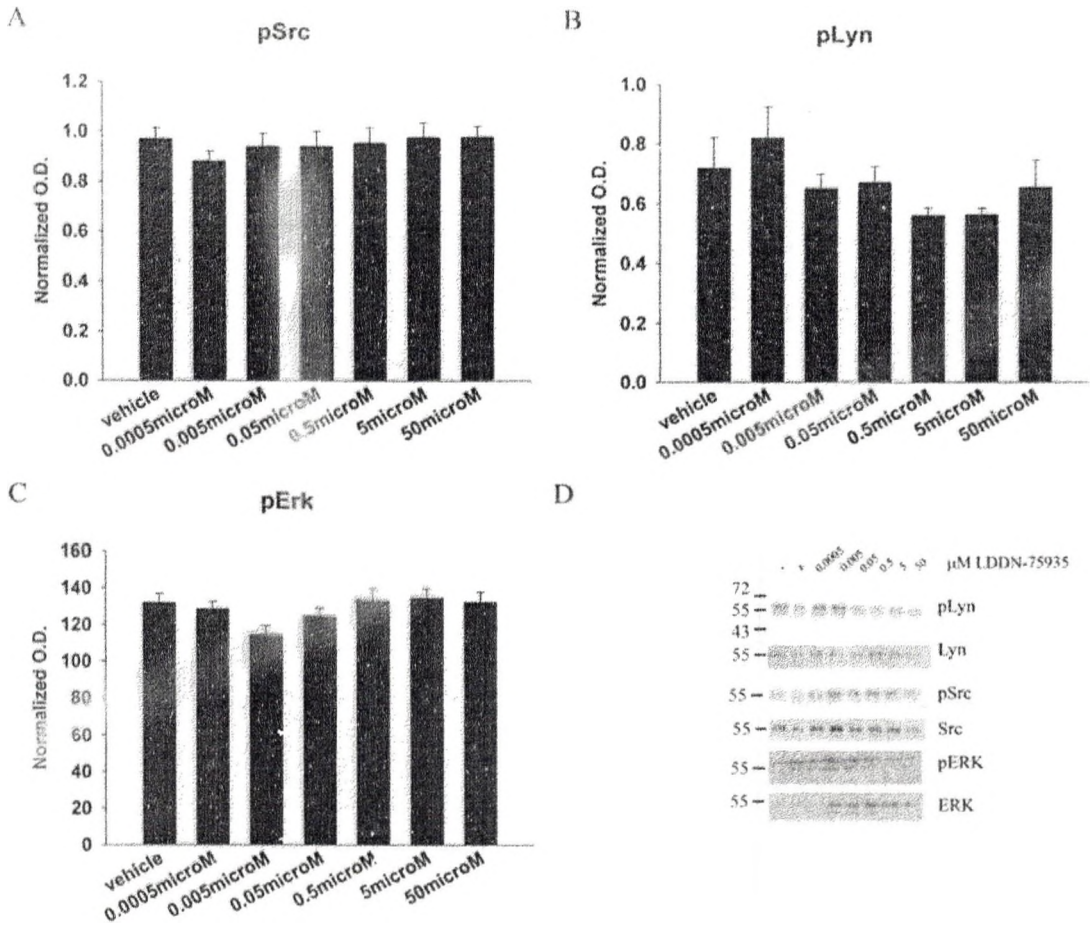

Figure 27. LDDN-0075935 did not attenuate active, phosphorylated Src, Lyn, or ERK levels in BV2 cells. Microglial BV2 cells were vehicle treated, or treated with 0.5nM, 5nM, 50nM, 0.5 μM, 5μM and 50 μM LDDN-0075935 for 24h. Cells lysates were used for dot-blot analyses with anti-pSrc (Tyr 416) **(A)**, anti-pLyn (Tyr 396) **(B)** and anti-pERK **(C)** antibodies with Src, Lyn and ERK2 antibodies as their respective loading controls. Optical densities were graphed and averaged +/- SD. **(D)** Cell lysates were resolved via SDS-PAGE and Western blotted using anti-pSrc, anti-pLyn, anti-pERK, anti-c-Src, anti-Lyn and anti-ERK2 antibodies. A representative Western blot is shown.

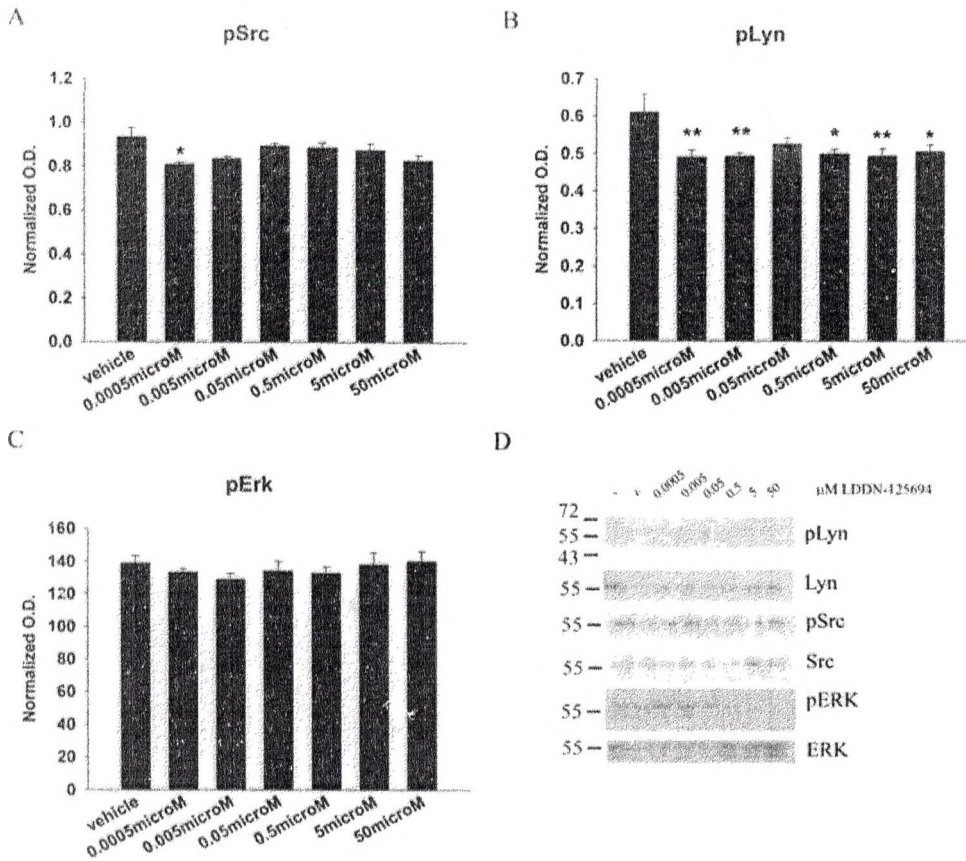

Figure 28. LDDN-0125694 did not dose dependently attenuate active, phosphorylated Src, Lyn, or ERK levels in BV2 cells. Microglial BV2 cells were vehicle treated, or treated with 0.5nM, 5nM, 50nM, 0.5 μM, 5μM and 50 μM LDDN-0075935 for 24h. Cells lysates were used for dot-blot analyses with anti-pSrc (Tyr 416) **(A)**, anti-pLyn (Tyr 396) **(B)** and anti-pERK **(C)** antibodies with Src, Lyn and ERK2 antibodies as their respective loading controls. Optical densities were graphed and averaged +/- SD. **(D)** Cell lysates were resolved via SDS-PAGE and Western blotted using anti-pSrc, anti-pLyn, anti-pERK, anti-c-Src, anti-Lyn and anti-ERK2 antibodies. A representative Western blot is shown.

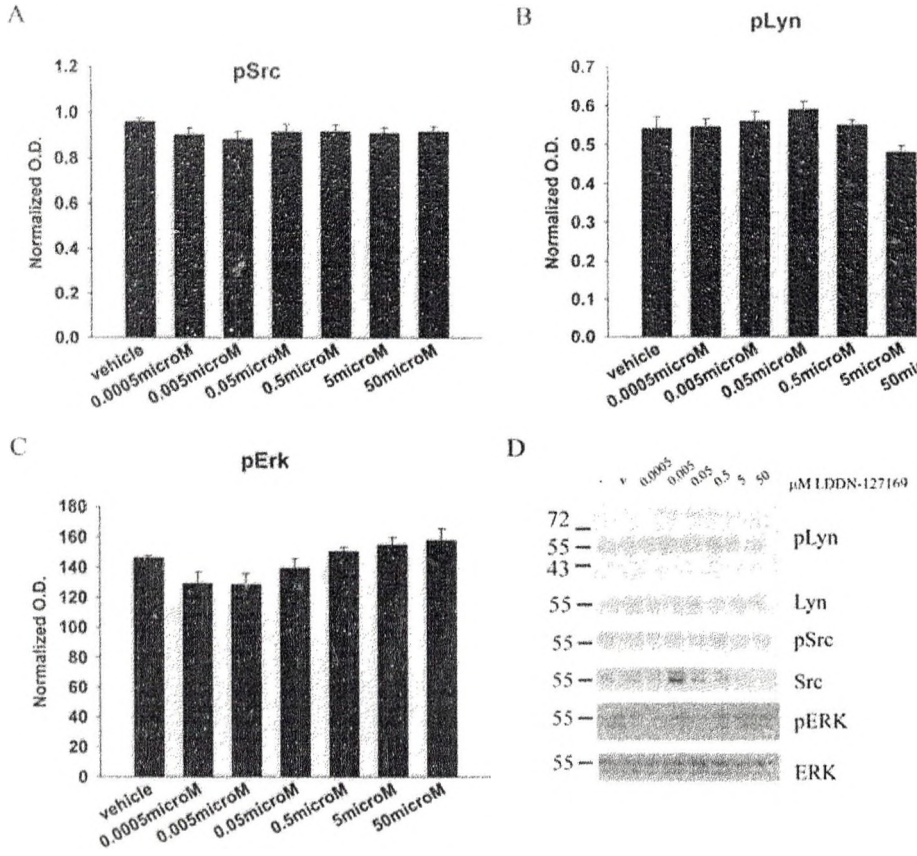

Figure 29. LDDN-0127164 did not attenuate active, phosphorylated Src, Lyn or ERK levels in BV2 cells. Microglial BV2 cells were vehicle treated, or treated with 0.5nM, 5nM, 50nM, 0.5 μM, 5μM and 50 μM LDDN-0075935 for 24h. Cells lysates were used for dot-blot analyses with anti-pSrc (Tyr 416) **(A)**, anti-pLyn (Tyr 396) **(B)** and anti-pERK **(C)** antibodies with Src, Lyn and ERK2 antibodies as their respective loading controls. Optical densities were graphed and averaged +/- SD. **(D)** Cell lysates were resolved via SDS-PAGE and Western blotted using anti-pSrc, anti-pLyn, anti-pERK, anti-c-Src, anti-Lyn and anti-ERK2 antibodies. A representative Western blot is shown.

LDDN-0003499 attenuated an Aβ dependent increase in active phosphorylated Src and Lyn kinases levels in primary microglia cultures.

Based on our earlier data and other work, it has been very well established that fibrillar Aβ and LPS can act as pro-inflammatory stimuli for microglia in the brain. However the primary rationale for this drug discovery effort was to identify small molecule capable of decreasing Aβ stimulation of microglia. To assess the ability of LDDN-0003499 to decrease Aβ or LPS stimulated tyrosine kinase changes in primary microglia cultures, cells were first stimulated with increasing concentrations of $A\beta_f$ and LPS to determine a concentration with adequate changes in increased active Lyn levels. As expected there was a dose dependent increase in total protein phosphotyrosine levels observed with Aβ treatment of the microglia (Fig.30). Aβ also stimulated increase in active, phosphorylated form of Src and Lyn kinases. Upon pretreatment on primary microglia cultures with 50μM LDDN-0003499, the Aβ stimulated increase in pLyn and pSrc levels was attenuated, as compared to vehicle treated cells.

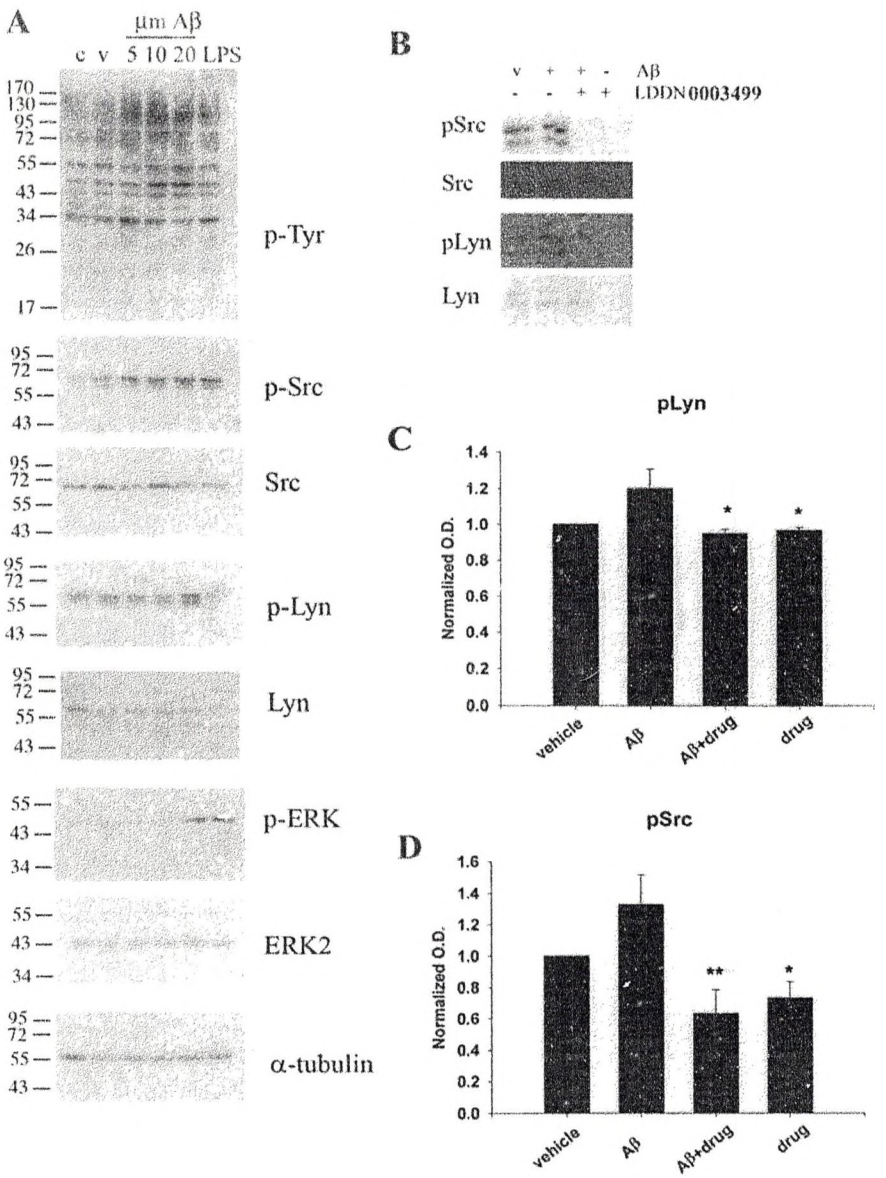

Figure 30. LDDN-0003499 attenuated an Aβ-dependent increase in active, phosphorylated Src and Lyn levels in primary microglia cultures. (A) Primary microglia cultures were untreated, vehicle treated (v) or treated with 5 μM, 10μM, 20 μM Aβ or 25ng/ml LPS for 5 minutes. Cell lysates were resolved by SDS-PAGE for anti-pTyr (4G10), anti-pSrc, anti-Lyn, anti-pERK, anti-Src, anti-Lyn, anti-ERK and anti-α-

tubulin antibodies. Representative Western blots are shown. Primary microglia cultures were vehicle treated (v) or treated with 10 μM Aβ in presence and absence of 50 μM LDDN-0003499. **(B)** Cell lysates were resolved by SDS-PAGE and blotted using anti-pSrc and anti-pLyn antibodies with Src and Lyn as loading controls. **(C)** Optical densities were averaged and graphed +/- SD (*$p<0.05$, **$p<0.01$ vs. Aβ treated cells)

LDDN-0003499 attenuated LPS-mediated secretion of the pro-inflammatory cytokine, TNF-α, in primary microglia cultures.

In order to determine whether the LPS-stimulated change in increased active tyrosine kinase levels was required for changes in phenotype, increased secretion of the pro-inflammatory cytokine, TNF-α, was quantified from the primary microglia cultures in the presence or absence of LDDN-0003499. LPS stimulated a significant increase in TNF-α secretion compared to control or vehicle treated microglial cells (Fig. 31). This increase in TNF-α secretion was attenuated by pretreatment with 50μM drug with no effect of cellular viability (Fig. 31). The data demonstrated that inhibition of Src family kinase activity was sufficient to prevent microglia from acquiring are reactive secretory phenotype upon pro-inflammatory stimulation *in vitro*.

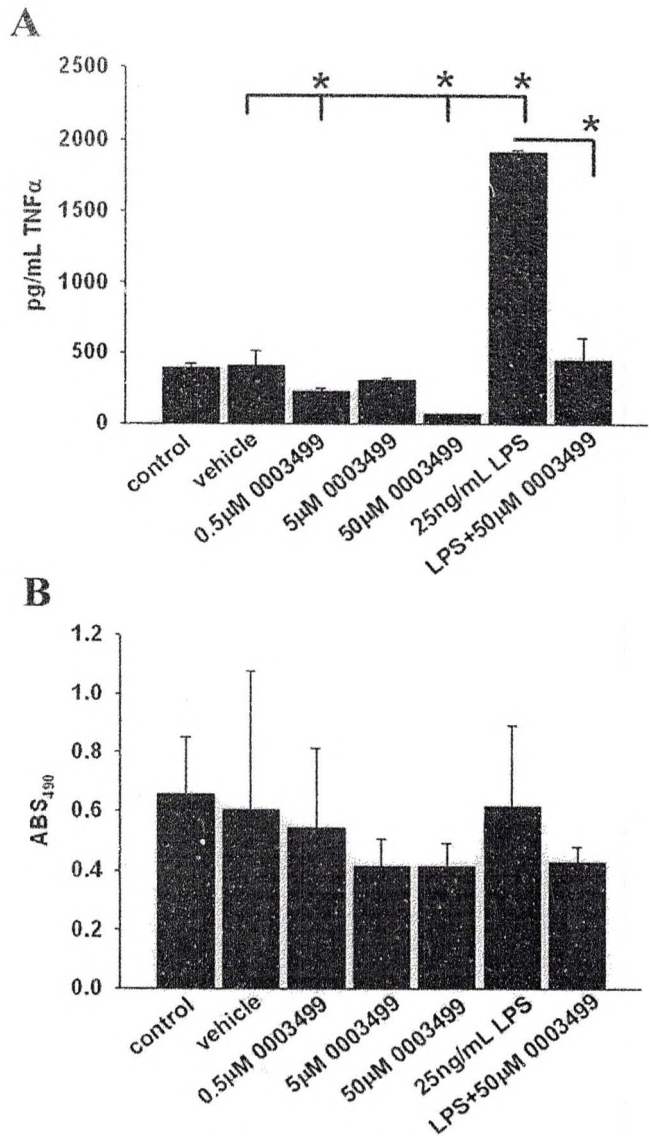

Figure 31. LDDN-0003499 attenuated LPS stimulated-microglial secretion of the proinflammatory cytokine, TNF-α. Primary microglia were unstimulated (control), DMSO vehicle treated (v), treated with 0.5 μM, 5μM and 50 μM LDDN-0003499 or stimulated for 24 hours with 25ng/ml LPS in the presence/absence of the 50 μM LDDN-0003499 drug. (A) Media was collected from the treated cells and used to quantify

changes in TNF-α secretion via ELISA. Secreted values were averaged +/-SD (*p< 0.05). (B) Media from treated cells was also used for to ˛ ssess cell viability via the LDH release assay. Absorbance values (490nm) were averaged+/-SD.

CHAPTER 6

DISCUSSION

This work demonstrates that Aβ oligomers and fibrils stimulate microglial activation *in vitro* via a tyrosine kinase associated pathway that results in increased secretion of the proinflammatory cytokine, TNF-α. It is possible to attenuate the oligomer-stimulated microglial phenotype change using a non-receptor tyrosine kinase inhibitor, dasatinib. The *in vitro* observations of oligomeric stimulation of microglia were validated *in vivo* demonstrating that intracerebroventricular infusion of oligomeric Aβ also stimulated increased microgliosis via a tyrosine kinase-dependent mechanism that was attenuated by co-delivery of dasatinib. Finally, the rodent findings correlated with a reactive microglial increase in protein phospho-tyrosine, p-Lyn and p-Src levels in AD brains compared to controls. Since total protein phosphotyrosine, more specifically active, phosphorylated Lyn and Src kinase are associated with plaques as well as distinct microglia in AD brains, role of fibrillar Aβ in activation of microglia phenotype cannot be ruled out. Collectively, all this data suggests that amyloid dependent microgliosis occurs through a tyrosine kinase dependent pathway. This mechanism of activation could prove to be very important therapeutically for attenuating pro-inflammatory microglial activation. In order to further understand the signaling pathway involved in amyloid based microglial activation, for pharmacological intervention purposes, a transgenic mouse model of AD, APP/PS1 mice, were also studied to assess protein phosphotyrosine changes with age. An age-dependent increase in plaque deposition in APP/PS1 mice

correlated with increased phosphotyrosine immunoreactivity and microgliosis in these mice. In order to assess whether inhibition of tyrosine kinases attenuated pro-inflammatory changes, dasatinib was subcutaneously infused into aged (13 month) old APP/PS1 mice with established plaques and reactive microglia. The infusions demonstrated that dasatinib attenuated overall tyrosine phosphorylation and active Src levels, in particular, in the hippocampus. The drug did not affect Aβ plaque load but reduced microgliosis and TNF-α levels in these animals without affecting other cell types, neurons and astrocytes. Moreover, dasatinib provided a significant increase in cognitive performance in correlation with this anti-inflammatory action. Collectively, these findings support the idea that Aβ fibrils and oligomers can serve as a microglial activating ligand in disease contributing to their proinflammatory phenotype and use of selective non-receptor tyrosine kinase inhibitors is an effective strategy to limit microglial-mediated changes during disease (Fig. 32).

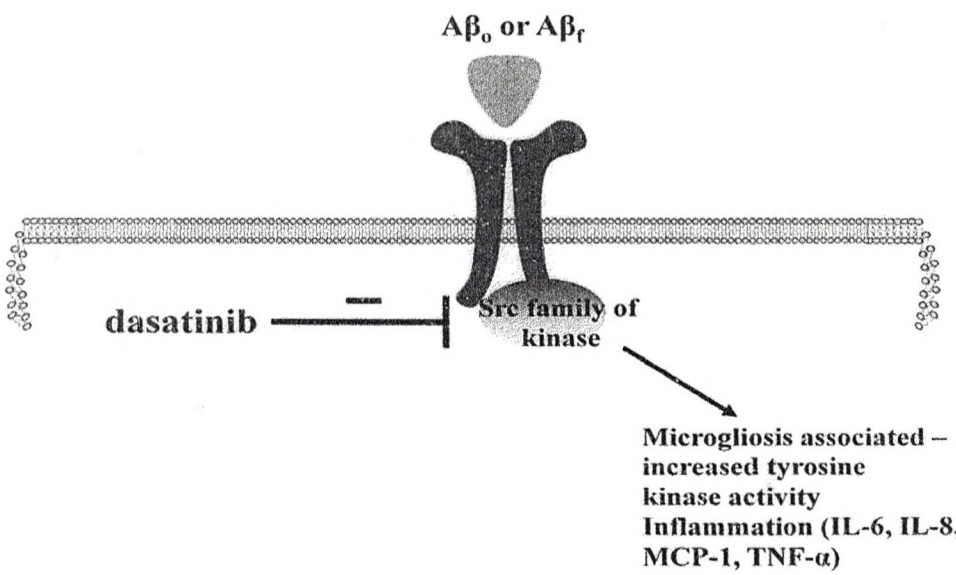

Figure 32: Amyloid dependent microgliosis occurs through a Src kinase activation pathway

Although it has been suggested that Aβ-stimulated microglial activation contributes to the pathophysiology of AD (Banati et al., 1993; Del Bo et al., 1995; Giulian et al., 1995; Klegeris et al., 1997; Combs et al., 2000; Combs et al., 2001a; Combs et al., 2001b; Floden and Combs, 2006) and a broad range of microglial secreted inflammatory markers are elevated in AD brains, including IL-1α, IL-1β, TGF-β and TNF-α (Akiyama et al., 2000; Jara et al., 2007), enthusiasm for an anti-inflammatory approach to treating AD has decreased, in part, due to lack of drug efficacy of a number of human trials that targeted cyclooxygenase (Cox) activity in AD patients (Rogers et al., 1993; Scharf et al., 1999; Aisen et al., 2002; Aisen et al., 2003; Thal et al., 2005). Indeed, Cox inhibition during later stages of disease had adverse effects and only demonstrated protection when administered long-term to asymptomatic individuals (Breitner et al., 2011). One possibility for the lack of efficacy of Cox inhibitors could be because Cox enzymes are expressed by multiple cell types in the brain and general drug inhibition has no cellular selectivity. Another possibility for the failed efficacy is that Cox 1 or 2 enzyme activities are simply not relevant targets for attenuating microglia-dependent changes. For this reason the direct signaling response initiated in microglia upon Aβ oligomer and fibril stimulation was the focus of this study. It has been reported from both AD brains (Tillotson and Wood, 1989a, b; Karp et al., 1994) and mouse models (Frautschy et al., 1998; Combs, 2009) that elevated protein phosphotyrosine levels are reliable markers of reactive microglia associated with plaques.

In spite of that fact that the specific stimuli driving microgliosis during disease may be heterogeneous, a common finding from our rodent *in vitro* and *in vivo* findings and AD brains is the increase in protein phospho-tyrosine levels. Our prior *in vitro* work

has demonstrated that specific non-receptor tyrosine kinase activities including Lyn and Syk are involved in the oligomer-dependent activation of microglia (Sondag et al., 2009) which correlated well with the increased phospho-tyrosine immunoreactivity observed in the intracerebroventricular infused animals. *In vitro* studies using monocytic lineage cells (McDonald et al., 1998; Combs et al., 2001a; Bamberger et al., 2003) and microglia (Combs et al., 1999; Sondag et al., 2009) have demonstrated that fibrillar Aβ stimulates a specific increase in overall protein tyrosine phosphorylation. Although numerous tyrosine kinases are expressed in microglia and it is likely that the temporal profile of kinase activities changes during chronic oligomer stimulation. During disease, stimulation with fibril, oligomer or other ligands may be superimposed (Sondag et al., 2009). Based upon the human disease and *in vitro* data, we demonstrated that active forms of non-receptor tyrosine kinases, Src and Lyn, are increased in reactive microglia. Indeed, the microglial phospho-Src and phospho-Lyn immunoreactivity changes observed in the AD brains is, to the best of our knowledge, a new contribution to the field. Thus, we have begun to identify particular kinase activities that may be responsible for the increase in phosphotyrosine immunoreactivity and microgliosis during disease.

This common change of increased forms of active non-receptor tyrosine kinases in the rodent and human findings served as the rationale for selecting a somewhat broad specificity agent, dasatinib, for its ability to attenuate the function of several different kinases, in particular the Src family members (Lombardo et al., 2004; Das et al., 2006) . The ability of dasatinib to limit protein phospho-tyrosine changes and cytokine secretion suggests that targeting kinase activity is a viable anti-inflammatory strategy for treating AD. It is interesting to note that limiting tyrosine kinase-dependent microgliosis is not the

only attractive reason for targeting these enzymes. For instance, tau phosphorylation is regulated via activity of the tyrosine kinase Abl modulating Cdk5 activation in a transgenic mouse model of AD (Alvarez et al., 2004; Cancino et al., 2009). Very recently, another tyrosine kinase inhibitor anti-cancer drug, imatinib, has been shown to target gamma-secretase activating protein as a therapeutic approach for Alzheimer's disease in a rodent model (He et al., 2010). Not surprisingly, recruitment of Src and Abl tyrosine kinases to APP has been demonstrated (Trommsdorff et al., 1998). Prior work has also verified an increased association of Src with APP in human diseased brains (Austin et al., 2009). Although our intracerebroventricular infusions, transgenic animals and *in vitro* studies, focused on oligomer and fibril stimulated mechanism of proinflammatory microgliosis in AD, it is likely that a heterogeneous mixture of changes during disease offers the possibility that inhibition of this class of kinases will be attractive from a number of different therapeutic perspectives.

Both *in vitro* data and *in vivo* experiments demonstrated that an oligomeric preparation of Aβ corresponding roughly to the size of SDS-stable trimer/tetramers at initial stimulation could drive microgliosis via a tyrosine kinase-dependent mechanism that correlated with a similar change in protein tyrosine phosphorylation in human diseased brains. Despite the fact that the oligomeric Aβ was delivered in a HDL solution to ensure its stability as an oligomeric preparation while in the pump, it is possible that the multimeric species changed after infusion into the brain over the time course of 14 day administration resulting in higher molecular weight species. However, immunohistochemical analyses using anti-oligomer antibodies to observe for oligomeric Aβ immunoreactivity strongly suggests by the thioflavin negative, A11/Ill positive nature

of the deposited Aβ, that the peptide was retained in an oligomeric and not fibrillar form. The possibility that higher order multimers and possibly some undetected fibrils did accumulate in the tissue during the infusion period along with, perhaps, co-deposition of endogenous Aβ, cannot be excluded. With the understanding that there may be some multimeric species of Aβ involved, along with the SDS-stable trimeric/tetrameric infused Aβ, the changes observed in microgliosis and the ability of dasatinib to attenuate those changes remain novel and relevant to Aβ-dependent microglial changes during disease. With regard to human disease, we certainly do not exclude the likelihood that fibrillar deposits of Aβ are also potent stimuli of microglia. As already mentioned, increased protein phospho-tyrosine staining from both AD brains and transgenic mouse models (Wood and Zinsmeister, 1991; Frautschy et al., 1998) have characterized microglial activation in association with Aβ plaques. Furthermore, prior work has demonstrated that fibrils also stimulate microglia *in vitro* via tyrosine kinase-mediated mechanisms (McDonald et al., 1997; Combs et al., 1999). However, histologic analysis of human brains demonstrated that some reactive microglia were associated with oligomeric Aβ as well, a finding not widely reported. In addition, many phospho-tyrosine immunoreactive microglia in diseased brains were not associated with any observable Aβ deposits suggesting that non-deposited Aβ oligomers or other molecules could be activating these cells as well. Therefore, we propose that oligomers are one of the stimuli driving microgliosis during disease but recognize a likely role of fibrils as well as possible still unnamed ligands. It is for this reason that we chose to examine fibril activation as well both *in vitro* and in the APP/PS1 model. As expected, both oligomers and fibrils could

activate microglia via Src family activation in our rodent studies correlating well with the increased pSrc/pLyn immunoreactivity from AD brains.

Validation that an orally available, FDA approved drug, dasatinib, was efficacious in *in vivo* study supports the idea of therapeutic tyrosine kinase inhibition for AD. Dasatinib (commercially, Sprycel) is used for treating chronic myeloid leukemia (Shah et al., 2004) and has the ability to cross the blood brain barrier (Porkka et al., 2008). We have demonstrated that it also attenuates Aβ-dependent proinflammatory microgliosis and inhibits disease relevant non-receptor tyrosine kinases, and improves cognitive performance.

The effect of decreasing microglial active Src and brain TNFα levels does not necessarily prove that these changes were responsible for the improved cognitive performance observed in the transgenic mouse model of AD with subcutaneously infused dasatinib. However, the *in vitro* data clearly demonstrated that dasatinib treatment and Src inhibition led to attenuated TNFα secretion providing correlative evidence that Src inhibition in microglia *in vivo* contributed to the decrease in TNFα observed. Moreover, recent human data using TNFα neutralizing drugs demonstrated cognitive improvement in AD patients (Tobinick and Gross, 2008) suggesting that diminished TNFα levels in the mice could have contributed to the cognitive improvements observed. We also appreciate that dasatinib treatment may effect a number of other kinases *in vitro* and *in vivo* and numerous cells may express Src. Non-receptor Src family tyrosine kinases are expressed widely in the mammalian CNS and are known to play a role in proliferation and differentiation of the CNS (Yoshimura et al., 1981; Alema and Tato, 1987; Haltmeier and Rohrer, 1990; Hecker et al., 1991; Wong et al., 1992; Barone and Courtneidge, 1995;

Taylor and Shalloway, 1996; Broome and Hunter, 1997; Klinghoffer et al., 1999; Tatosyan and Mizenina, 2000). Indeed, Src family kinase activities are crucial for synaptic plasticity, including learning and memory (Grant et al., 1992; Maness, 1992; Grant and Silva, 1994; Kojima et al., 1997; Sinai et al., 2010). Therefore any strategy to manipulate activity of these enzymes in the brain should be carefully considered. By demonstrating specificity of dasatinib for Src versus the related family member Lyn *in vivo* as well as a clear improvement in cognitive performance, we suggest that reagents such as dasatinib can form the basis for not only human testing consideration but, more importantly, for further drug development.

This study intentionally focused on animals at 13 months of age with established plaques and reactive microglia to test the efficacy of our anti-inflammatory strategy in late-stage disease. However, it will be important in future work to determine if a strategy of kinase inhibition can attenuate or delay behavioral decline or microgliosis in earlier stage disease. Although our longitudinal assessment in these mice suggested that phosphotyrosine immunoreactive microglia correlated with increased fibrillar plaque deposition, our prior work and our infusion data indicated that soluble oligomeric forms of Aβ were also potent stimuli of microglia responsible for initiating a unique type of tyrosine kinase-based signaling response (Sondag et al., 2009). Therefore, fully determining the specific signaling pathways involved in different forms of Aβ stimulation of microglia may offer a strategy for inhibiting specific tyrosine kinase activities at different disease time points to maximally produce anti-inflammatory effects.

Based on all the data thus far, we suggest amyloid-dependent microgliosis occurs via a Src kinase activation mechanism and this pathway is an important therapeutic target

in the prevention of AD. This work dealt with using a general non-receptor tyrosine kinase inhibitor, dasatinib, that shows affinity for a number of non-receptor tyrosine kinases including Src, Lyn, Fck and Yes. Dasatinib has higher affinity for Src and our *in vitro* and *in vivo* findings suggest that the drug has been effective in attenuating active Src levels. However, in human disease, another non-receptor tyrosine kinase, Lyn has been implicated in reactive plaque associated microglia. The Src family member, Lyn kinase has an important role in regulating immune cell phenotype. Lyn has been shown to physically associate with a number of hematopoetic cell surface receptors including BCR, CD40, LPS receptor and the FcεRI complex. Kinase dead mice, with mutations associated with loss of activity of Lyn show attenuated autoimmune disease, normally associated with Lyn deficiency (Verhagen et al., 2009) indicating a role of Lyn in B Cell regulation. Lyn also is an important target role in prostate cancer therapies (Goldenberg-Furmanov et al., 2004). Therefore, identifying the Lyn selective inhibitor to attenuate microgliosis in general and not just associated with AD, may prove to be crucial for therapeutically targeting several diseases. Based upon the observations that AD brains showed increased levels of pLyn in tissue lysates as well as plaque-associated immunoreactivity of active, phosphorylated Lyn, Lyn cannot be excluded as a valid target for attenuation of Aβ-associated microgliosis (Fig. 33). Following a high throughput screening kinase assay, four novel compounds were identified based upon their *in vitro* ability to inhibit Lyn. We further defined their ability to inhibit Lyn kinase basally as well in stimulated microglial *in vitro* models. We demonstrated that LDDN- 0003499, one compound in particular, was able to inhibit basal active, phosphorylated Lyn levels in the BV2 microglial cell line. LDDN-0003499 also decreased levels of active Lyn and Src in

Aβ and LPS stimulated microglia. Although this study was a characterization of the drugs in an *in vitro* system, there is a further need to modulate these drugs for *in vivo* use by characterization of particular specificities. At this point, we conclude that Lyn is also a relevant target for attenuating disease-associated microgliosis and propose that drug dependent strategies such as this we have undertaken may provide selective agents, for assessing the importance of Lyn vs. Src for contributing to microgliosis.

Since microglia are the primary immune cells in CNS, they have been implicated in a number of neurodegenerative disorders. As mentioned earlier, many pro-inflammatory and trophic factors are thought to be produced by activated microglia *in vitro* (Giulian et al., 1986; Hetier et al., 1988; Mallat et al., 1989; Sawada et al., 1989; Elkabes et al., 1996; Miwa et al., 1997). Microglia derived cytokines have been reported to be elevated in many cases besides Alzheimer's disease, including traumatic spinal cord lesion, traumatic brain injury, stroke, HIV-infection and multiple sclerosis (Lindholm et al., 1987; Griffin et al., 1989; Fagan and Gage, 1990; Merrill and Chen, 1991; Woodroofe et al., 1991; Taupin et al., 1993; Buttini et al., 1994; Merrill and Benveniste, 1996; Bartholdi and Schwab, 1997; Benveniste, 1997). Despite of the findings that the stimuli involved or the ligands responsible for microglial activation in disease conditions may be different, the fact remains that modulating microglial phenotype in order to attenuate pro-inflammatory effects becomes imperative in prevention of the adverse effects of microgliosis in all these diseases. Hence it is important to understand the mechanism(s) underlying the activation of microglia for pharmacologic intervention studies. Stimulation by β-amyloid peptides results in increased expression of CD40 on microglia leading to elevated TNF-α secretion (Tan et al., 1999b; Tan et al., 2000). Microglial

activation by either Aβ, CD40 ligand (CD40L) or LPS has been shown to involve activation of the MAPK pathway as well (Combs et al., 1999; Tan et al., 1999a). Lyn kinase has been shown to be involved in regulation of MAPK activation in microglia (Combs et al., 1999). Src is also reported to take part in regulation of MAPK in T cells, following stimulation (Tsuji-Takayama et al., 1997). Although, the mechanism of Src/MAPK regulation are complex, it appears that, in general, Src activation leads to downstream activation of MAP kinase, and production of neurotoxic and pro-inflammatory mediators. (Singer et al., 2011) (Figure 33). The process can also occur through activation of the PI3Kinase pathway (Combs et al., 1999). Src may also activate other signaling mediators like the JAK/STAT pathway leading to inflammatory gene expression (Simon et al., 2002; Simeone-Penney et al., 2008). Therefore, the signaling responses of pro-inflammatory signaling includes Src, activation is complex and is likely stimulant dependent. Our data indicates a role for Lyn and Src kinases in reactive microgliosis in AD. The retrospective studies involving NSAIDs possibly suggest that microglial inhibition is the basis of the beneficial effects in AD. Clearly, further experiments are needed to better understand the signaling cascade and the intracellular interactions involved for driving microglial activation during disease. It is only by detecting the intrinsic mechanisms of microglial activation that the most relevant target and therefore, drugs can be developed.

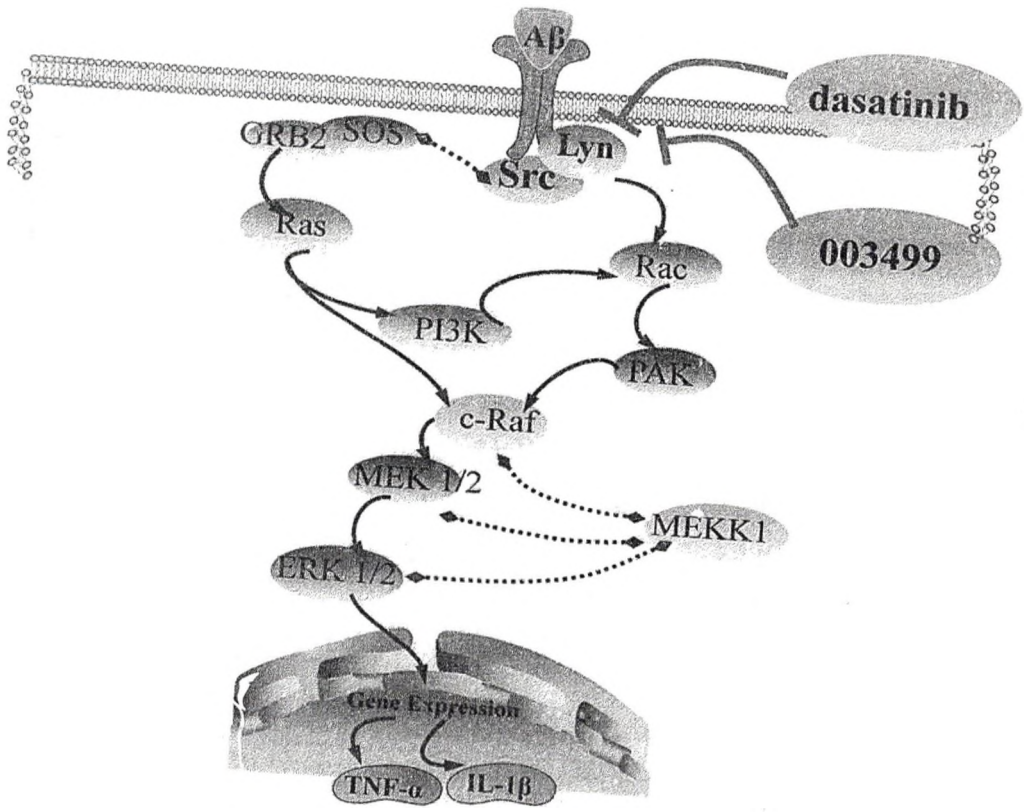

Figure 33. Schematic of Src/Lyn signaling pathway

APPENDIX

APP	Amyloid Precursor Protein
Aβ	Amyloid-β
$A\beta_f$	Amyloid-β fibril
$A\beta_o$	Amyloid-β oligomer
AD	Alzheimer's Disease
ALL	Acute Lymphoblastic Leukemia
ANOVA	Analysis of Variation
ApoE	Apolipoprotein E
ATP	Adenosine Tri Phosphate
CaCl2	Calcium Chloride
CCL-2	Chemokine (C-C motif) ligand 2
CD40	Cluster of Differentiation 40
CML	Chronic Myelogenous Leukemia
CNS	Central Nervous System
CO_2	Carbon di Oxide
Cox	Cyclooxygenase
CP-CML	Chromosome positive-Chronic Mylougenous Leukemia
CSF	Cerebrospinal Fluid
CT	Computer Topography
DAPI	4',6-diamidino-2-phenylindole
DMEM	Dulbecco's Modified Eagle Medium
EDTA	Ethylene diamine Tetraacetic acid
EGFR	Epidermal Growth Factor Receptor
EGTA	Ethylene Glycol Tetraacetic Acid
ERK	Extracellular Regulated Kinase
FAD	Familial Alzheimer's Disease
FAK	Focal Adhesion Kinase
FBS	Fetal Bovine Serum
FDA	Federal Drug Administration
FGFR	Fibroblast Growth Factor Receptor
FITC	Fluorescein Isothiocyanate

gp130	Glycoprotein 130
HDL	High Density Lipoprotein
HEPES	(4-(2-hydroxyethyl)-1-piperazineethanesulfonic acid)
HFIP	Hexafluoroisopropanol
HIV	Human immunodeficiency virus
HRP	Horse Radish Peroxidase
IFN	Interferon
IL	Interleukin
JAK	Janus Kinase
LDDN	Laboratory of Drug Discovery in Neurodegeneration
LPS	Lipopolysaccaride
MAPK	Mitogen Activated Protein Kinase
MCI	Mild Cognitive Impairment
MCP-1	Monocyte Chemotactic Protein-1
MHC	Major Histocompatibility Complex
mRNA	Messenger Ribonucleic Acid
N_2	Nitrogen
Na_2VO_4	Sodium Orthovandate
NaF	Sodium Flouride
NF-κB	Nuclear Factor-KappaB
NSAID	Non-Steroidal Anti-Inflammatory Drug
OD	Optical Density
PAGE	Poly Acrylamide Gel Electrphoresis
PBS	Phosphate Buffered Saline
PDGFR	Platelet Derived Growth Factor Receptor
PET	Positron Emission Tomography
PHF	Paired Helical Filament
PP1	4-Amino-5-(4-methylphenyl)-7-(t-butyl)pyrazolo[3,4-d]-pyrimidine
PP2	4-amino-5-(4-chloro-phenyl)-7-(t-butyl)pyrazolo[3,4-d]-pyrimidine
PPAR	Peroxisome Proliferator-activated Receptor
PS1	Presinilin 1
PSEN1	Presinilin 1
PSEN2	Presinilin 2
PVDF	Poly Vinylidene Di Flouride
RIPA	RadioImmunoPrecipitation Assay
SAD	Sporadic Alzheimer's disease
SD	Standard Deviation
SDS	Sodium Dodecyl Sulphate
SEM	Standard Error of Mean

STAT	Signal Transducer and Activator of Transcription
TBS	Tris-Buffered Saline
TBS-T	Tris-Buffered Saline Tween-20
Tg	Transgenic
TGF	Transforming Growth Factor
TNF	Tumor Necrosis Factor
Tyr	Tyrosine
VEGF	Vascular endothelial growth factor
VEGFR	Vascular endothelial growth factor Receptor

REFERENCES

Abbas N, Bednar I, Mix E, Marie S, Paterson D, Ljungberg A, Morris C, Winblad B, Nordberg A, Zhu J (2002) Up-regulation of the inflammatory cytokines IFN-gamma and IL-12 and down-regulation of IL-4 in cerebral cortex regions of APP(SWE) transgenic mice. J Neuroimmunol 126:50-57.

Aderem A, Underhill DM (1999) Mechanisms of phagocytosis in macrophages. Annu Rev Immunol 17:593-623.

Agostinho P, Cunha RA, Oliveira C (2010) Neuroinflammation, Oxidative Stress and the Pathogenesis of Alzheimer's Disease. Curr Pharm Des.

Aisen PS, Schmeidler J, Pasinetti GM (2002) Randomized pilot study of nimesulide treatment in Alzheimer's disease. Neurology 58:1050-1054.

Aisen PS, Marin DB, Brickman AM, Santoro J, Fusco M (2001) Pilot tolerability studies of hydroxychloroquine and colchicine in Alzheimer disease. Alzheimer Dis Assoc Disord 15:96-101.

Aisen PS, Schafer KA, Grundman M, Pfeiffer E, Sano M, Davis KL, Farlow MR, Jin S, Thomas RG, Thal LJ (2003) Effects of rofecoxib or naproxen vs placebo on Alzheimer disease progression: a randomized controlled trial. Jama 289:2819-2826.

Akiyama H, McGeer PL (1990) Brain microglia constitutively express beta-2 integrins. J Neuroimmunol 30:81-93.

Akiyama H, Mori H, Saido T, Kondo H, Ikeda K, McGeer PL (1999) Occurrence of the diffuse amyloid beta-protein (Abeta) deposits with numerous Abeta-containing glial cells in the cerebral cortex of patients with Alzheimer's disease. Glia 25:324-331.

Akiyama H, Barger S, Barnum S, Bradt B, Bauer J, Cole GM, Cooper NR, Eikelenboom P, Emmerling M, Fiebich BL, Finch CE, Frautschy S, Griffin WS, Hampel H, Hull M, Landreth G, Lue L, Mrak R, Mackenzie IR, McGeer PL, O'Banion MK, Pachter J, Pasinetti G, Plata-Salaman C, Rogers J, Rydel R, Shen Y, Streit W, Strohmeyer R, Tooyoma I, Van Muiswinkel FL, Veerhuis R, Walker D, Webster S, Wegrzyniak B, Wenk G, Wyss-Coray T (2000) Inflammation and Alzheimer's disease. Neurobiol Aging 21:383-421.

Alema S, Tato F (1987) Interaction of retroviral oncogenes with the differentiation program of myogenic cells. Adv Cancer Res 49:1-28.

Aleshin A, Finn RS (2010) SRC: a century of science brought to the clinic. Neoplasia 12:599-607.

Alvarez AR, Sandoval PC, Leal NR, Castro PU, Kosik KS (2004) Activation of the neuronal c-Abl tyrosine kinase by amyloid-beta-peptide and reactive oxygen species. Neurobiol Dis 17:326-336.

Alzheimer A (1987) About a peculiar disease of the cerebral cortex [Translation]. Alzheimer Dis Assoc Disord 1:7-8.

Apelt J, Schliebs R (2001) Beta-amyloid-induced glial expression of both pro- and anti-inflammatory cytokines in cerebral cortex of aged transgenic Tg2576 mice with Alzheimer plaque pathology. Brain Res 894:21-30.

Austin SA, Sens MA, Combs CK (2009) Amyloid precursor protein mediates a tyrosine kinase-dependent activation response in endothelial cells. J Neurosci 29:14451-14462.

Bamberger ME, Harris ME, McDonald DR, Husemann J, Landreth GE (2003) A cell surface receptor complex for fibrillar beta-amyloid mediates microglial activation. J Neurosci 23:2665-2674.

Banati RB, Gehrmann J, Schubert P, Kreutzberg GW (1993) Cytotoxicity of microglia. Glia 7:111-118.

Barber EK, Dasgupta JD, Schlossman SF, Trevillyan JM, Rudd CE (1989) The CD4 and CD8 antigens are coupled to a protein-tyrosine kinase (p56lck) that phosphorylates the CD3 complex. Proc Natl Acad Sci U S A 86:3277-3281.

Barone MV, Courtneidge SA (1995) Myc but not Fos rescue of PDGF signalling block caused by kinase-inactive Src. Nature 378:509-512.

Bartholdi D, Schwab ME (1997) Expression of pro-inflammatory cytokine and chemokine mRNA upon experimental spinal cord injury in mouse: an in situ hybridization study. Eur J Neurosci 9:1422-1438.

Beaty CD, Franklin TL, Uehara Y, Wilson CB (1994) Lipopolysaccharide-induced cytokine production in human monocytes: role of tyrosine phosphorylation in transmembrane signal transduction. Eur J Immunol 24:1278-1284.

Benveniste EN (1997) Role of macrophages/microglia in multiple sclerosis and experimental allergic encephalomyelitis. J Mol Med (Berl) 75:165-173.

Benzing WC, Wujek JR, Ward EK, Shaffer D, Ashe KH, Younkin SG, Brunden KR (1999) Evidence for glial-mediated inflammation in aged APP(SW) transgenic mice. Neurobiol Aging 20:581-589.

Biscardi JS, Tice DA, Parsons SJ (1999) c-Src, receptor tyrosine kinases, and human cancer. Adv Cancer Res 76:61-119.

Block ML, Zecca L, Hong JS (2007) Microglia-mediated neurotoxicity: uncovering the molecular mechanisms. Nat Rev Neurosci 8:57-69.

Boulet I, Ralph S, Stanley E, Lock P, Dunn AR, Green SP, Phillips WA (1992) Lipopolysaccharide- and interferon-gamma-induced expression of hck and lyn tyrosine kinases in murine bone marrow-derived macrophages. Oncogene 7:703-710.

Bradford MM (1976) A rapid and sensitive method for the quantitation of microgram quantities of protein utilizing the principle of protein-dye binding. Anal Biochem 72:248-254.

Breitner JC, Baker LD, Montine TJ, Meinert CL, Lyketsos CG, Ashe KH, Brandt J, Craft S, Evans DE, Green RC, Ismail MS, Martin BK, Mullan MJ, Sabbagh M, Tariot PN (2011) Extended results of the Alzheimer's disease anti-inflammatory prevention trial. Alzheimers Dement 7:402-411.

Broome MA, Hunter T (1997) The PDGF receptor phosphorylates Tyr 138 in the c-Src SH3 domain in vivo reducing peptide ligand binding. Oncogene 14:17-34.

Buttini M, Sauter A, Boddeke HW (1994) Induction of interleukin-1 beta mRNA after focal cerebral ischaemia in the rat. Brain Res Mol Brain Res 23:126-134.

Cancino GI, Perez de Arce K, Castro PU, Toledo EM, von Bernhardi R, Alvarez AR (2009) c-Abl tyrosine kinase modulates tau pathology and Cdk5 phosphorylation in AD transgenic mice. Neurobiol Aging.

Caveggion E, Continolo S, Pixley FJ, Stanley ER, Bowtell DD, Lowell CA, Berton G (2003) Expression and tyrosine phosphorylation of Cbl regulates macrophage chemokinetic and chemotactic movement. J Cell Physiol 195:276-289.

Chang Q, Jorgensen C, Pawson T, Hedley DW (2008) Effects of dasatinib on EphA2 receptor tyrosine kinase activity and downstream signalling in pancreatic cancer. Br J Cancer 99:1074-1082.

Cleary JP, Walsh DM, Hofmeister JJ, Shankar GM, Kuskowski MA, Selkoe DJ, Ashe KH (2005) Natural oligomers of the amyloid-beta protein specifically disrupt cognitive function. Nat Neurosci 8:79-84.

Cohen J (2002) The immunopathogenesis of sepsis. Nature 420:885-891.

Combs CK (2009) Inflammation and microglia actions in Alzheimer's disease. J Neuroimmune Pharmacol 4:380-388.

Combs CK, Bates P, Karlo JC, Landreth GE (2001a) Regulation of beta-amyloid stimulated proinflammatory responses by peroxisome proliferator-activated receptor alpha. Neurochem Int 39:449-457.

Combs CK, Karlo JC, Kao SC, Landreth GE (2001b) beta-Amyloid stimulation of microglia and monocytes results in TNFalpha-dependent expression of inducible nitric oxide synthase and neuronal apoptosis. J Neurosci 21:1179-1188.

Combs CK, Johnson DE, Cannady SB, Lehman TM, Landreth GE (1999) Identification of microglial signal transduction pathways mediating a neurotoxic response to amyloidogenic fragments of beta-amyloid and prion proteins. J Neurosci 19:928-939.

Combs CK, Johnson DE, Karlo JC, Cannady SB, Landreth GE (2000) Inflammatory mechanisms in Alzheimer's disease: inhibition of beta-amyloid-stimulated proinflammatory responses and neurotoxicity by PPARgamma agonists. J Neurosci 20:558-567.

Craig-Schapiro R, Fagan AM, Holtzman DM (2009) Biomarkers of Alzheimer's disease. Neurobiol Dis 35:128-140.

Cras P, Kawai M, Siedlak S, Mulvihill P, Gambetti P, Lowery D, Gonzalez-DeWhitt P, Greenberg B, Perry G (1990) Neuronal and microglial involvement in beta-amyloid protein deposition in Alzheimer's disease. Am J Pathol 137:241-246.

Das J, Chen P, Norris D, Padmanabha R, Lin J, Moquin RV, Shen Z, Cook LS, Doweyko AM, Pitt S, Pang S, Shen DR, Fang Q, de Fex HF, McIntyre KW, Shuster DJ, Gillooly KM, Behnia K, Schieven GL, Wityak J Barrish JC (2006) 2-aminothiazole as a novel kinase inhibitor template. Structure-activity relationship studies toward the discovery of N-(2-chloro-6-methylphenyl)-2-[[6-[4-(2-hydroxyethyl)-1- piperazinyl)]-2-methyl-4-pyrimidinyl]amino)]-1,3-thiazole-5-carboxamide (dasatinib, BMS-354825) as a potent pan-Src kinase inhibitor. J Med Chem 49:6819-6832.

De Franceschi L, Fumagalli L, Olivieri O, Corrocher R, Lowell CA, Berton G (1997) Deficiency of Src family kinases Fgr and Hck results in activation of erythrocyte K/Cl cotransport. J Clin Invest 99:220-227.

Del Bo R, Angeretti N, Lucca E, De Simoni MG, Forloni G (1995) Reciprocal control of inflammatory cytokines, IL-1 and IL-6, and beta-amyloid production in cultures. Neurosci Lett 188:70-74.

Dickson DW (1997) The pathogenesis of senile plaques. J Neuropathol Exp Neurol 56:321-339.

Dickson DW, Lee SC, Mattiace LA, Yen SH, Brosnan C (1993) Microglia and cytokines in neurological disease, with special reference to AIDS and Alzheimer's disease. Glia 7:75-83.

Drubin DG, Kirschner MW (1986) Tau protein function in living cells. J Cell Biol 103:2739-2746.

Duncan PM, Duncan NC (1971) Free-operant and T-maze avoidance performance by septal and hippocampal-damaged rats. Physiol Behav 7:687-693.

El Khoury J, Hickman SE, Thomas CA, Cao L, Silverstein SC, Loike JD (1996) Scavenger receptor-mediated adhesion of microglia to beta-amyloid fibrils. Nature 382:716-719.

Elkabes S, DiCicco-Bloom EM, Black IB (1996) Brain microglia/macrophages express neurotrophins that selectively regulate microglial proliferation and function. J Neurosci 16:2508-2521.

Eriksen JL, Sagi SA, Smith TE, Weggen S, Das P, McLendon DC, Ozols VV, Jessing KW, Zavitz KH, Koo EH, Golde TE (2003) NSAIDs and enantiomers of flurbiprofen target gamma-secretase and lower Abeta 42 in vivo. J Clin Invest 112:440-449.

Fagan AM, Gage FH (1990) Cholinergic sprouting in the hippocampus: a proposed role for IL-1. Exp Neurol 110:105-120.

Fitzer-Attas CJ, Lowry M, Crowley MT, Finn AJ, Meng F, DeFranco AL, Lowell CA (2000) Fcgamma receptor-mediated phagocytosis in macrophages lacking the Src family tyrosine kinases Hck, Fgr, and Lyn. J Exp Med 191:669-682.

Floden AM, Combs CK (2006) Beta-amyloid stimulates murine postnatal and adult microglia cultures in a unique manner. J Neurosci 26:4644-4648.

Frautschy SA, Yang F, Irrizarry M, Hyman B, Saido TC, Hsiao K, Cole GM (1998) Microglial response to amyloid plaques in APPsw transgenic mice. Am J Pathol 152:307-317.

Galimberti D, Fenoglio C, Scarpini E (2008) Inflammation in neurodegenerative disorders: friend or foe? Curr Aging Sci 1:30-41.

Gandy S (2005) The role of cerebral amyloid beta accumulation in common forms of Alzheimer disease. J Clin Invest 115:1121-1129.

Garcia-Alloza M, Robbins EM, Zhang-Nunes SX, Purcell SM, Betensky RA, Raju S, Prada C, Greenberg SM, Bacskai BJ, Frosch MP (2006) Characterization of amyloid deposition in the APPswe/PS1dE9 mouse model of Alzheimer disease. Neurobiol Dis 24:516-524.

Gardai S, Whitlock BB, Helgason C, Ambruso D, Fadok V, Bratton D, Henson PM (2002) Activation of SHIP by NADPH oxidase-stimulated Lyn leads to enhanced apoptosis in neutrophils. J Biol Chem 277:5236-5246.

Giulian D, Baker TJ, Shih LC, Lachman LB (1986) Interleukin 1 of the central nervous system is produced by ameboid microglia. J Exp Med 164:594-604.

Giulian D, Haverkamp LJ, Li J, Karshin WL, Yu J, Tom D, Li X, Kirkpatrick JB (1995) Senile plaques stimulate microglia to release a neurotoxin found in Alzheimer brain. Neurochem Int 27:119-137.

Gnoni A, Marech I, Silvestris N, Vacca A, Lorusso V (2011) Dasatinib: an anti-tumour agent via Src inhibition. Curr Drug Targets 12:563-578.

Goldenberg-Furmanov M, Stein I, Pikarsky E, Rubin H, Kasem S, Wygoda M, Weinstein I, Reuveni H, Ben-Sasson SA (2004) Lyn is a target gene for prostate cancer: sequence-based inhibition induces regression of human tumor xenografts. Cancer Res 64:1058-1066.

Grant SG, Silva AJ (1994) Targeting learning. Trends Neurosci 17:71-75.

Grant SG, O'Dell TJ, Karl KA, Stein PL, Soriano P, Kandel ER (1992) Impaired long-term potentiation, spatial learning, and hippocampal development in fyn mutant mice. Science 258:1903-1910.

Greenberg S, Chang P, Wang DC, Xavier R, Seed B (1996) Clustered syk tyrosine kinase domains trigger phagocytosis. Proc Natl Acad Sci U S A 93:1103-1107.

Griffin WS, Stanley LC, Ling C, White L, MacLeod V, Perrot LJ, White CL, 3rd, Araoz C (1989) Brain interleukin 1 and S-100 immunoreactivity are elevated in Down syndrome and Alzheimer disease. Proc Natl Acad Sci U S A 86:7611-7615.

Grundke-Iqbal I, Iqbal K, Tung YC, Quinlan M, Wisniewski HM, Binder LI (1986) Abnormal phosphorylation of the microtubule-associated protein tau (tau) in Alzheimer cytoskeletal pathology. Proc Natl Acad Sci U S A 83:4913-4917.

Guarino M (2010) Src signaling in cancer invasion. J Cell Physiol 223:14-26.

Haltmeier H, Rohrer H (1990) Distinct and different effects of the oncogenes v-myc and v-src on avian sympathetic neurons: retroviral transfer of v-myc stimulates neuronal proliferation whereas v-src transfer enhances neuronal differentiation. J Cell Biol 110:2087-2098.

Hanahan D, Weinberg RA (2000) The hallmarks of cancer. Cell 100:57-70.

Hardy J (1999) The shorter amyloid cascade hypothesis. Neurobiol Aging 20:85; discussion 87.

Hardy J (2002) Testing times for the "amyloid cascade hypothesis". Neurobiol Aging 23:1073-1074.

Hardy J (2006) Alzheimer's disease: the amyloid cascade hypothesis: an update and reappraisal. J Alzheimers Dis 9:151-153.

Hardy J, Selkoe DJ (2002) The amyloid hypothesis of Alzheimer's disease: progress and problems on the road to therapeutics. Science 297:353-356.

Hardy JA, Higgins GA (1992) Alzheimer's disease: the amyloid cascade hypothesis. Science 256:184-185.

He G, Luo W, Li P, Remmers C, Netzer WJ, Hendrick J, Bettayeb K, Flajolet M, Gorelick F, Wennogle LP, Greengard P (2010) Gamma-secretase activating protein is a therapeutic target for Alzheimer's disease. Nature 467:95-98.

Hecker G, Lewis DL, Rausch DM, Jelsema CL (1991) Nerve-growth-factor-treated and v-src-expressing PC 12 cells: a model for neuronal differentiation. Biochem Soc Trans 19:385-386.

Hernandez F, Avila J (2007) Tauopathies. Cell Mol Life Sci 64:2219-2233.

Hetier E, Ayala J, Denefle P, Bousseau A, Rouget P, Mallat M, Prochiantz A (1988) Brain macrophages synthesize interleukin-1 and interleukin-1 mRNAs in vitro. J Neurosci Res 21:391-397.

in't Veld BA, Ruitenberg A, Hofman A, Stricker BH, Breteler MM (2001) Antihypertensive drugs and incidence of dementia: the Rotterdam Study. Neurobiol Aging 22:407-412.

Itagaki S, McGeer PL, Akiyama H, Zhu S, Selkoe D (1989) Relationship of microglia and astrocytes to amyloid deposits of Alzheimer disease. J Neuroimmunol 24:173-182.

Jakubowska J, Czyz M (2006) [Novel inhibitors of Bcr-Abl]. Postepy Hig Med Dosw (Online) 60:697-706.

Janelsins MC, Mastrangelo MA, Oddo S, LaFerla FM, Federoff HJ, Bowers WJ (2005) Early correlation of microglial activation with enhanced tumor necrosis factor-alpha and monocyte chemoattractant protein-1 expression specifically within the entorhinal cortex of triple transgenic Alzheimer's disease mice. J Neuroinflammation 2:23.

Jara JH, Singh BB, Floden AM, Combs CK (2007) Tumor necrosis factor alpha stimulates NMDA receptor activity in mouse cortical neurons resulting in ERK-dependent death. J Neurochem 100:1407-1420.

Jarrett JT, Berger EP, Lansbury PT, Jr. (1993a) The carboxy terminus of the beta amyloid protein is critical for the seeding of amyloid formation: implications for the pathogenesis of Alzheimer's disease. Biochemistry 32:4693-4697.

Jarrett JT, Berger EP, Lansbury PT, Jr. (1993b) The C-terminus of the beta protein is critical in amyloidogenesis. Ann N Y Acad Sci 695:144-148.

Johnson FM, Saigal B, Talpaz M, Donato NJ (2005) Dasatinib (BMS-354825) tyrosine kinase inhibitor suppresses invasion and induces cell cycle arrest and apoptosis of head and neck squamous cell carcinoma and non-small cell lung cancer cells. Clin Cancer Res 11:6924-6932.

Kanda S, Miyata Y, Kanetake H, Smithgall TE (2007) Non-receptor protein-tyrosine kinases as molecular targets for antiangiogenic therapy (Review). Int J Mol Med 20:113-121.

Karp HL, Tillotson ML, Soria J, Reich C, Wood JG (1994) Microglial tyrosine phosphorylation systems in normal and degenerating brain. Glia 11:284-290.

Kauwe JS, Wang J, Mayo K, Morris JC, Fagan AM, Holtzman DM, Goate AM (2009) Alzheimer's disease risk variants show association with cerebrospinal fluid amyloid beta. Neurogenetics 10:13-17.

Kayed R, Head E, Thompson JL, McIntire TM, Milton SC, Cotman CW, Glabe CG (2003) Common structure of soluble amyloid oligomers implies common mechanism of pathogenesis. Science 300:486-489.

Kayed R, Head E, Sarsoza F, Saing T, Cotman CW, Necula M, Margol L, Wu J, Breydo L, Thompson JL, Rasool S, Gurlo T, Butler P, Glabe CG (2007) Fibril specific, conformation dependent antibodies recognize a generic epitope common to amyloid fibrils and fibrillar oligomers that is absent in prefibrillar oligomers. Mol Neurodegener 2:18.

Khadaroo RG, Kapus A, Powers KA, Cybulsky MI, Marshall JC, Rotstein OD (2003) Oxidative stress reprograms lipopolysaccharide signaling via Src kinase-dependent pathway in RAW 264.7 macrophage cell line. J Biol Chem 278:47834-47841.

Khadaroo RG, He R, Parodo J, Powers KA, Marshall JC, Kapus A, Rotstein OD (2004) The role of the Src family of tyrosine kinases after oxidant-induced lung injury in vivo. Surgery 136:483-488.

Kilarski WW, Jura N, Gerwins P (2003) Inactivation of Src family kinases inhibits angiogenesis in vivo: implications for a mechanism involving organization of the actin cytoskeleton. Exp Cell Res 291:70-82.

Klegeris A, Walker DG, McGeer PL (1997) Interaction of Alzheimer beta-amyloid peptide with the human monocytic cell line THP-1 results in a protein kinase C-dependent secretion of tumor necrosis factor-alpha. Brain Res 747:114-121.

Klinghoffer RA, Sachsenmaier C, Cooper JA, Soriano P (1999) Src family kinases are required for integrin but not PDGFR signal transduction. Embo J 18:2459-2471.

Klyubin I, Walsh DM, Lemere CA, Cullen WK, Shankar GM, Betts V, Spooner ET, Jiang L, Anwyl R, Selkoe DJ, Rowan MJ (2005) Amyloid beta protein immunotherapy neutralizes Abeta oligomers that disrupt synaptic plasticity in vivo. Nat Med 11:556-561.

Klyubin I, Betts V, Welzel AT, Blennow K, Zetterberg H, Wallin A, Lemere CA, Cullen WK, Peng Y, Wisniewski T, Selkoe DJ, Anwyl R, Walsh DM, Rowan MJ (2008) Amyloid beta protein dimer-containing human CSF disrupts synaptic plasticity: prevention by systemic passive immunization. J Neurosci 28:4231-4237.

Kojima N, Wang J, Mansuy IM, Grant SG, Mayford M, Kandel ER (1997) Rescuing impairment of long-term potentiation in fyn-deficient mice by introducing Fyn transgene. Proc Natl Acad Sci U S A 94:4761-4765.

Kusaka G, Ishikawa M, Nanda A, Granger DN, Zhang JH (2004) Signaling pathways for early brain injury after subarachnoid hemorrhage. J Cereb Blood Flow Metab 24:916-925.

Lammich S, Kojro E, Postina R, Gilbert S, Pfeiffer R, Jasionowski M, Haass C, Fahrenholz F (1999) Constitutive and regulated alpha-secretase cleavage of Alzheimer's amyloid precursor protein by a disintegrin metalloprotease. Proc Natl Acad Sci U S A 96:3922-3927.

Landreth GE, Heneka MT (2001) Anti-inflammatory actions of peroxisome proliferator-activated receptor gamma agonists in Alzheimer's disease. Neurobiol Aging 22:937-944.

Lawson LJ, Perry VH, Gordon S (1992) Turnover of resident microglia in the normal adult mouse brain. Neuroscience 48:405-415.

Lehmann JM, Lenhard JM, Oliver BB, Ringold GM, Kliewer SA (1997) Peroxisome proliferator-activated receptors alpha and gamma are activated by indomethacin and other non-steroidal anti-inflammatory drugs. J Biol Chem 272:3406-3410.

Lendon CL, Ashall F, Goate AM (1997) Exploring the etiology of Alzheimer disease using molecular genetics. Jama 277:825-831.

Lennmyr F, Ericsson A, Gerwins P, Akterin S, Ahlstrom H, Terent A (2004) Src family kinase-inhibitor PP2 reduces focal ischemic brain injury. Acta Neurol Scand 110:175-179.

Lesne S, Koh MT, Kotilinek L, Kayed R, Glabe CG, Yang A, Gallagher M, Ashe KH (2006) A specific amyloid-beta protein assembly in the brain impairs memory. Nature 440:352-357.

Lindholm D, Heumann R, Meyer M, Thoenen H (1987) Interleukin-1 regulates synthesis of nerve growth factor in non-neuronal cells of rat sciatic nerve. Nature 330:658-659.

Ling EA (1979) Transformation of monocytes into amoeboid microglia in the corpus callosum of postnatal rats, as shown by labelling monocytes by carbon particles. J Anat 128:847-858.

Loesche J, Steward O (1977) Behavioral correlates of denervation and reinnervation of the hippocampal formation of the rat: recovery of alternation performance following unilateral entorhinal cortex lesions. Brain Res Bull 2:31-39.

Lombardo LJ, Lee FY, Chen P, Norris D, Barrish JC, Behnia K, Castaneda S, Cornelius LA, Das J, Doweyko AM, Fairchild C, Hunt JT, Inigo I, Johnston K, Kamath A, Kan D, Klei H, Marathe P, Pang S, Peterson R, Pitt S, Schieven GL, Schmidt RJ, Tokarski J, Wen ML, Wityak J, Borzilleri RM (2004) Discovery of N-(2-chloro-6-methyl- phenyl)-2-(6-(4-(2-hydroxyethyl)- piperazin-1-yl)-2-methylpyrimidin-4- ylamino)thiazole-5-carboxamide (BMS-354825), a dual Src/Abl kinase inhibitor with potent antitumor activity in preclinical assays. J Med Chem 47:6658-6661.

Lowell CA (2004) Src-family kinases: rheostats of immune cell signaling. Mol Immunol 41:631-643.

Lowell CA, Berton G (1999) Integrin signal transduction in myeloid leukocytes. J Leukoc Biol 65:313-320.

Lue LF, Kuo YM, Roher AE, Brachova L, Shen Y, Sue L, Beach T, Kurth JH, Rydel RE, Rogers J (1999) Soluble amyloid beta peptide concentration as a predictor of synaptic change in Alzheimer's disease. Am J Pathol 155:853-862.

Mackenzie IR, Munoz DG (1998) Nonsteroidal anti-inflammatory drug use and Alzheimer-type pathology in aging. Neurology 50:986-990.

Mackenzie IR, Hao C, Munoz DG (1995) Role of microglia in senile plaque formation. Neurobiol Aging 16:797-804.

Mallat M, Houlgatte R, Brachet P, Prochiantz A (1989) Lipopolysaccharide-stimulated rat brain macrophages release NGF in vitro. Dev Biol 133:309-311.

Maness PF (1992) Nonreceptor protein tyrosine kinases associated with neuronal development. Dev Neurosci 14:257-270.

Martin LJ, Pardo CA, Cork LC, Price DL (1994) Synaptic pathology and glial responses to neuronal injury precede the formation of senile plaques and amyloid deposits in the aging cerebral cortex. Am J Pathol 145:1358-1381.

Mattiace LA, Davies P, Dickson DW (1990) Detection of HLA-DR on microglia in the human brain is a function of both clinical and technical factors. Am J Pathol 136:1101-1114.

McAlpine FE, Lee JK, Harms AS, Ruhn KA, Blurton-Jones M, Hong J, Das P, Golde TE, LaFerla FM, Oddo S, Blesch A, Tansey MG (2009) Inhibition of soluble TNF signaling in a mouse model of Alzheimer's disease prevents pre-plaque amyloid-associated neuropathology. Neurobiol Dis 34:163-177.

McDonald DR, Brunden KR, Landreth GE (1997) Amyloid fibrils activate tyrosine kinase-dependent signaling and superoxide production in microglia. J Neurosci 17:2284-2294.

McDonald DR, Bamberger ME, Combs CK, Landreth GE (1998) beta-Amyloid fibrils activate parallel mitogen-activated protein kinase pathways in microglia and THP1 monocytes. J Neurosci 18:4451-4460.

McGeer EG, McGeer PL (1999) Brain inflammation in Alzheimer disease and the therapeutic implications. Curr Pharm Des 5:821-836.

McGeer PL, Itagaki S, Tago H, McGeer EG (1987) Reactive microglia in patients with senile dementia of the Alzheimer type are positive for the histocompatibility glycoprotein HLA-DR. Neurosci Lett 79:195-200.

McKhann G, Drachman D, Folstein M, Katzman R, Price D, Stadlan EM (1984) Clinical diagnosis of Alzheimer's disease: report of the NINCDS-ADRDA Work Group under the auspices of Department of Health and Human Services Task Force on Alzheimer's Disease. Neurology 34:939-944.

McLean CA, Cherny RA, Fraser FW, Fuller SJ, Smith MJ, Beyreuther K, Bush AI, Masters CL (1999) Soluble pool of Abeta amyloid as a determinant of severity of neurodegeneration in Alzheimer's disease. Ann Neurol 46:860-866.

McLean GW, Carragher NO, Avizienyte E, Evans J, Brunton VG, Frame MC (2005) The role of focal-adhesion kinase in cancer - a new therapeutic opportunity. Nat Rev Cancer 5:505-515.

McNaull BB, Todd S, McGuinness B, Passmore AP (2010) Inflammation and anti-inflammatory strategies for Alzheimer's disease--a mini-review. Gerontology 56:3-14.

Merrill JE, Chen IS (1991) HIV-1, macrophages, glial cells, and cytokines in AIDS nervous system disease. Faseb J 5:2391-2397.

Merrill JE, Benveniste EN (1996) Cytokines in inflammatory brain lesions: helpful and harmful. Trends Neurosci 19:331-338.

Meyer-Luehmann M, Spires-Jones TL, Prada C, Garcia-Alloza M, de Calignon A, Rozkalne A, Koenigsknecht-Talboo J, Holtzman DM, Bacskai BJ, Hyman BT (2008) Rapid appearance and local toxicity of amyloid-beta plaques in a mouse model of Alzheimer's disease. Nature 451:720-724.

Miwa T, Furukawa S, Nakajima K, Furukawa Y, Kohsaka S (1997) Lipopolysaccharide enhances synthesis of brain-derived neurotrophic factor in cultured rat microglia. J Neurosci Res 50:1023-1029.

Moore AH, O'Banion MK (2002) Neuroinflammation and anti-inflammatory therapy for Alzheimer's disease. Adv Drug Deliv Rev 54:1627-1656.

Morgan D, Gordon MN, Tan J, Wilcock D, Rojiani AM (2005) Dynamic complexity of the microglial activation response in transgenic models of amyloid deposition: implications for Alzheimer therapeutics. J Neuropathol Exp Neurol 64:743-753.

Morris JC (1993) The Clinical Dementia Rating (CDR): current version and scoring rules. Neurology 43:2412-2414.

Nakajima K, Kohsaka S (2001) Microglia: activation and their significance in the central nervous system. J Biochem 130:169-175.

Nam S, Kim D, Cheng JQ, Zhang S, Lee JH, Buettner R, Mirosevich J, Lee FY, Jove R (2005) Action of the Src family kinase inhibitor, dasatinib (BMS-354825), on human prostate cancer cells. Cancer Res 65:9185-9189.

Nijhuis E, Lammers JW, Koenderman L, Coffer PJ (2002) Src kinases regulate PKB activation and modulate cytokine and chemoattractant-controlled neutrophil functioning. J Leukoc Biol 71:115-124.

Okutani D, Lodyga M, Han B, Liu M (2006) Src protein tyrosine kinase family and acute inflammatory responses. Am J Physiol Lung Cell Mol Physiol 291:L129-141.

Parsons JT, Parsons SJ (1997) Src family protein tyrosine kinases: cooperating with growth factor and adhesion signaling pathways. Curr Opin Cell Biol 9:187-192.

Pasinetti GM, Aisen PS (1998) Cyclooxygenase-2 expression is increased in frontal cortex of Alzheimer's disease brain. Neuroscience 87:319-324.

Patel NS, Paris D, Mathura V, Quadros AN, Crawford FC, Mullan MJ (2005) Inflammatory cytokine levels correlate with amyloid load in transgenic mouse models of Alzheimer's disease. J Neuroinflammation 2:9.

Patterson C, Feightner JW, Garcia A, Hsiung GY, MacKnight C, Sadovnick AD (2008) Diagnosis and treatment of dementia: 1. Risk assessment and primary prevention of Alzheimer disease. Cmaj 178:548-556.

Paul R, Zhang ZG, Eliceiri BP, Jiang Q, Boccia AD, Zhang RL, Chopp M, Cheresh DA (2001) Src deficiency or blockade of Src activity in mice provides cerebral protection following stroke. Nat Med 7:222-227.

Perlmutter LS, Barron E, Chui HC (1990) Morphologic association between microglia and senile plaque amyloid in Alzheimer's disease. Neurosci Lett 119:32-36.

Perrin RJ, Fagan AM, Holtzman DM (2009) Multimodal techniques for diagnosis and prognosis of Alzheimer's disease. Nature 461:916-922.

Petersen RC, Smith GE, Waring SC, Ivnik RJ, Tangalos EG, Kokmen E (1999) Mild cognitive impairment: clinical characterization and outcome. Arch Neurol 56:303-308.

Petreaca ML, Yao M, Liu Y, Defea K, Martins-Green M (2007) Transactivation of vascular endothelial growth factor receptor-2 by interleukin-8 (IL-8/CXCL8) is required for IL-8/CXCL8-induced endothelial permeability. Mol Biol Cell 18:5014-5023.

Pike CJ, Burdick D, Walencewicz AJ, Glabe CG, Cotman CW (1993) Neurodegeneration induced by beta-amyloid peptides in vitro: the role of peptide assembly state. J Neurosci 13:1676-1687.

Playford MP, Schaller MD (2004) The interplay between Src and integrins in normal and tumor biology. Oncogene 23:7928-7946.

Podlisny MB, Ostaszewski BL, Squazzo SL, Koo EH, Rydell RE, Teplow DB, Selkoe DJ (1995) Aggregation of secreted amyloid beta-protein into sodium dodecyl sulfate-stable oligomers in cell culture. J Biol Chem 270:9564-9570.

Poli V (1998) The role of C/EBP isoforms in the control of inflammatory and native immunity functions. J Biol Chem 273:29279-29282.

Porkka K, Koskenvesa P, Lundan T, Rimpilainen J, Mustjoki S, Smykla R, Wild R, Luo R, Arnan M, Brethon B, Eccersley L, Hjorth-Hansen H, Hoglund M, Klamova H, Knutsen H, Parikh S, Raffoux E, Gruber F, Brito-Babapulle F, Dombret H, Duarte RF, Elonen E, Paquette R, Zwaan CM, Lee FY (2008) Dasatinib crosses the blood-brain barrier and is an efficient therapy for central nervous system Philadelphia chromosome-positive leukemia. Blood 112:1005-1012.

Prathapam T, Tegen S, Oskarsson T, Trumpp A, Martin GS (2006) Activated Src abrogates the Myc requirement for the G0/G1 transition but not for the G1/S transition. Proc Natl Acad Sci U S A 103:2695-2700.

Quintas-Cardama A, Kantarjian H, Cortes J (2007) Flying under the radar: the new wave of BCR-ABL inhibitors. Nat Rev Drug Discov 6:834-848.

Rane SG, Reddy EP (2002) JAKs, STATs and Src kinases in hematopoiesis. Oncogene 21:3334-3358.

Ray WJ, Ashall F, Goate AM (1998) Molecular pathogenesis of sporadic and familial forms of Alzheimer's disease. Mol Med Today 4:151-157.

Reddy VP, Zhu X, Perry G, Smith MA (2009) Oxidative stress in diabetes and Alzheimer's disease. J Alzheimers Dis 16:763-774.

Reines SA, Block GA, Morris JC, Liu G, Nessly ML, Lines CR, Norman BA, Baranak CC (2004) Rofecoxib: no effect on Alzheimer's disease in a 1-year, randomized, blinded, controlled study. Neurology 62:66-71.

Roche S, Fumagalli S, Courtneidge SA (1995) Requirement for Src family protein tyrosine kinases in G2 for fibroblast cell division. Science 269:1567-1569.

Rogers J, Lue LF (2001) Microglial chemotaxis, activation, and phagocytosis of amyloid beta-peptide as linked phenomena in Alzheimer's disease. Neurochem Int 39:333-340.

Rogers J, Strohmeyer R, Kovelowski CJ, Li R (2002) Microglia and inflammatory mechanisms in the clearance of amyloid beta peptide. Glia 40:260-269.

Rogers J, Kirby LC, Hempelman SR, Berry DL, McGeer PL, Kaszniak AW, Zalinski J, Cofield M, Mansukhani L, Willson P, et al. (1993) Clinical trial of indomethacin in Alzheimer's disease. Neurology 43:1609-1611.

Roher AE, Chaney MO, Kuo YM, Webster SD, Stine WB, Haverkamp LJ, Woods AS, Cotter RJ, Tuohy JM, Krafft GA, Bonnell BS, Emmerling MR (1996) Morphology and toxicity of Abeta-(1-42) dimer derived from neuritic and vascular amyloid deposits of Alzheimer's disease. J Biol Chem 271:20631-20635.

Rojo LE, Fernandez JA, Maccioni AA, Jimenez JM, Maccioni RB (2008) Neuroinflammation: implications for the pathogenesis and molecular diagnosis of Alzheimer's disease. Arch Med Res 39:1-16.

Sakai R, Iwamatsu A, Hirano N, Ogawa S, Tanaka T, Mano H, Yazaki Y, Hirai H (1994) A novel signaling molecule, p130, forms stable complexes in vivo with v-Crk and v-Src in a tyrosine phosphorylation-dependent manner. Embo J 13:3748-3756.

Sasaki A, Yamaguchi H, Ogawa A, Sugihara S, Nakazato Y (1997) Microglial activation in early stages of amyloid beta protein deposition. Acta Neuropathol 94:316-322.

Sasaki A, Shoji M, Harigaya Y, Kawarabayashi T, Ikeda M, Naito M, Matsubara E, Abe K, Nakazato Y (2002) Amyloid cored plaques in Tg2576 transgenic mice are characterized by giant plaques, slightly activated microglia, and the lack of paired helical filament-typed, dystrophic neurites. Virchows Arch 441:358-367.

Sawada M, Kondo N, Suzumura A, Marunouchi T (1989) Production of tumor necrosis factor-alpha by microglia and astrocytes in culture. Brain Res 491:394-397.

Schaeffer M, Schneiderbauer M, Weidler S, Tavares R, Warmuth M, de Vos G, Hallek M (2001) Signaling through a novel domain of gp130 mediates cell proliferation and activation of Hck and Erk kinases. Mol Cell Biol 21:8068-8081.

Scharf S, Mander A, Ugoni A, Vajda F, Christophidis N (1999) A double-blind, placebo-controlled trial of diclofenac/misoprostol in Alzheimer's disease. Neurology 53:197-201.

Schlachetzki JC, Hull M (2009) Microglial activation in Alzheimer's disease. Curr Alzheimer Res 6:554-563.

Schwab C, Klegeris A, McGeer PL (2010) Inflammation in transgenic mouse models of neurodegenerative disorders. Biochim Biophys Acta 1802:889-902.

Selkoe DJ (1994) Normal and abnormal biology of the beta-amyloid precursor protein. Annu Rev Neurosci 17:489-517.

Seubert P, Vigo-Pelfrey C, Esch F, Lee M, Dovey H, Davis D, Sinha S, Schlossmacher M, Whaley J, Swindlehurst C, et al. (1992) Isolation and quantification of soluble Alzheimer's beta-peptide from biological fluids. Nature 359:325-327.

Severgnini M, Takahashi S, Tu P, Perides G, Homer RJ, Jhung JW, Bhavsar D, Cochran BH, Simon AR (2005) Inhibition of the Src and Jak kinases protects against lipopolysaccharide-induced acute lung injury. Am J Respir Crit Care Med 171:858-867.

Shah NP, Tran C, Lee FY, Chen P, Norris D, Sawyers CL (2004) Overriding imatinib resistance with a novel ABL kinase inhibitor. Science 305:399-401.

Shankar GM, Welzel AT, McDonald JM, Selkoe DJ, Walsh DM (2011) Isolation of low-n amyloid beta-protein oligomers from cultured cells, CSF, and brain. Methods Mol Biol 670:33-44.

Shankar GM, Li S, Mehta TH, Garcia-Munoz A, Shepardson NE, Smith I, Brett FM, Farrell MA, Rowan MJ, Lemere CA, Regan CM, Walsh DM, Sabatini BL, Selkoe DJ (2008) Amyloid-beta protein dimers isolated directly from Alzheimer's brains impair synaptic plasticity and memory. Nat Med 14:837-842.

Sicheri F, Kuriyan J (1997) Structures of Src-family tyrosine kinases. Curr Opin Struct Biol 7:777-785.

Simeone-Penney MC, Severgnini M, Rozo L, Takahashi S, Cochran BH, Simon AR (2008) PDGF-induced human airway smooth muscle cell proliferation requires STAT3 and the small GTPase Rac1. Am J Physiol Lung Cell Mol Physiol 294:L698-704.

Simon AR, Takahashi S, Severgnini M, Fanburg BL, Cochran BH (2002) Role of the JAK-STAT pathway in PDGF-stimulated proliferation of human airway smooth muscle cells. Am J Physiol Lung Cell Mol Physiol 282:L1296-1304.

Sinai L, Duffy S, Roder JC (2010) Src inhibition reduces NR2B surface expression and synaptic plasticity in the amygdala. Learn Mem 17:364-371.

Singer CA, Lontay B, Unruh H, Halayko AJ, Gerthoffer WT (2011) Src mediates cytokine-stimulated gene expression in airway myocytes through ERK MAPK. Cell Commun Signal 9:14.

Soininen H, West C, Robbins J, Niculescu L (2007) Long-term efficacy and safety of celecoxib in Alzheimer's disease. Dement Geriatr Cogn Disord 23:8-21.

Sondag CM, Dhawan G, Combs CK (2009) Beta amyloid oligomers and fibrils stimulate differential activation of primary microglia. J Neuroinflammation 6:1.

Stalder M, Phinney A, Probst A, Sommer B, Staufenbiel M, Jucker M (1999) Association of microglia with amyloid plaques in brains of APP23 transgenic mice. Am J Pathol 154:1673-1684.

Stefanova I, Corcoran ML, Horak EM, Wahl LM, Bolen JB, Horak ID (1993) Lipopolysaccharide induces activation of CD14-associated protein tyrosine kinase p53/56lyn. J Biol Chem 268:20725-20728.

Stewart S, Cacucci F, Lever C (2011) Which memory task for my mouse? A systematic review of spatial memory performance in the tg2576 Alzheimer's mouse model. J Alzheimers Dis 26:105-126.

Stewart WF, Kawas C, Corrada M, Metter EJ (1997) Risk of Alzheimer's disease and duration of NSAID use. Neurology 48:626-632.

Streit WJ, Conde JR, Harrison JK (2001) Chemokines and Alzheimer's disease. Neurobiol Aging 22:909-913.

Streit WJ, Mrak RE, Griffin WS (2004) Microglia and neuroinflammation: a pathological perspective. J Neuroinflammation 1:14.

Strittmatter WJ, Roses AD (1996) Apolipoprotein E and Alzheimer's disease. Annu Rev Neurosci 19:53-77.

Styren SD, Civin WH, Rogers J (1990) Molecular, cellular, and pathologic characterization of HLA-DR immunoreactivity in normal elderly and Alzheimer's disease brain. Exp Neurol 110:93-104.

Suen PW, Ilic D, Caveggion E, Berton G, Damsky CH, Lowell CA (1999) Impaired integrin-mediated signal transduction, altered cytoskeletal structure and reduced motility in Hck/Fgr deficient macrophages. J Cell Sci 112 (Pt 22):4067-4078.

Sunderland T, Linker G, Mirza N, Putnam KT, Friedman DL, Kimmel LH, Bergeson J, Manetti GJ, Zimmermann M, Tang B, Bartko JJ, Cohen RM (2003) Decreased beta-amyloid1-42 and increased tau levels in cerebrospinal fluid of patients with Alzheimer disease. Jama 289:2094-2103.

Szczepanik AM, Rampe D, Ringheim GE (2001) Amyloid-beta peptide fragments p3 and p4 induce pro-inflammatory cytokine and chemokine production in vitro and in vivo. J Neurochem 77:304-317.

Tan J, Town T, Mullan M (2000) CD45 inhibits CD40L-induced microglial activation via negative regulation of the Src/p44/42 MAPK pathway. J Biol Chem 275:37224-37231.

Tan J, Town T, Saxe M, Paris D, Wu Y, Mullan M (1999a) Ligation of microglial CD40 results in p44/42 mitogen-activated protein kinase-dependent TNF-alpha production that is opposed by TGF-beta 1 and IL-10. J Immunol 163:6614-6621.

Tan J, Town T, Paris D, Mori T, Suo Z, Crawford F, Mattson MP, Flavell RA, Mullan M (1999b) Microglial activation resulting from CD40-CD40L interaction after beta-amyloid stimulation. Science 286:2352-2355.

Tatosyan AG, Mizenina OA (2000) Kinases of the Src family: structure and functions. Biochemistry (Mosc) 65:49-58.

Taupin V, Toulmond S, Serrano A, Benavides J, Zavala F (1993) Increase in IL-6, IL-1 and TNF levels in rat brain following traumatic lesion. Influence of pre- and post-traumatic treatment with Ro5 4864, a peripheral-type (p site) benzodiazepine ligand. J Neuroimmunol 42:177-185.

Taylor SJ, Shalloway D (1996) Src and the control of cell division. Bioessays 18:9-11.

Thal LJ, Ferris SH, Kirby L, Block GA, Lines CR, Yuen E, Assaid C, Nessly ML, Norman BA, Baranak CC, Reines SA (2005) A randomized, double-blind, study of rofecoxib in patients with mild cognitive impairment. Neuropsychopharmacology 30:1204-1215.

Tillotson ML, Wood JG (1989a) Tyrosine phosphorylation in the postnatal rat brain: a developmental, immunohistochemical study. J Comp Neurol 282:133-141.

Tillotson ML, Wood JG (1989b) Phosphotyrosine antibodies specifically label ameboid microglia in vitro and ramified microglia in vivo. Glia 2:412-419.

Tobinick EL, Gross H (2008) Rapid cognitive improvement in Alzheimer's disease following perispinal etanercept administration. J Neuroinflammation 5:2.

Trommsdorff M, Borg JP, Margolis B, Herz J (1998) Interaction of cytosolic adaptor proteins with neuronal apolipoprotein E receptors and the amyloid precursor protein. J Biol Chem 273:33556-33560.

Tsuji-Takayama K, Matsumoto S, Koide K, Takeuchi M, Ikeda M, Ohta T, Kurimoto M (1997) Interleukin-18 induces activation and association of p56(lck) and MAPK in a murine TH1 clone. Biochem Biophys Res Commun 237:126-130.

Tuppo EE, Arias HR (2005) The role of inflammation in Alzheimer's disease. Int J Biochem Cell Biol 37:289-305.

Verhager AM, Wallace ME, Goradia A, Jones SA, Croom HA, Metcalf D, Collinge JE, Maxwell MJ, Hibbs ML, Alexander WS, Hilton DJ, Kile BT, Starr R (2009) A kinase-dead allele of Lyn attenuates autoimmune disease normally associated with Lyn deficiency. J Immunol 182:2020-2029.

Villemagne VL, Perez KA, Pike KE, Kok WM, Rowe CC, White AR, Bourgeat P, Salvado O, Bedo J, Hutton CA, Faux NG, Masters CL, Barnham KJ (2010) Blood-borne amyloid-beta dimer correlates with clinical markers of Alzheimer's disease. J Neurosci 30:6315-6322.

Weggen S, Eriksen JL, Sagi SA, Pietrzik CU, Ozols V, Fauq A, Golde TE, Koo EH (2003) Evidence that nonsteroidal anti-inflammatory drugs decrease amyloid beta 42 production by direct modulation of gamma-secretase activity. J Biol Chem 278:31831-31837.

Wegiel J, Imaki H, Wang KC, Wronska A, Osuchowski M, Rubenstein R (2003) Origin and turnover of microglial cells in fibrillar plaques of APPsw transgenic mice. Acta Neuropathol 105:393-402.

Wegiel J, Wang KC, Imaki H, Rubenstein R, Wronska A, Osuchowski M, Lipinski WJ, Walker LC, LeVine H (2001) The role of microglial cells and astrocytes in fibrillar plaque evolution in transgenic APP(SW) mice. Neurobiol Aging 22:49-61.

Weingarten MD, Lockwood AH, Hwo SY, Kirschner MW (1975) A protein factor essential for microtubule assembly. Proc Natl Acad Sci U S A 72:1858-1862.

Weldon DT, Rogers SD, Ghilardi JR, Finke MP, Cleary JP, O'Hare E, Esler WP, Maggio JE, Mantyh PW (1998) Fibrillar beta-amyloid induces microglial phagocytosis, expression of inducible nitric oxide synthase, and loss of a select population of neurons in the rat CNS in vivo. J Neurosci 18:2161-2173.

Weng Z, Thomas SM, Rickles RJ, Taylor JA, Brauer AW, Seidel-Dugan C, Michael WM, Dreyfuss G, Brugge JS (1994) Identification of Src, Fyn, and Lyn SH3-binding proteins: implications for a function of SH3 domains. Mol Cell Biol 14:4509-4521.

Wenk GL (1998) Current Protocols in Neuroscience. In: Behavioral Neuroscience, pp 8.5B.1-8.5B.7.

Werdich XQ, Penn JS (2005) Src, Fyn and Yes play differential roles in VEGF-mediated endothelial cell events. Angiogenesis 8:315-326.

Wilson CJ, Finch CE, Cohen HJ (2002) Cytokines and cognition--the case for a head-to-toe inflammatory paradigm. J Am Geriatr Soc 50:2041-2056.

Wong G, Muller O, Clark R, Conroy L, Moran MF, Polakis P, McCormick F (1992) Molecular cloning and nucleic acid binding properties of the GAP-associated tyrosine phosphoprotein p62. Cell 69:551-558.

Wood JG, Zinsmeister P (1991) Tyrosine phosphorylation systems in Alzheimer's disease pathology. Neurosci Lett 121:12-16.

Woodroofe MN, Sarna GS, Wadhwa M, Hayes GM, Loughlin AJ, Tinker A, Cuzner ML (1991) Detection of interleukin-1 and interleukin-6 in adult rat brain, following mechanical injury, by in vivo microdialysis: evidence of a role for microglia in cytokine production. J Neuroimmunol 33:227-236.

Yamamoto M, Horiba M, Buescher JL, Huang D, Gendelman HE, Ransohoff RM, Ikezu T (2005) Overexpression of monocyte chemotactic protein-1/CCL2 in beta-amyloid precursor protein transgenic mice show accelerated diffuse beta-amyloid deposition. Am J Pathol 166:1475-1485.

Yamamoto M, Kiyota T, Horiba M, Buescher JL, Walsh SM, Gendelman HE, Ikezu T (2007) Interferon-gamma and tumor necrosis factor-alpha regulate amyloid-beta plaque deposition and beta-secretase expression in Swedish mutant APP transgenic mice. Am J Pathol 170:680-692.

Yates SL, Burgess LH, Kocsis-Angle J, Antal JM, Dority MD, Embury PB, Piotrkowski AM, Brunden KR (2000) Amyloid beta and amylin fibrils induce increases in proinflammatory cytokine and chemokine production by THP-1 cells and murine microglia. J Neurochem 74:1017-1025.

Yeatman TJ (2004) A renaissance for SRC. Nat Rev Cancer 4:470-480.

Yeh M, Gharavi NM, Choi J, Hsieh X, Reed E, Mouillesseaux KP, Cole AL, Reddy ST, Berliner JA (2004) Oxidized phospholipids increase interleukin 8 (IL-8) synthesis by activation of the c-src/signal transducers and activators of transcription (STAT)3 pathway. J Biol Chem 279:30175-30181.

Yin YI, Bassit B, Zhu L, Yang X, Wang C, Li YM (2007) {gamma}-Secretase Substrate Concentration Modulates the Abeta42/Abeta40 Ratio: IMPLICATIONS FOR ALZHEIMER DISEASE. J Biol Chem 282:23639-23644.

Yoshimura M, Iwasaki Y, Kaji A (1981) In vitro differentiation of chicken embryo skin cells transformed by Rous sarcoma virus. J Cell Physiol 109:373-385.

Ziegler SF, Wilson CB, Perlmutter RM (1988) Augmented expression of a myeloid-specific protein tyrosine kinase gene (hck) after macrophage activation. J Exp Med 168:1801-1810.